Doctoral Thesis

Development of a Reverse Osmosis (RO)-Based Water Treatment System for Potable Water Production from Contaminated Source Water

A dissertation submitted in partial fulfillment of the requirements for the degree of

Doctor of Engineering (D.Eng.)

By

A.K.M. Ashadullah

Supervised by

Professor Naoyuki Kishimoto

And

Co-supervised by

Associate Professor Hiromoto Koshikawa

Ryukoku University

2016

Department of Environmental Solution Technology

Graduate School of Science and Technology, Ryukoku University, Japan.

Acknowledgement

All praise is to ALLAH Subhanahu Wa Ta'ala, who gave me an opportunity for pursuing Doctor of Engineering (D.Eng.) in the Department of Environmental Solution Technology, Ryukoku University, Japan, under kind supervision of honorable Professor Naoyuki Kishimoto. I would like to thanks co-supervisors Professor Yoichi Ichikawa and Associate Professor Hiromoto Koshikawa and oral-examiners Professor Thomas Lei and Associate Professor Tetsuji Okuda for guiding me in a proper way for the completion my doctoral thesis. I feel proud to be a student of the water quality system engineering laboratory belong to Prof. Kishimoto as well as really grateful to the members of this laboratory who contributed immensely to my personal and experimental research activities directly or indirectly. It's my pleasure that in three years experimental based doctoral research study I learned a lot from Prof. Kishimoto not only in theoretical concept but also in practical aspect in the diversified water treatment areas. His excellent teaching technique and affectional friendly behavior touched my heart very deeply. Moreover, his encouragement, effort, and precise time-to-time supervision helped me to construct the doctoral research module and to finalize the thesis paper in a proper manner.

I would like to thanks Japan Student Services Organization (JASSO) for providing Monbukagakusho Honors Scholarship for funding me financially from October, 2013 to March, 2014. Then, I would like to special thanks to Kato Asao International Scholarship Foundation (KAISF) for supporting me financially from April, 2014 to September, 2016. In addition, I would like to thanks Ryukoku University, Graduate School of Science and Technology Doctoral Fellowship, Research Grants for Students in the Doctoral Program of the graduate School of Science and Technology, and Research Grants for Science and Technology Conferences for supporting me financially to participate in the domestic and international conferences.

I exclusively want to thanks my parents who raised me with love of affection and supported me each and every moment financially and mentally. Last but not least special gratitude for my loving wife Mst. Naznin Akter for her all sorts of support, encouragement, and sacrifice in the different stages of this doctoral program.

A.K.M. Ashadullah
Ryukoku University
2016

Abstract

A proper management of water treatment systems is not an easy task and it is still imperfect in many developing countries in the world, whereas, safe water supply systems are diffusing into their society. This situation is caused by many crucial factors like political, social, and economical obstacles in developing countries, which directly or indirectly affect the urban water supply system development and deteriorate the quality of water reaching the consumer. Water quality control is typically one of the foremost responsibilities of government or local organizations to protect the inhabitants from water borne diseases. Many authorities conventionally adopt central water treatment plants (CWTPs) for potable water production. But, unfortunately the produced potable water is often contaminated by polluted water reaching the consumer prior to consumption. Even though such contaminations occur, many people continue to use the contaminated water in their daily lives like drinking, cooking, bathing, and washing. It has also been seen that in many cases some people boil water or use some conventional and unconventional technologies for minimum drinking purpose. Boiling water could be an instant alternative solution for getting safer drinking water, but the removal of heat resistant microorganisms, organic, and inorganic particles are less expected. Many advanced technologies like microfiltration (MF) and ultrafiltration (UF) also fail to purify the water to potable level in some cases. As a result, every year millions of people die in the world due to unhygienic water consumption, especially in developing countries. Thus, an appropriate advanced water treatment system is desirable for potable water production from contaminated water sources.

Considering this notion, I proposed and evaluated a reverse osmosis (RO)-based water treatment system for safe and hygienic drinking water production from contaminated water sources, because of globalization RO membranes are available everywhere and they can provide an absolute barrier to all types of pathogens and dissolved particulate matter. Since RO is a sophisticated technology, its performance and operational life-time depend on pre-treatment processes applied. Fouling is one of the major problems and foremost antagonist in RO operations. In general foulants are categorized into four types namely particles, organic, inorganic, and microorganisms. All foulants have a negative effect on the performance of RO membrane by increasing the operational pressure simultaneously decreasing the permeate flux. Hence, to protect the RO membrane from particulate, organic, and inorganic fouling a series of pre-treatment processes, namely a depth filtration with surface-charge control followed by electrolysis was developed in this research.

In Chapter I of this thesis I summarized contaminated potable water issues in developing countries and described the concept and ideas behind the development of RO-based water treatment system for potable water production from contaminated source water.

In Chapter II, I discussed the applicability of a reverse osmosis (RO) membrane for potable water production and major foulants in RO operation with effective permeate flux recovery methods. A commercially available spiral-wound polyamide thin-film composite type RO membrane element (TW30-1812-36, Dow Filmtec, USA) was used in this research, because of its low hydraulic resistance with a greater membrane stability. One of the specific objectives was to evaluate the rejection rates of physical, chemical, and biological indices of synthetic contaminated source water containing nitrite nitrogen (NO_2^--N), nitrate nitrogen (NO_3^--N), iron (Fe^{2+}), and manganese (Mn^{2+}). In addition, the main causes of fouling and an effective method for successive permeate flux recovery techniques were also discussed for extending the operational life-time. The synthetic contaminated source water was prepared by a 5-time dilution of municipal wastewater in Ryukoku University with normal tap water and the addition of NO_2^--N, NO_3^--N, Fe^{2+}, and Mn^{2+} at the concentrations of about 10, 20, 10, and 5 mg/L, respectively. The experimental results showed that the RO membrane was able to reject suspended solids (SS), biochemical oxygen demand (BOD), chemical oxygen demand (COD), and total coliform (TC) completely. Besides, the ions rejection rates were 98% for iron, 97% for manganese, 94% for chloride, 80% for nitrite nitrogen, and 77% for nitrate nitrogen, respectively. The ammonium (NH_4^+) rejection rate was found to be poor and it was only 45% probably due to its lower molecular weight. As a result, a pre- or post-treatment process would be required to meet the drinking water quality standards, especially for NH_4^+. The contaminated source water contained organic aggregates and inorganic particles like iron (Fe) colloids and they were found to be major membrane foulants. The back-flushing operation through the concentrate port could improve the permeate flux of a RO membranes fouled by organic aggregates to the permeate flux recovery rate of 37.0% using pure water, and 79.4% using pure water followed by the 1,000 mg/L of sodium hydroxide (NaOH) solution. The hydrolyzation and solubilization of organic matter by NaOH was inferred to be responsible for the permeate flux recovery. On the contrary, the permeate flux of RO membrane fouled by Fe colloids was completely recovered by back-flushing using pure water, when the back-flushing was applied just after the fouling. This suggested that the membrane fouling by Fe colloids was mainly caused by the physical clogging in the membrane element. In addition, NaOH solution showed a better performances in permeate flux recovery of matured Fe colloidal fouled membrane. The permeate flux recovery rate reached 89.1%. Consequently, I recommend back-flushing through the concentrate port using 1,000 mg/L of NaOH solution as a back-flushing solution.

From the reverse osmosis (RO) experiments in Chapter II, it was found that the RO process can produce good quality water for potable use. However, a few foulants, like organic aggregates and iron (Fe) colloids, were found to be problematic for the continuous operation of the system. Accordingly, a pre-treatment of suspended solids (SS) like organic aggregates and Fe colloids

should be introduced prior to the RO process. Hence, I discussed the depth filtration with surface-charge control of depth filter in Chapter III for the removal of organic aggregates and Fe colloids. A conducting carbon fiber felt made from polyacrylonitrile fibers 5.3 μm in diameter (Weight per area: 250 g/m^2; Kanai Juyo Kogyo, Osaka, Japan) was used as filter media, and kaolin powder of 0.1-4.0 μm in diameter (Nacalai, Tesque, Kyoto, Japan) and ferrous sulfate heptahydrate ($FeSO_4.7H_2O$) were used as micro-particles and Fe colloids sources, respectively. The surface-charge of depth filter was controlled by impressing the terminal voltage of +1.0 V at the filtration operation and of -1.0 V at the back-washing operation. Since these terminal voltages were within the potential window of water electrolysis, the electricity was used only for charging the electrical double layers (EDLs) of the filter media and the counter electrode. The kaolin particles and Fe colloids removal efficiencies were observed in pure water, water containing anionic surfactant, and synthetic contaminated source water. In addition, back-washing experiments were conducted to observe the washout removal efficiency of the particles that desorbed on the filter media in the filtration step. The kaolin particle removal efficiency of 100% was observed at the terminal voltage of +1.0 V in pure water with 292.2 mg/L sodium chloride (NaCl) at the hydraulic loading of 283 L m^{-2} min^{-1}. However, the kaolin particle removal efficiency decreased to 22.2-45.7% in synthetic contaminated source water and 51.1% in the anionic surfactant-contained water. Fe colloids removal efficiency was observed 96.4-98.1% at alkaline pH and it decreased to 29.9-47.5% in acidic pH. On the contrary, the kaolin particle washout efficiency of 72.5% was observed at the terminal voltage of -1.0 V and the hydraulic loading of 1274 L m^{-2} min^{-1}. But, the kaolin particle washout efficiency was decreased to 55.0-59.5% in synthetic contaminated source water and 4.6-12.5% in the anionic surfactant-contaminated water. The hydrophobic tails of the anionic surfactant inhibited in repulsive force mechanism between the filter medium and the particles, which affected the washout efficiency. The Fe colloids suspension washout efficiency of 59.7% was observed in an anionic surfactant-free water, but it dropped to 6.4% in the anionic surfactant-contained water. Consequently, I recommend the hydraulic loading of 283 L m^{-2} min^{-1} with the terminal voltage of +1.0 V for the filtration mode and the hydraulic loading of 1274 L m^{-2} min^{-1} of 292.2 mg/L-NaCl contained pure water with the terminal voltage of -1.0 V for the back-washing mode.

Chapter II revealed that the reverse osmosis (RO) process has the potential to produce potable water with acceptable water quality from contaminated source water. However, the rejection efficiency of ammonium (NH_4^+) was relatively low even if the RO process was applied. Therefore, a process assisting the RO process should be introduced for the removal of NH_4^+. Furthermore, the membrane fouling was a serious thread for extended operation of the RO process. In order to remove foulants from the feed water to the RO process, the depth filtration with the active control of the surface-charge of the filter media was discussed as a pre-treatment technique in Chapter III. The depth

filtration successfully removed particulate foulants from the contaminated source water. However, a certain amount of total coliform (TC) and general bacteria (GB) passed through the depth filter, which would cause the biofouling of the RO membrane. Accordingly, a pre-treatment technique for the removal of TC and GB should be also introduced prior to the RO process. In Chapter IV, I discussed the removal of NH_4^+ and microorganisms like TC and GB through electrolysis. A two-compartment electrochemical flow cell with copper mesh cathodes and a platinum-coated titanium anode was used in this study. The cell had a cation-exchange membrane (Nafion NE-1110, DuPont, USA) separator for dividing an anodic compartment from a cathodic. Potassium nitrate (KNO_3) and sodium chloride (NaCl) were used for the sources of nitrate and chloride at the final concentration of 1.42 mM for KNO_3 (NO_3^--N=20 mg/L) and 329.68-1318.72 mg/L for NaCl (Cl^-=100-800 mg/L). I used a 5-time diluted municipal wastewater from Ryukoku University with normal tap water as the source of ammonium, TC, and GB for synthetic contaminated source water. A series of electrolysis experiments revealed that the volumetric electric charge was a critical factor for conversion of nitrate into nitrite and ammonium as well as anodic production of chlorine. An increase in the flow rate also enhanced the electrochemical reactions due to the promotion of the mass transfer process. Higher chloride ion concentration improved the current efficiency of chlorine production by decreasing the equilibrium electrode potential for chlorine (Cl_2) evolution. As a result, total nitrogen removal via the break-point chlorination mechanism was enhanced. However, the current efficiency remained low, namely a maximum of 6.1% at a chloride ion concentration of 800 mg/L. In spite of the low current efficiency, the 1.42 mM initial nitrate was decreased to 0.48 mM (NO_3^--N=6.78 mg/L) without nitrite and ammonium accumulation during a 1.0 minute contact time for nitrate reduction and a 15-second contact time for chlorine production at the volumetric electric charge of 5,100 C/L and Cl^- concentration of 800 mg/L at pH 7. Under this condition, TC and GB were removed completely. Consequently, the electrochemical flow cell could provide a rapid removal technique of nitrogenous compounds and microorganisms from water stream. Finally, I proposed 5,100 C/L volumetric electric charge with 800 mg/L chloride ion concentration at pH 7 as an optimum operational condition for the removal of nitrogenous compounds, TC, and GB.

The final conclusion of this research was summarized in Chapter V. An integrated water treatment system was proposed to get potable water from contaminated source water, which was composed of a depth filter with surface charge control and a reservoir equipped with an electrolysis system and a RO membrane unit that produced potable water as a final product. The depth filter and the RO membrane unit also had a back-flushing system to extend the operational life-time. As a whole, this integrated water treatment system was thought to be effective in solving the problems derived from contaminated source water.

論文要旨

水処理システムの適正管理は必ずしも容易なものではなく，安全な水道システムが普及しつつある多くの発展途上国においても，未だ不適切な管理が散見される。この状況は，政治的，社会的，経済的な様々な要因に起因し，直接・間接的に水道システムの発展を妨げ，消費者に供給される水の質的悪化をもたらしている。安全な水道水の供給は，住民を水系伝染病から守るために，政府や地域団体が負う重要な責任の一つである。一般に，多くの機関において中央集約型浄水システムが採用されている。しかし，そこで生産された水道水は，しばしば消費される前に，汚染水の混入などにより汚染されることがある。たとえそのような汚染が起こったとしても，多くの人々は，飲用や調理，入浴，洗浄など，日々の生活を営むためにそのような汚染された水道水を使うことを余儀なくされている。一部の人々は，水の煮沸やその他の方法で最低限の飲料水を確保している。水の煮沸は，より安全な飲料水を得るための簡便な手法である。しかし，耐熱細菌や有機および無機粒子の除去はあまり期待できない。これに対し，精密ろ過（MF）や限外ろ過（UF）のような高度処理技術もあるが，有害溶解性物質による汚染などに対しては飲用可能レベルまで水を浄化することは困難である。結果として，特に発展途上国において，毎年，何百万人もの人々が非衛生的な水の利用によって命を落としている。したがって，汚染された原水から飲料水を製造可能な適切な高度水処理システムの構築が望まれている。

このような状況を考え，この論文では，汚染された原水から安全で衛生的な飲料水を作ることができる逆浸透（RO）法を基盤とした水処理システムを提案し，評価した。というのも，産業のグローバル化の進展に伴って，RO 膜がどこでも容易に手に入るようになり，かつ，RO 膜は全ての病原体や溶解性物質に対する有効な防護手段を提供できると考えるからである。RO 技術は繊細な技術であり，その性能や膜寿命は，組み合わせる前処理技術の適否に依存している。膜の閉塞（ファウリング）は RO 操作における主要な問題の一つである。一般に，膜閉塞を引き起こす物質（ファウラント）は 4 つの種類に分類される。すなわち，粒子状物質および有機物，無機物，微生物である。全てのファウラントは，膜間差圧の増大やろ過流束の低下というように，RO 膜性能に負の影響をもたらす。そこで，本研究では，ファウリングから RO 膜を保護するための一連の前処理プロセスとして，ろ材表面電位制御機構を有する深層ろ過プロセスと電解プロセスを開発，検討した。

第 I 章では，序論として，発展途上国における水道水汚染問題についてまとめるとともに，汚染原水から飲料水を製造するための RO 法を基盤とした水処理システムの開発に至った考え方を説明した。

第 II 章では，飲料水製造への RO 膜の適用可能性および RO 操作における主要なファウラントについて検討し，効果的なろ過流束回復手法を提示した。本研究では，通水抵抗の低さや膜の安定性を考慮し，RO 膜に，商業的に利用可能なポリアミド薄膜型 RO 膜エレメント（TW30-1812-36, Dow Filmtec, USA）を用い，亜硝酸イオン（NO_2^-）や硝酸イオン（NO_3^-），鉄（Fe^{2+}），

マンガン（Mn^{2+}）を含む汚染原水中の物理・化学・生物学的水質項目の阻止率を評価した。その後，膜寿命の向上を図るために，ファウリング要因や有効なろ過流束回復手法を検討した。汚染原水は，龍谷大学で発生した下水を水道水で 5 倍希釈した希釈水をベースに，NO_2^-や NO_3^-，Fe^{2+}，Mn^{2+}をそれぞれ約 10, 20, 10, 5 mg/L となるように添加して作成した。様々な実験の結果，RO 膜は浮遊物質および生物化学的酸素要求量，化学的酸素要求量，大腸菌群数を完全に除去することが可能であった。一方，イオン類の阻止率は，鉄で 98%，マンガンで 97%，塩化物イオンで 94%，亜硝酸イオンで 80%，硝酸イオンで 77%であり，アンモニアに至っては 45%と低い阻止率にとどまった。アンモニアの分子量が小さいことが，低い阻止率の一要因であると考えられた。結果として，飲料水質基準を満たすためには，特にアンモニアに関して，何らかの前処理，もしくは後処理が必要となることが示唆された。使用した汚染原水は有機性凝集粒子や鉄コロイドのような無機粒子を含んでおり，これらは本 RO 膜の主たるファウラントとして機能していた。RO 膜エレメントの濃縮液排出口から逆流洗浄を行うことで，有機性凝集粒子によりファウリングした RO 膜のろ過流束の回復が可能であり，ろ過流束回復率は，純水による逆流洗浄では 37%，1000 mg/L の水酸化ナトリウム溶液による逆流洗浄では 79%であった。水酸化ナトリウムによる有機物の加水分解作用や可溶化作用が，水酸化ナトリウム溶液による逆流洗浄の高い有効性に寄与していたと考えられた。一方，鉄コロイドでファウリングした RO 膜については，ファウリング直後に純水による逆流洗浄を行うことで，ろ過流速は完全に回復した。このことから，鉄コロイドによるファウリングは，主に，RO 膜エレメントの物理的な目詰まりによるものであると考えられた。他方，鉄コロイドでファウンリングした RO 膜を，ファウリング後，一定時間放置した場合は，純水による逆流洗浄効果は不十分であり，水酸化ナトリウム溶液による逆流洗浄が有効で，ろ過流束回復率は 89%であった。最終的に，本 RO 膜エレメントの推奨される洗浄方法として，1000 mg/L の水酸化ナトリウム溶液を洗浄液に用い，濃縮液排出口から逆流洗浄を行うことが望ましいと判断された。

第 II 章の RO 処理実験の結果，RO 処理は飲用に耐える処理水を作り出せることが分かった。しかし，有機性凝集粒子や鉄コロイドなどのファウラントが連続運転をする上で障害となることが示唆された。したがって，これらの浮遊物質を除去する前処理法を導入すべきであると判断された。第 III 章では，これらの浮遊物質を除去するために，ろ材表面電位制御機構を有する深層ろ過法について検討した。ろ材には，ポリアクリロニトリル繊維から製造した線径 5.3 μm の導電性炭素繊維を用いた炭素繊維不織布（目付 250 g/m^2，金井重要工業）を積層させて使用した。浮遊物質および鉄コロイドには，それぞれ粒径 0.1～4.0 μm のカオリン粒子（ナカライテスク）と硫酸鉄(II) 7 水和物（試薬特級，ナカライテスク）が空気酸化されて生じるコロイドを用いた。ろ材表面電位は，ろ材を陽極とし，対極（陰極）としてステンレス板をもちいて，両極間に直流電圧を印加することにより制御した。ろ過時は，極間電位を+1.0 V に設定し，逆流洗浄時は極間電位を−1.0 V に設定した。印加電圧は水の電位窓の範囲内なので，ろ材表面電位制御の

ための電力は，ろ材表面や対極の電気二重層の充電のみに使用され，電解電流は観測されなかった。カオリン粒子および鉄コロイドの除去実験は，292.2 mg/L 塩化ナトリウム含有水，陰イオン界面活性剤含有水，および汚染原水中で実施した。また，逆流洗浄は，ろ材に捕捉された粒子の脱着除去を行わせるために実施した。292.2 mg/L 塩化ナトリウム含有水を用いた実験では，水量負荷 283 L m^{-2} min^{-1} の条件で+1.0 V の電圧を印加することで 100%のカオリン粒子除去率を達成した。しかし，カオリン粒子除去率は汚染原水中では 22～46%，陰イオン界面活性剤含有水中では 51%に低下した。一方，逆流洗浄においては，水量負荷 1274 L m^{-2} min^{-1} の条件下で−1.0 V の電圧を印加することで，292.2 mg/L 塩化ナトリウム含有水を用いた実験で 73%の洗浄効率（脱着率）を達成した。しかし，洗浄効率は，汚染原水を用いた実験では 55～60%，陰イオン界面活性剤含有排水を用いた実験では 4.6～13%まで低下した。鉄コロイド除去実験での鉄コロイド除去率は，292.2 mg/L 塩化ナトリウム含有水中で 96%，陰イオン界面活性剤含有水中で 98%となり，陰イオン界面活性剤による除去率低下は認められなかった。一方，陰イオン界面活性剤が共存することで，洗浄効率は 59.7%から 6.4%へ大幅に低下した。陰イオン界面活性剤は，ろ材に吸着し，ろ材表面を被覆することで，ろ材表面電位を負に変化させる。その結果，外部電源によるろ材表面電位制御機能が低下し，処理能力の低下をもたらしたと考えられた。このような課題は残るものの，ろ材表面電位制御による深層ろ過性能向上効果が認められたことから，水量負荷 283 L m^{-2} min^{-1}，印加電圧+1.0 V の条件でろ過操作を実施し，水量負荷 1274 L m^{-2} min^{-1}，印加電圧−1.0 V の条件で逆流洗浄操作を行うことが望ましいと判断された。

第 II 章において，RO 膜のアンモニア阻止率が低いという課題が認められ，アンモニア除去のための補完プロセスの必要性が示唆された。また，RO 膜のファウリング抑止のための前処理プロセスとして，第 III 章において，ろ材表面電位制御を行う深層ろ過を導入した。これにより粒子状のファウラントの分離除去が可能となったが，バクテリアの除去率は低く，バイオファウリングが引き続き，懸念される状況にある。そこで，第 IV 章では，電解技術を導入し，そのアンモニア除去特性や微生物除去特性を評価，検討した。本研究では，銅カソードと白金鍍金チタンアノードを備え，陽イオン交換膜（Nafion NE-1110, DuPont, USA）を隔膜とした二室型電解フローセルを用い，被処理水をカソード室に流入させたのち，アノード室に流入させる形で電解処理を行った。被処理水には，硝酸イオン源として硝酸カリウム（試薬特級，ナカライテスク）を，塩化物イオン源として塩化ナトリウム（試薬特級，ナカライテスク）を，それぞれ 1.42 mM (NO_3^--N=20 mg/L)，100～800 mg-Cl^-/L となるように添加した。また，アンモニア，大腸菌群，および一般細菌源として龍谷大学で発生した下水を 20%添加した。一連の電解処理実験の結果，容積あたり通電量が，硝酸イオンの亜硝酸イオンもしくはアンモニウムイオンへの電解還元や遊離塩素の電解生成の支配因子であった。また，通水速度を増大させると，物質移動過程が促進されることで，電極反応も促進された。塩化物イオン濃度の増加も遊離塩素の電解生成を促進したが，800 mg-Cl^-/L の塩化ナトリウムを添加した場合でも電流効率は 6.1%と低い値にと

どまった。電流効率は低いものの，カソード室滞留時間 1.0 分，アノード室滞留時間 15 秒，通電量 5.1 kC/L の運転条件下で，硝酸イオン濃度は 1.42 mM (NO_3^--N=20 mg/L) から 0.48 mM (NO_3^--N=6.78 mg/L) に低減し，亜硝酸イオンやアンモニアの蓄積も見られなかった。これは，硝酸イオンの電解還元により生成したアンモニアと塩化物イオンの電解酸化により生成した遊離塩素が反応し，不連続点塩素処理のメカニズムで窒素ガスに変換されたためであると考えられた。一方，同じ条件での大腸菌群数および一般細菌の除去率は，どちらも 100%であった。結果として，電解フローセルを用いることにより，無機窒素化合物および微生物の迅速な除去が可能であった。最終的に，無機窒素化合物除去および微生物除去のための電解フローセルの運転条件として，塩化ナトリウムを約 800 mg-Cl^-/L となるように原水に添加した上で，5.1 kC/L の通電量で電解を行うことが適切であると判断された。

第 V 章では，本論文の結論として，汚染原水から飲料水を製造するための統合水処理システムを提示した。このシステムでは，まず，ろ材表面電位制御深層ろ過で，粒子状物質を取り除き，その処理水を貯留タンクに貯留する。処理水貯留タンクには，電解フローセルと RO 膜エレメントへの水循環系が別個に構築されており，電解フローセルにより無機窒素化合物や微生物の除去が行われ，RO 膜エレメントでは飲料水の製造が行われる。処理水貯留タンクの水は必要に応じて深層ろ過のろ床の逆流洗浄水としても用いられる。また，RO 膜エレメントの逆流洗浄水には水酸化ナトリウムを添加した RO 膜処理水を用いる。全体として，本統合水処理システムは，汚染された原水に付随する諸課題の解決に貢献できると考えられた。

Table of Contents

Chapter I
General Introduction

1.1 Introduction

Potable water supply systems in the world are categorized into centralized, decentralized, or hybrid ones incorporated with both centralized and decentralized components. Generally, in centralized water treatment systems potable water is produced in one or a small number of water treatment plants. Then, water is distributed from there using a pressurized system to consumers throughout the urban areas. By contrast, in a decentralized water treatment system water is treated on-site and supplied to the users locally at a house-hold or community level on a small scale. A hybrid system integrates a centralized water treatment system as a backbone along with decentralized systems in selected locations. Currently, a decentralized advanced water treatment system in a particular house-hold or a community is a radical concept in most of developing countries in the world. A decentralized water treatment system refers to a small scale potable water supply system. In this context, decentralized water treatment systems are considered as specialized projects particularly in individual residential areas, multipurpose hotels, schools, colleges, universities, and public officials or a group of community (Daigger and Crawford, 2007).

The term Millennium Development Goals (MDGs) is a very well-known common phrase in the 20th century. To achieve MDGs in developing countries many international, domestic, and local organizations are working together in the field of environment, and putting special emphasis on hygienic drinking water for everyone (United Nations, 2006). The population growth along with migration from rural to urban areas is a very common phenomenon in developing countries. Due to rapid unplanned urbanization residents of urban areas face many unexpected crises, among them water shortage for daily uses is the most noticeable (Lee and Schwab, 2005). Regrettably, gradual decreases of natural ground water sources and discharge of large quantities of polluted water to open water bodies like lakes and rivers have complicated the procurement of safe water sources for the potable use (United Nations Environment Programme, 2002).

On the other hand, political, social, and economical complications are very common manifestations in daily lives for the people of developing countries, which directly or indirectly affect the urban water supply system development and deteriorate the quality of water reaching the consumers (WHO and UNICEF, 2000). Furthermore, water produced by central water treatment plants (CWTPs) is often adulterated prior to consumption by untreated water either inefficiently or unintentionally. The latter is caused by an improper treatment or cross contamination in the distribution system after treatment (Ford, 1999). Countless literatures have pointed out that developing countries experience a serious deterioration of infrastructure such as vast distribution

system failure compared with advanced countries (Craun and Calderon, 2001; Gadgil, 1998; Kyessi, 2005; Zerah, 2000). Depending on various contaminated sources the point-of-use water quality parameters are often found to be over the standard limits proposed by World Health Organization (WHO) all the year round as are shown in Table 1.1 (Agrad et al., 2000; Alberini et al., 1996; Dany et al., 2000; Kelkar et al., 2001; Mermin et al., 1999; Shar et al., 2007).

Table 1.1 List of some water quality parameters in contaminated water at the point-of-use (POU).

Sl. No.	Name of common contaminants	Most probable causes of contamination	Contamination level	Target water quality at POU by WHO
01.	Suspended solids (SS)	Distribution pipe leakage and cross connection with the sewerage channel	50 (mg/L)	0.0 (mg/L)
02.	Turbidity	Distribution pipe leakage and cross connection with the sewerage channel	50 (mg/L-kaolin)	< 1.0 (mg/L-kaolin)
03.	Color	Distribution pipe leakage and cross connection with the sewerage channel	50 (Pt-Co)	< 1.0 (Pt-Co)
04.	Iron (Fe^{2+})	Ground water and aged iron made distribution pipe	10 (mg/L)	< 0.5 (mg/L)
05.	Manganese (Mn^{2+})	Ground water	5 (mg/L)	< 0.5 (mg/L)
06.	Nitrite nitrogen (NO_2^--N)	Surface water, contaminated ground water, and cross connection with the sewerage line	10 (mg/L)	< 1.0 (mg/L)
07.	Nitrate nitrogen (NO_3^--N)	Surface water, contaminated ground water, and cross connection with the sewerage line	20 (mg/L)	< 10.0 (mg/L)
08.	Ammonium nitrogen (NH_4^+-N)	Surface water, contaminated ground water, and cross connection with the sewerage line	5 (mg/L)	< 0.5 (mg/L)
09.	Biochemical oxygen demand (BOD)	Surface water, contaminated ground water, and cross connection with the sewerage line	50 (mg/L)	< 1.0 (mg/L)
10.	Chemical oxygen demand (COD)	Surface water, contaminated ground water, and cross connection with the sewerage line	75 (mg/L)	< 1.0 (mg/L)
11.	Total coliform (TC)	Surface water, contaminated ground water, and cross connection with the sewerage line	2 Log10 (CFU/mL)	0.0 (CFU/mL)
12.	General bacteria (GB)	Surface water, contaminated ground water, and cross connection with the sewerage line	2 Log10 (CFU/mL)	0.0 (CFU/mL)

POU=Point of Use; WHO=World Health Organization.

Undoubtedly, water strongly acts as a passive carrier for pathogenic infections and causes protozoal, parasitic, bacterial, viral, and algal infectious diseases like various forms of diarrheal illnesses that are the most prominent examples. According to the WHO (2015) around 2 million people die every year due to unsafe water supply, sanitation, and hygiene. However, since there is no alternative, people are bound to use unclean and harmful water for drinking, cooking, bathing, and washing for survival. It has also been observed that in such critical circumstances some dwellers normally boil water at least for drinking purpose (Uddin and Baten, 2011). It is supposed that boiling water could be an instant solution to unclean water for drinking purpose. But, there may exist many heat resistant virus, bacteria, protozoa, and so on, which could directly affect human health (Spinks, 2006). Furthermore, water boiling method may not remove or decrease organic and inorganic pollutants at all (Gupta et al., 2012).

Facing such life-threatening problems and presence of various contaminants in water, some water purification systems are used in developing countries to counter these problems, which include advanced technologies like microfiltration (MF), ultrafiltration (UF), nanofiltration (NF), and reverse osmosis (RO) (Mocanu, 2000; Tam et al., 2007). Among these technologies the RO membrane process plays a vital role in response to higher impurities rejection rates, essentially producing high quality clean water in compared to other membrane-based technologies at a lower cost (Bruggen et al., 2003; Pandey et al., 2012). Figure 1.1 shows the comparison of various membrane-based process with respect to particle rejection adopted from Saxena et al. (2009).

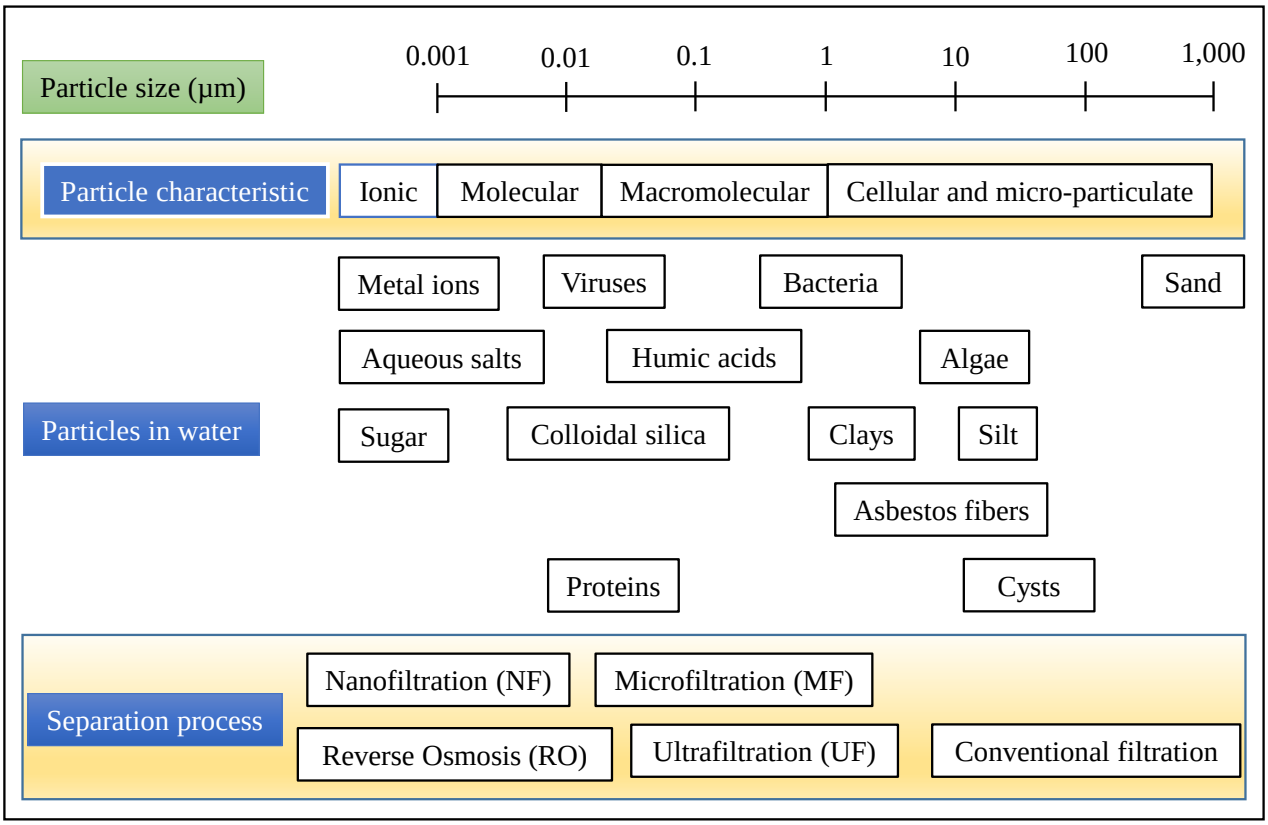

Figure 1.1 Comparison of various membrane-based process on particle rejection.

Although these methods may work well for a short time, the systems will deteriorate with extended operation and finally become unusable due to improper maintenance, management, and arrangement if professionals are not related to the operation. Among these water treatment technologies, the application of RO membrane is considered the most effective, since it can provide an absolute barrier for all types of pathogens along with turbid materials, and thus can increase the potability of water. Moreover, due to globalization RO membranes are available everywhere in the world even in developing countries. At the same time, the costs of RO membranes have decreased rapidly during the last decades. Therefore, RO membrane systems have become a feasible option for the decentralized concept due to its low-cost, ease of operation, sustainability, and low maintenance with independence of utilities in the developing countries (Varbanets et al., 2009). In

fact, the performance and efficiency of a RO system is directly affected by the quality of feed water. The impurities in feed water have various negative effects on membrane performance through fouling, scaling, or membrane degradation. The fouling results in a decline in the performance of RO membrane not due to the change of membrane structure, but due to substances accumulating on the membrane surface. The most common types of foulants are listed in Table 1.2 (Jarusutthirak and Amy, 2006; Liikanen et al., 2002; Sablani et al., 2005).

Table 1.2 List of some common foulants in RO membrane operation.

Sl. No.	Foulants	Examples	Fouling mechanism
01.	Insoluble solid particles	Sand, silt, and clay particles	Settling and accumulation on the membrane surface
02.	Metal oxides	Iron (Fe), manganese (Mn), copper (Cu), nickel (Ni), and zinc (Zn)	Settling and accumulation on the membrane surface
03.	Micro-biological organisms	Bacteria, virus, slime, and algae	Settling, growth, and accumulation on the membrane surface
04.	Soluble organic matter	Humic acid and fulvic acid	Adsorption (Hydrophobic interaction)
05.	Cationic charged elements	Coagulant, detergent, and biocides	Adsorption (Electrostatic interaction)

Figure 1.2 shows various types of fouling with fouling mechanism in a cross flow membrane operation adopted from Herzberg and Elimelech (2007), Lee et al. (2006), and Zhu and Elimelech (1997).

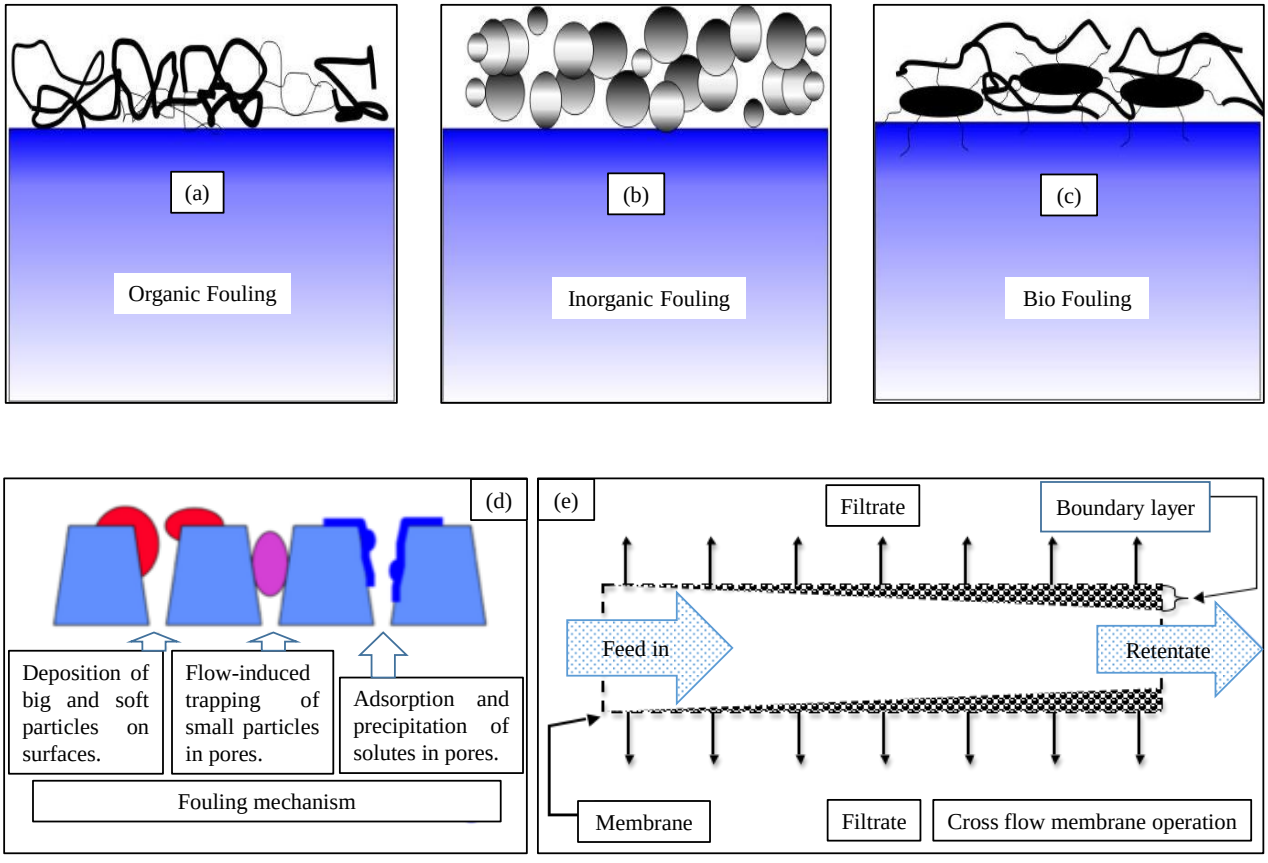

Figure 1.2 (a) Organic fouling, (b) Inorganic fouling, (c) Bio fouling, (d) Fouling mechanism, and (e) Cross flow membrane filtration.

Foulants adsorb on the membrane surface and clog membrane pores, which result in a decrease in the permeate flux through the membrane. As a result, pre-treatment is very essential for efficient and continuous operation of a RO membrane system in an economic way. Various types of conventional pre-treatment technologies like clarification and coagulation-flocculation as well as unconventional pre-treatment technologies like MF, UF, NF, and membrane bioreactors (MBRs) are used coupling with RO operation. Overall, it has been found that conventional pre-treatment technologies have lower total cost, labor cost, and unit cost in comparison with unconventional technologies. In addition, due to their comparatively smaller pore size, unconventional technologies like MF, UF, and NF also have fouling problems like RO membranes (Adham et al., 1996; Pearce, 2008). To overcome these problems and considering the long operational life-span without addition of costly chemicals, two pre-treatment methods, namely, active surface-charge control depth filtration and electrolysis were investigated in this research through laboratory scale experiments to protect the RO membrane from various fouling materials stated in Table 1.2. Since conventional pre-treatment techniques such as gravitational sedimentation and coagulation-flocculation are not effective enough to remove suspended solids (SS) and micro particles completely, they will result in RO membrane fouling (Chakravorty and Layson, 1997). Hence, to protect the RO membrane from particle, organic, and inorganic fouling the conventional depth filtration method has to be upgraded to a satisfactory level. The depth filtration has several advantages with respect to other technologies. For instance, porous filtration media in depth filtration retains particles throughout the filter bed, rather than just on the surface of the filter. Moreover, due to having tortuous channels among media the particles are retained not only on the media, but also in the media (Tien and Payatakes, 1979). Figure 1.3 shows the particle separation mechanism through the depth filtration adopted from Tobiason and O'Melia (1988).

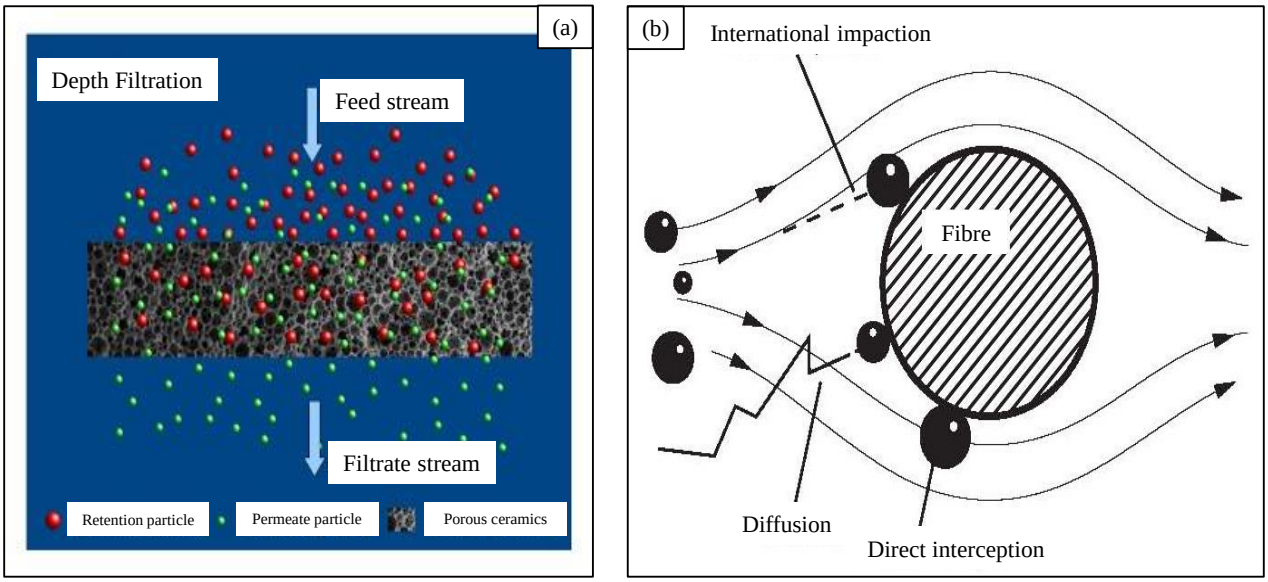

Figure 1.3 (a) Depth filtration through porous media and (b) Particle collection mechanism in a depth filtration.

However, even if a high performance depth filtration system is established, the system cannot efficiently remove microbial organisms like virus, bacteria, slime, and algae, which cause microbial fouling in the RO membrane. Moreover, some chemicals whose molecular weight are less than water molecule like ammonia cannot reject the RO membrane completely (Yoon and Lueptow, 2005). As a result, to protect the RO membrane from microbial fouling and to compensate for the low ammonia removal by the RO system, the break-point chlorination combined with an electrolysis technique is proposed as a pre-treatment technique. Electrolysis has significant advantages over other technologies, because it is simple and convenient in operation, and does not require chemical substances (Chopra et al., 2011). Figure 1.4 shows the basic principal and configuration of electrolysis in water and wastewater treatment adopted from Mollah et al. (2004). Table 1.3 shows some examples of electrochemical reduction of nitrogenous compounds with treatment efficiency at various cathode materials.

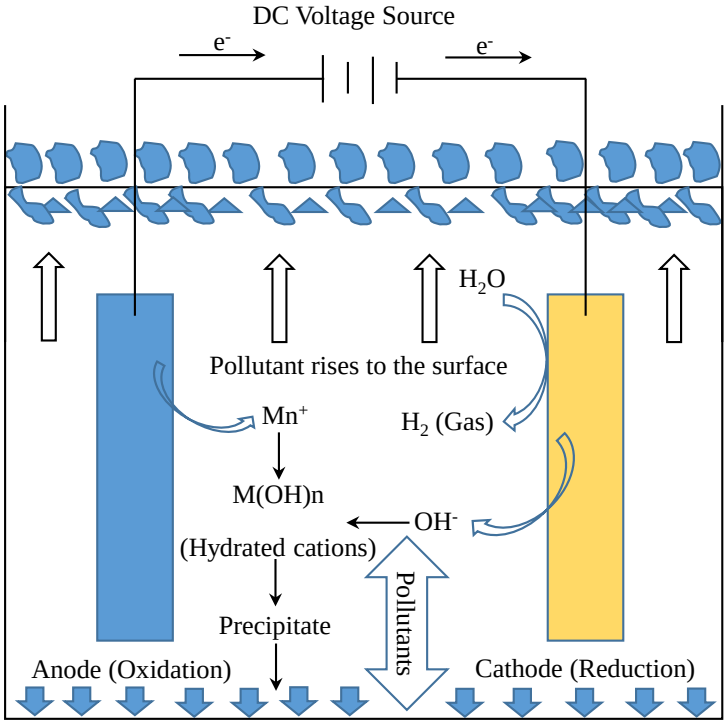

Figure 1.4 Basic principle and configuration of electrolysis in water and wastewater treatment.

Table 1.3 Some research works on electrochemical process for nitrogenous compound removal.

Name of cathode electrodes	Name of pollutants	Current density (mA/cm^2)	Contact time (minutes)	Treatment efficiency (%)	References
Nickel (Ni)	Nitrite (NO_2^-)	3.75	10	95	Salem et al., 2011.
Aluminum (Al) and Iron (Fe)	Nitrate (NO_3^-)	6-14	10-90	78-91	Pak, 2015.
Coper (Cu)/Zinc (Zn)	Nitrite (NO_2^-) and Ammonia (NH_3)	30	120	100	Wang et al., 2012.
Stainless Steel (SS)	Ammonium (NH_4^+)	15-90	360	100	Cabeza et al., 2007.
Aluminum (Al) and Iron (Fe)	Nitrite (NO_2^-), Nitrate (NO_3^-), and Ammonia (NH_3)	40-80	5	65-95	Ugurlu, 2004.

1.2 Overall Objectives in This Research

The overall objectives of this research were to develop an integrated water purification system at low-cost with easy operation and maintenance using RO membrane as a core technology. Since RO membrane is a very sophisticated technology and fouling phenomena by particle, organic and inorganic chemicals, microorganisms, and so on are the main problems in RO operation. As a result, to protect the RO membrane from them pre-treatment methods, namely, active surface-charge depth filtration and electrolysis are proposed for extending the operational life-time of the RO membrane.

Various types of conventional and unconventional pre-treatment technologies are used to protect the RO membrane from fouling, conventional pre-treatment technologies like coagulation-flocculation requires higher chemical doses, larger manpower, and high operational cost. But, unconventional pre-treatment technologies like MF, UF, and NF are also costly and suffer from fouling problems that need very frequent replacement, which increases the overall operational cost (Jamaly et al., 2014; Yamamura et al., 2007). As a result, an active surface-charge control depth filtration system will be introduce, which will be effective in SS, organic, inorganic, and micro-particles removal and the back-washing technique will help to refresh the filter media for the next operation economically. Almost all natural particles and colloids found in water are negatively charged. In such a case, controlling the surface charge of the filter media to positive will help to remove submicron particles and colloids smaller than the filter media pore size through an electro-kinetic adsorption mechanism.

In general, disinfectants like bleaching powder are used in water purification system for killing microorganisms, viruses, and bacteria or for the removal of ammonia through break-point chlorination mechanism. But, the biggest problem of adding bleaching powder is in maintaining the proper chlorination ratio and this always needs manpower to maintain and manage the operation with continuous supply of chemicals (Burch and Thomas, 1998). Moreover, excessive amount of chlorine (Cl_2) causes negative effect on RO membranes. To overcome these problems, an automatic electrolysis method will be introduce as a practical option, which will produce an exact amount of Cl_2 under the appropriate chloride ion (Cl^-) concentration and will remove the nitrogenous compounds like ammonia and microorganisms such as total coliform and general bacteria through break-point chlorination mechanism.

1.3 References

Adham, S. S., Jacangelo, J. G., Laine, J. M., (1996). Characteristics and costs of MF and UF plants. American Water Works Association., 88 (5), 22-31.

Agard, L., Alexander, C., Green, S., Jackson, M., Patel, S., Adesiyun, A., (2000). Microbial quality of water supply to an urban community in Trinidad. Journal of Food Protection., 65 (8), 1297-1303.

Alberini, A., Eskeland, G. S., Krupnick, A., McGranahan, G., (1996). Determinants of Diarrheal Disease in Jakarta. World Bank, Washington, DC, Policy Research Working Paper, WSP1568.

Bruggen, B. V. D., Vandecasteele, C., Gestel, T. V., Doyen, W., Leysen, R., (2003). A review of pressure-driven membrane process in wastewater treatment and drinking water production. Environmental Progress & Sustainable Energy., 22 (1), 46-56.

Burch, J. D., Thomas, K. E., (1998). Water disinfection for developing countries and potential for solar thermal pasteurization. Solar Energy., 64 (1-3), 87-97.

Cabeza, A., Urtiaga, A., Rivero, M., Ortiz, I., (2007). Ammonium removal from landfill leachate by anodic oxidation. Journal of Hazardous Materials., 144 (3), 715-719.

Chakravorty, B., Layson, A., (1997). Ideal feed pretreatment for reverse osmosis by continuous microfiltration. Desalination., 110 (1-2), 143-149.

Chopra, A. K., Sharma, A. K., Kumar, V., (2011). Overview of electrolytic treatment: An alternative technology for purification of wastewater. Archives of Applied Science Research., 3 (5), 191-206.

Craun, G. F., Calderon, R. L., (2001). Waterborne disease outbreaks caused by distribution system deficiencies. American Water Works Association., 93 (9), 67-75.

Daigger, G. T., Crawford, G. V., (2007). Enhancing water system security and sustainability by incorporating centralized and decentralized water reclamation and reuse into urban water management systems. Journal of Environmental Engineering Management., 17 (1), 1-10.

Dany, V., Visvanathan, C., Thanh, N. C., (2000). Evaluation of water supply systems in Phnom Penh city: A review of the present status and future prospects. International Journal of Water Resources Development., 16 (4), 677-689.

Ford, T. E., (1999). Microbiological safety of drinking water: United States and global perspectives. Environmental Health Perspectives., 107 (Suppl 1), 191-206.

Gadgil, A., (1998). Drinking water in developing countries. Annual Review of Energy and the Environment., 23, 253-286.

Gupta, V. K., Ali, I., Saleh, T. A., Nayak, A., Aqarwal, S., (2012). Chemical treatment technologies for waste-water recycling-an overview. RSC Advances., 16, 6380-6388.

Herzberg, M., Elimelech, M., (2007). Biofouling of reverse osmosis membranes: Role of biofilm-enhanced osmotic pressure. Journal of Membrane Science., 295 (1-2), 11-20.

Jamaly, S., Darwish, N. N., Ahmed, I., Hasan, S. W., (2014). A short review on reverse osmosis pretreatment technologies. Desalination., 354, 38-38.

Jarusutthirak, C., Amy, G., (2006). Role of soluble microbial products (SMP) in membrane fouling and flux decline. Environmental Science & Technology., 40 (3), 969-974.

Kelkar, P. S., Talkhande, A. V., Joshi, M. W., Andey, S. P., (2001). Water quality assessment in distribution system under intermittent and continuous modes of water supply. Journal of Indian Water Works Association., 33 (1), 39-44.

Kyessi, A. G., (2005). Community-based urban water management in fringe neighborhoods: the case of Dar es Salam, Tanzania. Habitat International., 29 (1), 1-25.

Lee, S., Ang, W. S., Elimelech, M., (2006). Fouling of reverse osmosis membranes by hydrophilic organic matter: implications for water reuse. Desalination., 187 (1-3), 33-321.

Lee, J. L., Schwab, K. J., (2005). Deficiencies in drinking water distribution systems in developing countries. Journal of Water and Health., 3 (2), 109-127.

Liikanen, R., Yli-Kuivila, J., Laukkanen, R., (2002). Efficiency of various chemical cleanings for nanofiltration membrane fouled by conventionally-treated surface water. Journal of Membrane Science., 195 (2)., 265-276.

Mermin, J. H., Villar, R., Carpenter, J., Roberts, L., Hutwagner, L., Mead, P., Ross, B., Mintz, E. D., (1999). A massive epidemic of multidrug-resistant typhoid fever in Tajikistan associated with consumption of municipal water. The Journal of Infectious Diseases., 179 (6), 1416-1422.

Mocanu, M., (2000). Well-considered investments pay off in the long run. Water supply strategy for the municipality of Targoviste, Romania., Report, Good Practice Un-Habitat Vienna.

Mollah, M. Y. A., Morkovsky, P., Gomes, J. A. G., Kesmez, M., Parga, J., Cocke, D. L., (2004). Fundamentals, present and future perspectives of electrocoagulation. Journal of Hazardous Materials., 114 (1-3), 199-210.

Pak, K. S., (2015). Factors influencing treatment of nitrate contaminated water using batch electrocoagulation process. International Journal of Current Engineering and Technology., 5 (2), 714-718.

Pandey, S. R., Jegatheesan, V., Baskaran, K., Shu, L., (2012). Fouling in reverse osmosis (RO) membrane in water recovery from secondary effluent. A review. Reviews in Environmental Science and Bio/Technology., 11 (2), 125-145.

Pearce, G. K., (2008). UF/MF pre-treatment to RO in seawater and wastewater reuse applications: a comparison of energy costs. Desalination., 222 (1-3), 66-73.

Sablani, Al-Hinai, H., Al-Obeidani, S., Al-Belushi, R., Jackson, D., (2005). Fouling of reverse osmosis and ultrafiltration membranes: A critical review: Separation Science and Technology., 39 (10), 2261-2297.

Salem, M., Chakrabarti, M. H., Hasan, D. B., (2011). Electrochemical removal of nitrate in simulated aquaculture wastewater. African Journal of Biotechnology., 10 (73), 16566-16576.

Saxena, A., Tripathi, B. P., Kumar, M., Shahi, V. K., (2009). Membrane-based techniques for the separation and purification of proteins: An overview. Advances in Colloid and Interface Science., 145 (1-2), 1-22.

Shar, A. H., Kazi, Y. F., Zardari, M., Soomro, I. H., (2007). Enumeration of total and faecal coliform bacteria in drinking water of Khairpur City, Sindh, Pakistan. Bangladesh Journal of Microbiology., 24 (2), 163-165.

Spinks, A. T., Dunstan, R. H., Harrison, T., Coombes, P., Kuczera, G., (2006). Thermal inactivation of water-borne pathogenic and indicator bacteria at sub-boiling temperatures. Water Research., 40 (6), 1326-1332.

Tam, L. S., Tang, T. W., Lau, G. N., Sharma, K. R., Chen, G. H., (2007). A pilot study for wastewater reclamation and reuse with MBR/RO and MF/RO systems. Desalination., 202 (1-3), 106-113.

Tien, C., Payatakes, A. C., (1979). Advances in deep bed filtration. AlchE Journal., 25 (5), 737-759.

Tobiason, J. E., O'Melia, C. R., (1988). Physiochemical aspects of particle removal in depth filtration. American Water Works Association., 80 (12), 54-64.

Uddin, A. F. M. A., Baten, M. A., (2011). Water supply of Dhaka city: Murky future.

Ugurlu, M., (2004). The removal of some inorganic compounds from paper mill effluents by the electrocoagulation method. G. U. Journal of Science., 17 (3), 85-99.

United Nations Environment Programme, (2002). Vital water graphics: An Overview of the State of the World's Fresh and Marine Waters. United Nations, Nirobi.

United Nations, (2006). The Millennium Development Goals Report. United Nations Department of Economic and Social Affairs., DESA.

Varbanets, M. P., Zurbrugg, C., Swartz, C., Pronk, W., (2009). Decentralized systems for potable water and the potential of membrane technology. Water Research., 43 (2), 245-265.

Wang, Y., Guo, X., Li, J., Yang, Y., Lei, Z., Zhang, Z., (2012). Efficient electrochemical removal of ammonia with various cathodes and Ti/RuO_2-Pt anode. Open Journal of Applied Sciences., 2, 241-247.

WHO and UNICEF, (2000). Global Water Supply and Sanitation Assessment Report. Iseman Creative, Washington, DC.

WHO, (2015). Burden of disease and cost-effectiveness estimates. Water Sanitation Health.

Yamamura, H., Kimura, K., Watanabe, Y., (2007). Mechanism involved in the evolution of physically irreversible fouling in microfiltration and ultrafiltration membranes used for drinking water treatment. Environmental Science & Technology., 41 (19), 6789-6794

Yoon, Y., Lueptow, R. M., (2005). Removal of organic contaminants by RO and NF membranes. Journal of Membrane Science., 261, (76-86).

Zerah, M. H., (2000). Household strategies for coping with unreliable water supplies: the case of Delhi. Habitat International., 24 (3), 295-307.

Zhu, X., Elimelech, M., (1997). Colloidal fouling of reverse osmosis membranes. Measurements and fouling mechanisms. Environmental Science & Technology., 31 (12), 3654-3662.

Chapter II
Applicability of Reverse Osmosis (RO) Membrane to Potable Water Production

2.1 Introduction

Although, water is a finite natural resource, it is possible to reuse wastewater through proper treatments. As a consequence of sustainable development, perceptions of water purification, reuse, and recycling have become indispensable for future generations (Service, 2006). Purification of contaminated water is a difficult and challenging task, because it contains a lot of unknown and complex substances. Despite of many difficulties and limitations, conventional treatment processes like activated sludge processes combined with other methods have been widely used everywhere for water treatment from the end of 19th century. Generally, these technologies show good purification efficiency in normal polluted water, but in critical situations these processes are inefficient in removing parts of hydrophobic and hydrophilic organic composites such as disinfection by-products and pharmaceutical compounds (Isaias, 2001).

In such adversely contaminated water, the application of membranes like microfiltration (MF), ultrafiltration (UF), nanofiltration (NF), and reverse osmosis (RO) can be a viable alternative solution to evaporation-based technologies in the water treatment market (Amjad et al., 1998). MF and UF are characterized by their ability to remove suspended solids (SS) or colloidal particles via a sieving mechanism based on smaller pores of the membrane than the diameter of particulate matter. MF membranes are generally considered to have a pore size over 0.1 μm and for UF membranes the pore sizes are generally within the range from 0.01-0.05 μm (Perry et al., 1997). NF and RO are classified to one of membrane processes, which are often used for the removal of dissolved contaminants. The typical range of molecular weight cutoff (MWCO) level is between 200-1,000 daltons for NF membranes and less than 100 daltons for RO membranes (Baker, 2004).

RO membranes were commercially introduced when Gulf General Atomics and Aerojet General employed the cellulose acetate membrane in a spiral wound module for water purification (Loeb and Sourirajan, 1963). Cellulose acetate membranes were the common choice for RO until the advent of thin-film composite membranes in 1972. The thin-film composite membranes have excellent hydrolytic resistances with a greater membrane stability and membrane life, superior salts and organics rejection rates, and compaction-resistant sub-layers than those of cellulose acetate membranes. In addition, most of thin-film composite membranes are made with a porous and highly permeable support such as polysulfone, which is coated with a cross-linked aromatic polyamide thin film. This coating confers the salt rejection properties of the membrane. Figure 2.1 shows the representative chemical structure of commercial polyamide membranes used as the separation layer in thin-film composite membranes (Lloyd, 1985).

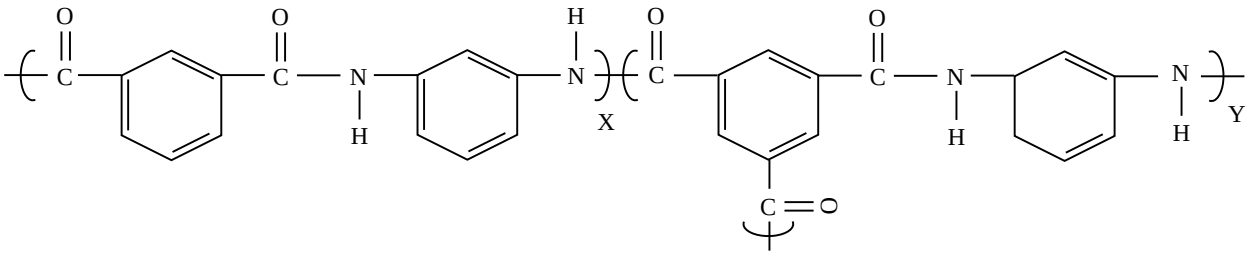

Figure 2.1 Chemical structure of commercial polyamide membranes used as the separation layer in thin-film composite membranes.

Over the years, purified water standards have become stringent and at the same time applications of RO membrane for water purification have risen significantly. Over the last half century, an emerging implementation of RO membranes in the area of water and wastewater treatment has grown very rapidly in comparison with other membranes (Gleick et al., 2006). The RO membranes are being employed extensively in the treatment of radioactive wastewater, municipal wastewater, contaminated groundwater, and wastewater from electroplating, metal finishing, pulp and paper, mining, petrochemical, textile, and food processing industries (Kamar et al., 2014). In addition, RO systems are being used in combination with other treatment processes such as an oxidation, adsorption, stripping, or biological treatment to produce a high quality product water that can be reused or discharged (Richardson et al., 2007).

Overall, the field application of RO membranes have advanced immensely in the water treatment areas due to low energy consumption, environmental friendliness, versatility, and easy operation and maintenance. At present, RO technologies are becoming more popular in the home market, because citizens are progressively more concerned about hazardous contaminants as well as non-hazardous chemicals that directly affect the physical and chemical parameters of potable water such as taste, odor, and color (Greenlee et al., 2009). Recently, ground water quality in many developing countries are found to be beyond the drinking water quality standards due to susceptible pollutants depending on agricultural byproducts, industrial, and other human activities. In such a scenario, nitrite nitrogen (NO_2^--N), nitrate nitrogen (NO_3^--N), iron (Fe^{2+}), and manganese (Mn^{2+}) are noticed in groundwater at the concentrations of nearly 10, 20, 10, and 5 mg/L, respectively (Hasan and Ali, 2010; Hossain et al., 2013; Uddin and Kurosawa, 2011). Accordingly, removing these substances using different types of conventional and unconventional water purification systems are being tried, but in many cases due to high contamination level in source water these technologies fail to purify the water at drinkable quality level (Akther et al., 2009). In this case, application of RO technology could be an alternative solution for producing high quality potable water.

However, in membrane technologies membrane fouling is one of the most significant factor that

limits its application in water and wastewater treatment. In general, fouling occurs either on the surface of the membrane or within its pores. There are mainly four types of fouling observed in RO membranes, namely bio-fouling, scaling, organic, and colloidal fouling. Bio-fouling results from the microbial contamination of feed water that produces a biofilm on the surface of the membrane. Scaling arises from the precipitation and deposition of salts on the membrane surface. Organic fouling originates from the organic substances such as humic substances, which coat over the surface of a membrane and plug the pores in the porous support layer. Colloidal fouling is mainly caused by particles, such as clay and silica accumulating on the surface of the membrane. As a whole, the deposition of unwanted materials on the membrane surface results in increasing filtration downtime and higher energy requirements for membrane operation (Le-Clech et al., 2006).

Certain fouling materials can be removed by hydraulic-means such as filter backwash or most can be removed by chemical-means such as cleaning-in-phase (CIP), or chemical cleaning. Chemical cleaning is thought to be an integral part of membrane process operation that has a profound impact on the performance and economics of membrane process (Ang et al., 2011; Mi and Elimelech, 2010). Considering the versatile application of RO membranes in the water treatment area a laboratory-based research work was executed using commercially available spiral wound polyamide thin-film composite type RO membrane. The specific objective of this research work was to investigate the optimum condition for the removal of physical, chemical, and biological indices of synthetic contaminated source water containing NO_2^-, NO_3^-, Fe^{2+}, and Mn^{2+}. In addition, the main causes of fouling and an effective method for successive permeate flux recovery techniques were also discussed for extending the operational life-time and lowering the energy requirements to reduce the water purification cost.

2.2 Materials and Methods

2.2.1 Experimental Apparatus, Ingredients, and Operational Conditions

Figure 2.2 shows the laboratory scale experimental setup, which was composed of a pressure boost pump (CDP6800, Aquatec, USA), a pressure gauge (PG-35, Copal Electronics, Japan), a spiral wound polyamide thin-film composite type RO membrane (TW30-1812-36, Dow Filmtec, USA), a water regulator (R91W-2AK-NLN, Norgren, UK), a flow meter (RK400, Kofloc, Japan), a mixer (SMT-102, AS ONE, Osaka, Japan), and a 50 liters capacity plastic bucket used as a reservoir tank. A rubber type brine seal and two O-rings were fitted in the feed and product port portion respectively, to prevent leakages while in operation. The membrane had 25.4 cm in width and 115 cm in length, which resulted in total surface area of 0.29 m^2. Table 2.1 shows a list of chemicals used to prepare the synthetic contaminated source water, test solution for salt rejection rate measurement, and back-

flushing solution for a fouled membrane.

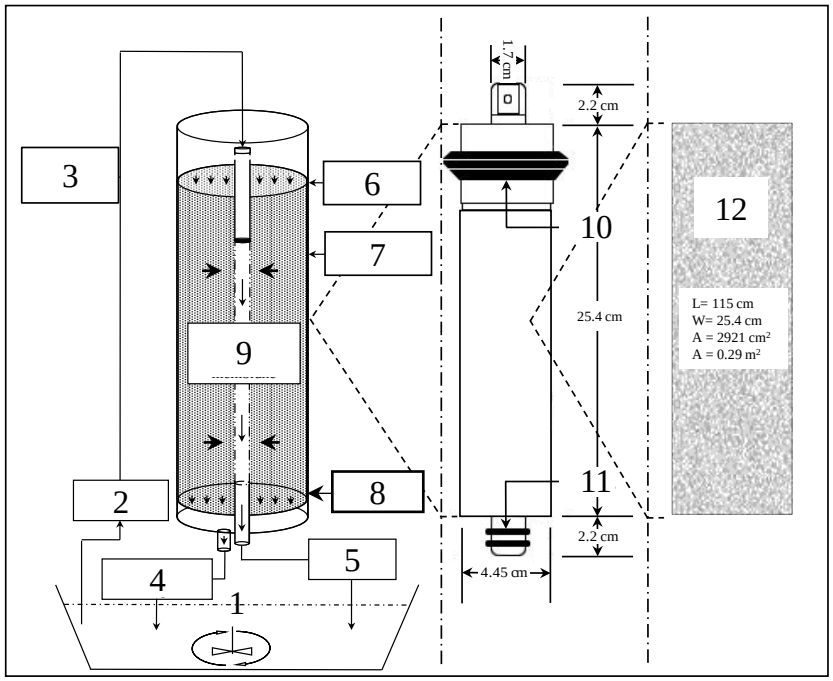

Figure 2.2 Experimental setup with reversed permeate and concentrate flow. 1: Reservoir tank, 2: Feed water pump, 3: Pressure gauge, 4: Concentrate flow regulator, 5: Permeate flow meter, 6: Water inlet portion, 7: Membrane housing, 8: Water outlet portion, 9: Membrane, 10: Brine seal, 11: O-ring, and 12: Surface area of the membrane.

These chemicals for synthetic contaminated source water were spiked into the 5-times diluted municipal wastewater in Ryukoku University at the final concentration shown in Table 2.1, though the chemicals for the test solution for rejection rate measurement and the back-flushing solution were spiked into deionized water (DW). Table 2.2 shows the synthetic contaminated source water characteristic for Run 1 (Phase I, II, and III). Table 2.3 shows the synthetic contaminated source water characteristics and operational conditions for Runs 2, 3, and 4. Table 2.4 shows the actual wastewater characteristics for Runs 5, 6, and 7. Table 2.5 shows the synthetic contaminated source water characteristics for Runs 8, 9, and 10.

Table 2.1 List of chemicals used in the experiment.

Name of chemicals	Concentrations	Functions
Sodium nitrite ($NaNO_2$)	49.25 mg/L (NO_2^--32.84 mg/L)/(NO_2^--N=10 mg/L)	Source of nitrite ion
Potassium nitrate (KNO_3)	144.43 mg/L (NO_3^--88.53 mg/L)/(NO_3^--N=20 mg/L)	Source of nitrate ion
Ferrous (II) sulfate heptahydrate ($FeSO_4.7H_2O$)	49.79 mg/L (Fe^{2+}-10 mg/L)	Source of ferrous ion
Manganese (II) chloride tetrahydrate ($MnCl_2.4H_2O$)	18.01 mg/L (Mn^{2+}-5 mg/L)	Source of manganese ion
Sodium chloride (NaCl)	2,000 (mg/L)	Used to check the salt rejection rate
Sodium lauryl sulfate ($CH_3(CH_2)_{11}OSO_3Na$)	1,000 (mg/L)	Used to backwash the fouled membrane
Sodium hydroxide (NaOH)	1,000 (mg/L)	Used to backwash the fouled membrane
Citric acid monohydrate ($C_6H_8O_7.H_2O$)	10 mM	Used to backwash the fouled membrane

Table 2.2 Synthetic contaminated source water characteristics of Run 1.

Runs	SS (mg/L)	Turbidity (mg/L-kaolin)	EC (μS/cm)	Color (Pt-Co)	Fe^{2+} (mg/L)	Mn^{2+} (mg/L)	Cl^- (mg/L)	NO_2^- (mg/L)	NO_3^- (mg/L)	NH_4^+ (mg/L)	BOD (mg/L)	COD (mg/L)	TC (CFU/mL)
Run 1 (Phase I)	100	197	480	190	9.14	5.13	36.47	41.20	66.15	4.90	63	89	122,000
Run 1 (Phase II)	16	36	430	170	8.17	6.46	28.35	38.16	80.67	5.49	49	102	46,333
Run 1 (Phase III)	42	69	380	140	7.32	5.13	30.10	29.27	82.37	3.01	75	128	29,333

EC=Electrical Conductivity; TC=Total Coliform.

Table 2.3 Synthetic contaminated source water characteristics and operational conditions of Runs 2, 3, and 4.

Runs	Operating days	SS (mg/L)	Permeate flux (L m^{-2} h^{-1})	Turbidity (mg/L-kaolin)	EC (μS/cm)	Color (Pt-Co)	Fe^{2+} (mg/L)	Mn^{2+} (mg/L)	Cl^- (mg/L)	NO_2^- (mg/L)	NO_3^- (mg/L)	NH_4^+ (mg/L)	BOD (mg/L)	COD (mg/L)	TC (CFU/mL)
Run 2	0	32	17.17	36	470	230	5.61	5.51	30.42	38.49	99.94	0.98	69.46	154.74	98,667
	1	2	14.07	5	470	12	0.29	5.45	31.76	42.68	108.89	1.48	33.66	88.42	12,000
	2	0	13.66	1	510	8	0.09	5.78	34.05	43.60	108.56	3.54	10.00	29.83	4,033
	3	0	13.45	0	510	8	0.06	5.59	34.01	46.87	116.42	2.95	4.69	25.39	1,700
	4	0	13.24	0	510	8	0.06	5.74	34.64	45.30	112.97	3.24	3.88	32.61	331
	5	0	13.24	0	580	7	0.06	5.83	37.35	48.64	121.63	3.85	3.47	31.50	325
	6	0	13.24	0	570	9	0.03	5.93	37.11	53.01	144.18	4.83	3.06	34.28	307
Run 3	0	0	16.14	69	740	130	10*	5.00	33.38	36.47	79.95	38.84	31.82	90.68	N. A.
	1	0	16.14	N. A.	N. A.	N. A.	20*	N. A.	N. A.	N. A.	N. A.	N. A.	N. A.	N. A.	N. A.
	2	0	16.14	N. A.	N. A.	N. A.	40*	N. A.	N. A.	N. A.	N. A.	N. A.	N. A.	N. A.	N. A.
	3	0	14.48	N. A.	N. A.	N. A.	80*	N. A.	N. A.	N. A.	N. A.	N. A.	N. A.	N. A.	N. A.
	4	0	14.48	N. A.	N. A.	N. A.	0.0*	N. A.	N. A.	N. A.	N. A.	N. A.	N. A.	N. A.	N. A.
	5	0	14.48	N. A.	N. A.	N. A.	0.0*	N. A.	N. A.	N. A.	N. A.	N. A.	N. A.	N. A.	N. A.
	6	0	14.07	9	1560	30	7.76	5.74	42.53	0.62	99.69	36.27	16.61	39.47	N. A.
Run 4	0	0	14.07	2	290	23	0.94	5.93	32.13	36.62	91.02	15.66	32.23	74.25	N. A.
	1	0	14.07	5	240	13	0.09	6.12	31.63	36.51	98.86	14.16	14.69	43.25	N. A.
	2	0	14.07	0	390	9	0.03	6.53	34.38	37.10	116.77	22.39	14.28	29.15	N. A.
	3	0	14.07	0	640	7	0.02	6.69	32.82	35.39	111.83	22.93	3.67	23.15	N. A.

EC=Electrical Conductivity; N. A. : Not Analyzed; *The spiked Fe concentration.

Table 2.4 Actual wastewater characteristics of Runs 5, 6, and 7.

Runs	SS (mg/L)	Turbidity (mg/L-kaolin)	EC (μS/cm)	Color (Pt-Co)	Fe^{2+} (mg/L)	Mn^{2+} (mg/L)	Cl^- (mg/L)	NO_2^- (mg/L)	NO_3^- (mg/L)	NH_4^+ (mg/L)	BOD (mg/L)	COD (mg/L)	TC (CFU/mL)
Run 5	300	238	410	260	0.0	0.0	75.10	0.0	0.0	41.92	610	1,372	1,386,667
Run 6	136	298	960	220	0.0	0.0	118.68	0.0	0.0	34.86	168	742	121,333
Run 7	46	256	890	270	0.0	0.0	134.08	0.0	0.0	16.77	181	782	N. A.

EC=Electrical Conductivity; N. A. : Not Analyzed.

Table 2.5 Synthetic contaminated source water characteristics of Runs 8, 9, and 10.

Runs	Operating time (Hours)	SS (mg/L)	EC (µS/cm)	Color (Pt-Co)	Fe^{2+} (mg/L)
Run 8	0	0.0	570	220	144.15
	16	0.0	590	14	23.91
Run 9	0	0.0	670	650	125.31
	16	0.0	650	16	26.89
Run 10	0	0.0	610	400	128.95
	21	0.0	620	16	19.22
EC=Electrical Conductivity.					

2.2.2 Experimental Procedure

The Run 1 was conducted to observe the relation between permeate flux and transmembrane pressure (TMP) along with permeate water quality in three phases at the SS concentration of 100 mg/L for phase I, 16 mg/L for phase II, and 42 mg/L for phase III, respectively. Runs 2, 3, and 4 were conducted to observe the effect of SS, Fe colloids, and dissolved matter on membrane fouling, respectively. Runs 5, 6, and 7 were conducted to observe the effect of back-flushing on permeate flux recovery of a fouled membrane mainly fouled by organic aggregates. Runs 8, 9, and 10 were conducted to observe the effect of back-flushing on permeate flux recovery of a fouled membrane mainly fouled by Fe colloids.

Before each experimental run, a new RO membrane was inserted into the membrane housing. Then the permeate port and concentrate port was connected properly following the Figure 2.2. After that, a new membrane was washed using DW for 30 minutes and then used for the experiments. In the case of Runs 1, 5, 6, and 7 permeate water was discharged, but concentrate water was returned into the reservoir tank. However, in the case of Runs 2, 3, 4, 8, 9, and 10 both permeate water and concentrate water were returned into the reservoir tank as shown in Figure 2.2. While running the experiments a mixer was continuously operated at 250 rpm to mix the feed water homogeneously.

After experimental run was finished, permeate flux recovery experiments were conducted in Runs 5-10 using the same configuration of Figure 2.2, but opposing the flow direction. In this study, DW, sodium lauryl sulfate ($CH_3(CH_2)_{11}OSO_3Na$), sodium hydroxide (NaOH), or citric acid monohydrate ($C_6H_8O_7.H_2O$) solutions was used as feed water, which was flowed from the concentrate port, but blocking the permeate port for the back-flushing of a fouled membrane at the flow rate of 1175±50 mL/min, and at the TMP of 17.50±2.89 kPa. Here, DW was considered as hydraulic-means to remove the physical clogging materials that deposited on the surface of the membrane. Surfactants

like $CH_3(CH_2)_{11}OSO_3Na$ was considered for its emulsifying and dispersion characteristics. Since surfactants are compounds that have both hydrophilic and hydrophobic structures, they can form micelles with fat, oil, and proteins in water. A caustic chemical of NaOH was considered for its hydrolyzation and solubilization characteristics that was expected to remove organic matter along with microorganisms. $C_6H_8O_7.H_2O$ was considered for its solubilization characteristics, which was expected to remove inorganic foulants like Fe oxides. All the runs were performed under air-conditioned room temperature at 25ºC. For sampling and analysis effluent was collected from the permeate port using laboratory grade plastic bottles.

2.2.3 Analytical Methods

The pH, dissolved oxygen (DO), and electrical conductivity (EC) were measured with a pH meter (B-212, Horiba, Japan), a DO meter (LDO, HQ10, Hach, USA), and an EC meter (Twin cond, B-173, Horiba, Japan), respectively. Turbidity and color were measured with a digital turbidity/color meter (Aqua Doctor, WA-PT-4DG, Kyoritsu Chemical-Check Lab, Japan). The concentrations of chloride (Cl^-), NO_2^-, and NO_3^- were determined by ion chromatography (PIA-1000, Shimadzu, Japan), and NH_4^+ was determined by phenate method (4500-NH_3 F) (Rice et al., 2012). The Fe^{2+} was measured by phenanthroline method (3500-Fe B) (Rice et al., 2012) and Mn^{2+} was measured by inductively coupled plasma spectrometry (ICP, Optima 5300DV, PerkinElmer, USA). Total coliform (TC) was measured by test papers for TC (Sibata, Saitama, Japan) using the colony count, most-probable-number (MPN) method with thermostat incubator (CALBOX, CB-101, Sibata, Saitama, Japan). Biochemical oxygen demand (BOD) was measured by 5-day BOD test (5210 B) (Rice et al., 2012) and chemical oxygen demand (COD) was measured by closed reflux colorimetric method (5220 D) (Rice et al., 2012). DW of EC less than 1 μS/cm was used for the dilution and preparation of standard solution, as obtained from a water purification system (Autostill, WA5000, Yamato, Japan).

2.3 Results and Discussion

2.3.1 Effect of Permeate Flux on Transmembrane Pressure (TMP) and Water Quality Assessment of Reverse Osmosis (RO) Membrane

In this experimental study, the RO system was operated one after another in three phases using a new membrane in each time. In the 1st phase, it was operated for four hours at an initial permeate flux of 6.21 L m^{-2} h^{-1}, transmembrane pressure (TMP) of 354 kPa (Figure 2.3 (a)), and SS concentration of influent was 100 mg/L (Table 2.2). Here, flux was calculated using the equation 1:

$$\text{Flux (L m}^{-2}\text{ h}^{-1}) = \frac{Q}{A} \qquad (1)$$

Where, Q is the filtration flow rate (L/h), and A is the effective surface area of the membrane (m^2). In the 2nd phase, it was operated for an hour at an initial permeate flux of 9.31 L m^{-2} h^{-1}, TMP of 407 kPa (Figure 2.3 (b)), and SS concentration of influent was 16 mg/L (Table 2.2). In the 3rd phase, it was also operated for an hour at an initial permeate flux of 12.41 L m^{-2} h^{-1}, TMP of 480 kPa (Figure 2.3 (c)), and SS concentration of influent was 42 mg/L (Table 2.2). The permeate water volume in 1st, 2nd, and 3rd phase was 7.20, 2.70, and 3.60 liters, respectively. The synthetic water in all of three phases had the dissimilar SS concentrations, but the changes in TMP and permeate flux over time were not remarkable. A slight TMP increasing phenomenon was observed in 1st phase from 354 to 363 kPa (Figure 2.3 (a)). A permeate flux decrease and TMP increase phenomenon is usually observed during the membrane process (Le-Clech et al., 2006). But, in this experiment both TMP and permeate flux was found to be almost constant at initial and ending stage in 2nd and 3rd phase, respectively. This might be due to relatively short operational time of the experiments.

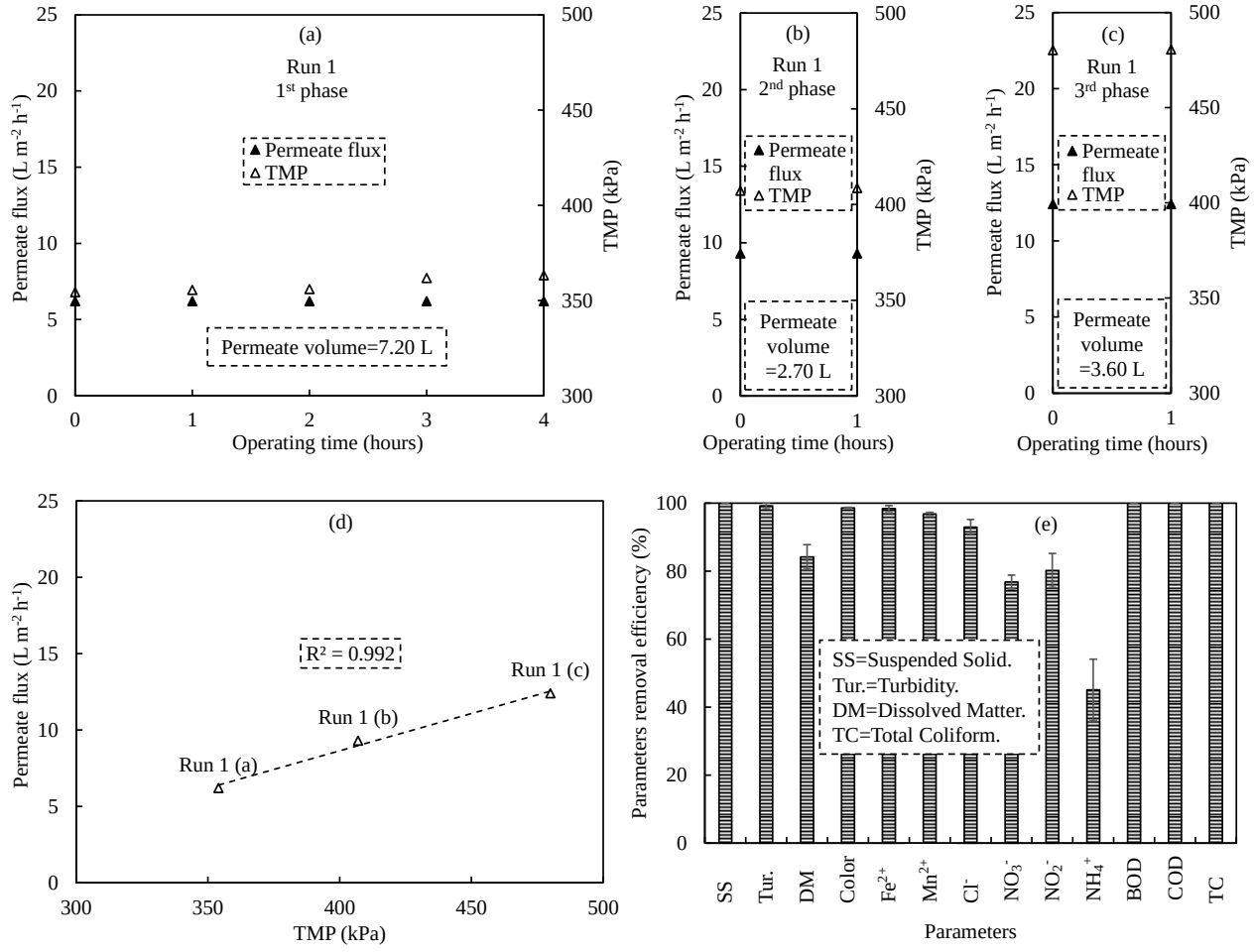

Figure 2.3 Experimental results of RO treatments under different TMP (Run 1). (a), (b), and (c) permeate flux and TMP changes over time, (d) Relationship between permeate flux and TMP, and (e) Removal efficiency of each index from Run 1 (a), (b), and (c). The error bars depict the unbiased standard deviation.

Figure 2.3 (d) shows the relationship between the permeate flux and TMP. Here, the permeate flux

was found to be linearly increased with the increasing of TMP at R^2 value of 0.992. Vrijenhoek et al. (2001) reported the similar result of linear relationship between permeate flux and TMP in a RO filtration system without fouling, which accords with my present experimental study.

The permeate water quality of RO was tested using synthetic contaminated source water shown in Table 2.2 (Run 1). Figure 2.3 (e) shows the effluent characteristics of Run 1. In this study, SS, TC, BOD, and COD were removed completely (100%) and the removal efficiencies of turbidity and color were found to be 99%, but dissolved matter removal efficiency was found to be 84% which was calculated in terms of EC. Here, cations of Fe^{2+} and Mn^{2+} and anions of Cl^-, NO_2^-, and NO_3^- were removed at the rate of 98%, 97%, 93%, 80%, and 77%, respectively. Thus, the NO_2^-, and NO_3^- rejection rates were slightly lower than those of other ions. The similar rejection tendencies of these indices in RO filtration system were experienced by Chianese et al. (1999), Comerton et al. (2005), and Fakhru'l-Razi et al. (2010), respectively. However, in comparison with other runs ammonium (NH_4^+) removal efficiency was found to be much less than that of other indices, and it was calculated to be 45%. In this case, the lower NH_4^+ removal efficiency was thought to be due to less molecular weight of NH_4^+ than that of other solutes. As a result, it may easily passed through the RO membrane and led to lower rejection rate. Funston et al. (2002) reported the similar experimental results in their study.

2.3.2 Influence of Organic Aggregates, Iron Colloids, and Dissolved Matter on Membrane Fouling

In the following experimental study, the RO system was operated using 20 liters of synthetic contaminated source water as influent (Figure 2.2). The operational period was 7 days for Runs 2 and 3, and 4 days for Run 4. Figure 2.4 (a) shows the effect of SS on membrane fouling in Run 2. The experiment was started at an initial permeate flux of 17.17 L m^{-2} h^{-1} and initial SS of synthetic contaminated source water was 32 mg/L, which was mainly composed of organic aggregates from municipal wastewater (Table 2.3). After 2 days operation, SS of the influent was found to be 0 mg/L and permeate flux decreased to 13.66 L m^{-2} h^{-1}. The permeate flux gradually decreased up to 4 days, and then it reached a constant level at 13.24 L m^{-2} h^{-1}. Since, both permeate and concentrate were returned to reservoir tank in this experiment, it was confirmed that the SS was accumulated in the membrane unit.

In the case of Run 3, SS of synthetic contaminated source water was completely removed using a glass fiber filter with 1μm particle rejection (GF/B, Whatman, Japan). Then, NO_2^-, NO_3^-, Fe^{2+}, and Mn^{2+} ions were spiked into filtrated synthetic contaminated source water (Table 2.3). Figure 2.4 (b)

shows the behavior of Fe colloids on membrane fouling. The experiment was started at an initial permeate flux of 16.14 L m^{-2} h^{-1}. At the operation time of 0, 1, 2, and 3 days Fe^{2+} was spiked into synthetic contaminated source water at the final concentration of 10, 20, 40, and 80 mg/L, respectively, but the permeate flux remained constant as initial (16.14 L m^{-2} h^{-1}) up to 2 days operation. When Fe^{2+} was spiked into the synthetic contaminated source water at the final concentration of 80 mg/L at 3 days operation, the permeate flux decreased to 14.48 L m^{-2} h^{-1}. Then, the run was continued in operation up to 6 days without addition of Fe^{2+}. The permeate flux was remained constant at 14.48 L m^{-2} h^{-1} from 3 to 5 days operation, but it slightly dropped to 14.07 L m^{-2} h^{-1} at the operation time of 6 days. Since both permeate and concentrate were returned to reservoir tank, the drop in the Fe concentration of 7.76 mg/L at 6 days indicates the accumulation of Fe colloids in the membrane unit as similar to the SS accumulation in Run 2.

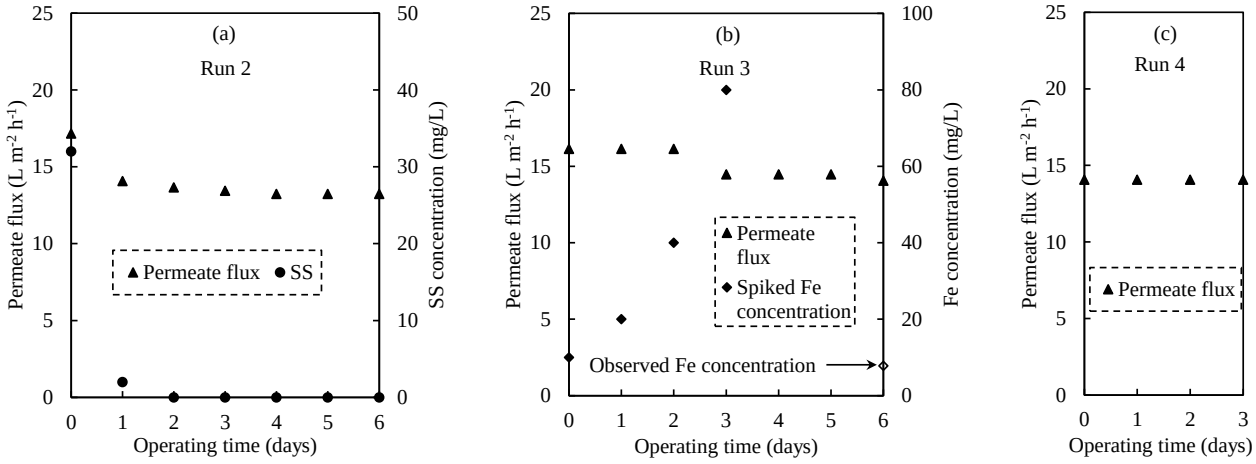

Figure 2.4 (a) Experimental results of RO treatments using normal synthetic contaminated source water (Run 2), (b) Synthetic contaminated source water with NO_2^-, NO_3^-, Fe^{2+}, and Mn^{2+} addition after SS removal (Run 3), and (c) Synthetic contaminated source water with NO_2^-, NO_3^-, Fe^{2+}, and Mn^{2+} addition before SS removal (Run 4).

In the case of Run 4, NO_2^-, NO_3^-, Fe^{2+}, and Mn^{2+} ions were spiked into the synthetic contaminated source water. Then, SS was completely removed using a glass fiber filter with 1μm particle rejection (GF/B, Whatman, Japan). As a result, the initial Fe^{2+} concentration in synthetic contaminated source water of Run 4 was found to be 0.94 mg/L (Table 2.3). This indicates that spiked Fe^{2+} was rapidly transformed into Fe colloids according to the equations (2) and (3) in synthetic contaminated source water and most of the Fe was removed by the microfiltration.

$$4Fe^{2+} + O_2 + 4H^+ \rightarrow 4Fe^{3+} + 2H_2O \quad (2)$$

$$Fe^{3+} + 3OH^- \rightarrow Fe(OH)_3\downarrow \quad (3)$$

Figure 2.4 (c) shows the influence of dissolved matter on membrane fouling. Here, the experiment was started at an initial permeate flux of 14.07 L m^{-2} h^{-1} with feed water EC of 290-640 μS/cm

(Table 2.3). The permeate flux remained constant at initial value (14.07 L m^{-2} h^{-1}) during the consecutive 4 days operational period (Figure 2.4 (c)). This results strongly supports that dissolved matter did not take part in membrane fouling.

2.3.3 Impact of In-situ Back-flushing on Permeate Flux Recovery of Fouled Membranes

As a result of Runs 2-4, the main fouling components were SS mainly composed of organic aggregates (Run 2) and Fe colloids (Run 3). To recover the permeate flux of fouled membranes, permeate flux recovery experiments were demonstrated on Runs 5-10, where Runs 5-7 were fouled by organic aggregates and Runs 8-10 were fouled by Fe colloids. The equation 4 was used to calculate the permeate flux recovery rate of a fouled membrane:

$$\text{Permeate flux recovery rate (\%)} = \frac{\text{Permeate flux after cleaning at DW}}{\text{Initial permeate flux at DW}} \times 100 \quad (4)$$

The membranes of Runs 5, 6, and 7 were fouled using actual wastewater shown in Table 2.4, and the membranes of Runs 8, 9, and 10 were fouled using synthetic contaminated source water shown in Table 2.5. After every step of permeate flux recovery experiment the salt rejection rate was checked using the NaCl solution (pH 6.2) at the NaCl concentration of 2,000 mg/L (EC=4,400 μS/cm) (Table 2.1). The salt rejection rate was calculated as follows:

$$\text{Salt rejection rate (\%)} = \frac{\text{Feed water EC} - \text{Permeate water EC}}{\text{Feed water EC}} \times 100 \quad (5)$$

Figure 2.5 (a) shows the permeate flux recovery phenomenon of Run 5 by back-flushing with DW (pH 7.1). An initial permeate flux of the membrane of 19.03 L m^{-2} h^{-1} was recorded with respect to DW. Then, it was used for the fouling experiment using actual wastewater with SS concentration of 300 mg/L and TMP of 320 kPa (Table 2.4). After 16 hours operation the membrane was fouled and final permeate flux was observed 2.07 L m^{-2} h^{-1} with respect to DW. Then, the fouled membrane was used for the permeate flux recovery experiment. Here, in the 1st step the fouled membrane was back-flushed with DW for 30 minutes. As a result, the permeate flux was recovered to 5.38 L m^{-2} h^{-1} that was equivalent to the permeate flux recovery rate of 28.3%. Next, in the 2nd step it was again back-flushed with DW for 2 hours at the same condition. The permeate flux was further improved to 6.62 L m^{-2} h^{-1} that was equivalent to the permeate flux recovery rate of 34.8%. The subsequent back-flushing with DW in the 3rd step for 2 hours, permeate flux further slightly improved to 7.03 L m^{-2} h^{-1} that was equivalent to the permeate flux recovery rate of 37.0%. However, additional back-flushing with DW in the 4th step for 2 hours were not effective in permeate flux recovery rate. The final salt rejection rate was found to be 92.7%.

Figure 2.5 (b) shows the permeate flux recovery phenomenon of Run 6 by back-flushing with DW followed by sodium lauryl sulfate solution (pH 6.2). An initial permeate flux of the membrane of 14.07 L m^{-2} h^{-1} was recorded with respect to DW. After that, it was used for the fouling experiment using actual wastewater with SS concentration of 136 mg/L and TMP of 370 kPa (Table 2.4). After 18 hours operation the membrane was fouled and permeate flux dropped to 5.79 L m^{-2} h^{-1}. Then, the fouled membrane was used for the permeate flux recovery experiment. Here, in the 1st step the fouled membrane was back-flushed with DW for 30 minutes. As a result, the permeate flux increased to 6.62 L m^{-2} h^{-1} that was equivalent to the permeate flux recovery rate of 47.1%. In the 2nd step it was again back-flushed with DW for 30 minutes at the same condition. Then, the permeate flux was further improved to 7.86 L m^{-2} h^{-1} that was equivalent to the permeate flux recovery rate of 55.9%. However, when it was back-flushed with sodium lauryl sulfate solution at the concentration of 1,000 mg/L in the 3rd step for 5 minutes and 4th step for 20 minutes sequentially, permeate flux decreased to 7.03 and 4.55 L m^{-2} h^{-1}, respectively. Therefore, sodium lauryl sulfate solution was thought to be an ineffective chemical in permeate flux recovery of fouled membrane with organic aggregates. The interaction between the membrane and the surfactant is mainly dominated by hydrophilic or hydrophobic interaction. Since the membrane used in this research was hydrophilic, a hydrophilic head of the surfactant was preferable adhered to the membrane surface, and a hydrophobic tail was oriented towards the aquatic phase. This arrangement makes the membrane in a hydrophobic coating condition and influence on decrease in permeate flux (Louie et al., 2006). After that, this fouled membrane was back-flushed with NaOH solution (pH 12.4) at the concentration of 1,000 mg/L for 30 minutes and permeate flux recovered to 8.28 L m^{-2} h^{-1} and salt rejection rate was found to be 97.6%. Then, this recovered membrane was applied for the second time in the Run 7.

Figure 2.5 (c) shows the permeate flux recovery phenomenon of Run 7 by back-flushing with DW and NaOH solution. An initial permeate flux of this membrane was considered to be the same as Run 6, namely 14.07 L m^{-2} h^{-1} with respect to DW. After that, it was used for the fouling experiment using actual wastewater with SS concentration of 46 mg/L and TMP of 390 kPa (Table 2.4). After 16 hours operation the membrane was fouled and permeate flux decreased to 5.17 L m^{-2} h^{-1} with respect to DW. Then, the fouled membrane was used for the permeate flux recovery experiment. Here, in the 1st step the fouled membrane was back-flushed with DW for 30 minutes. As a result, the permeate flux was observed to 6.21 L m^{-2} h^{-1} that was equivalent to the permeate flux recovery rate of 44.1%. In the 2nd step it was back-flushed with NaOH solution at the concentration of 1,000 mg/L for 2 hours and permeate flux resulted in 10.34 L m^{-2} h^{-1} that was equivalent to the permeate flux recovery rate of 73.5%. The subsequent back-flushing with NaOH solution in the 3rd step for

2 hours further improved the permeate flux to 11.17 L m^{-2} h^{-1} that was equivalent to the permeate flux recovery rate of 79.4%.

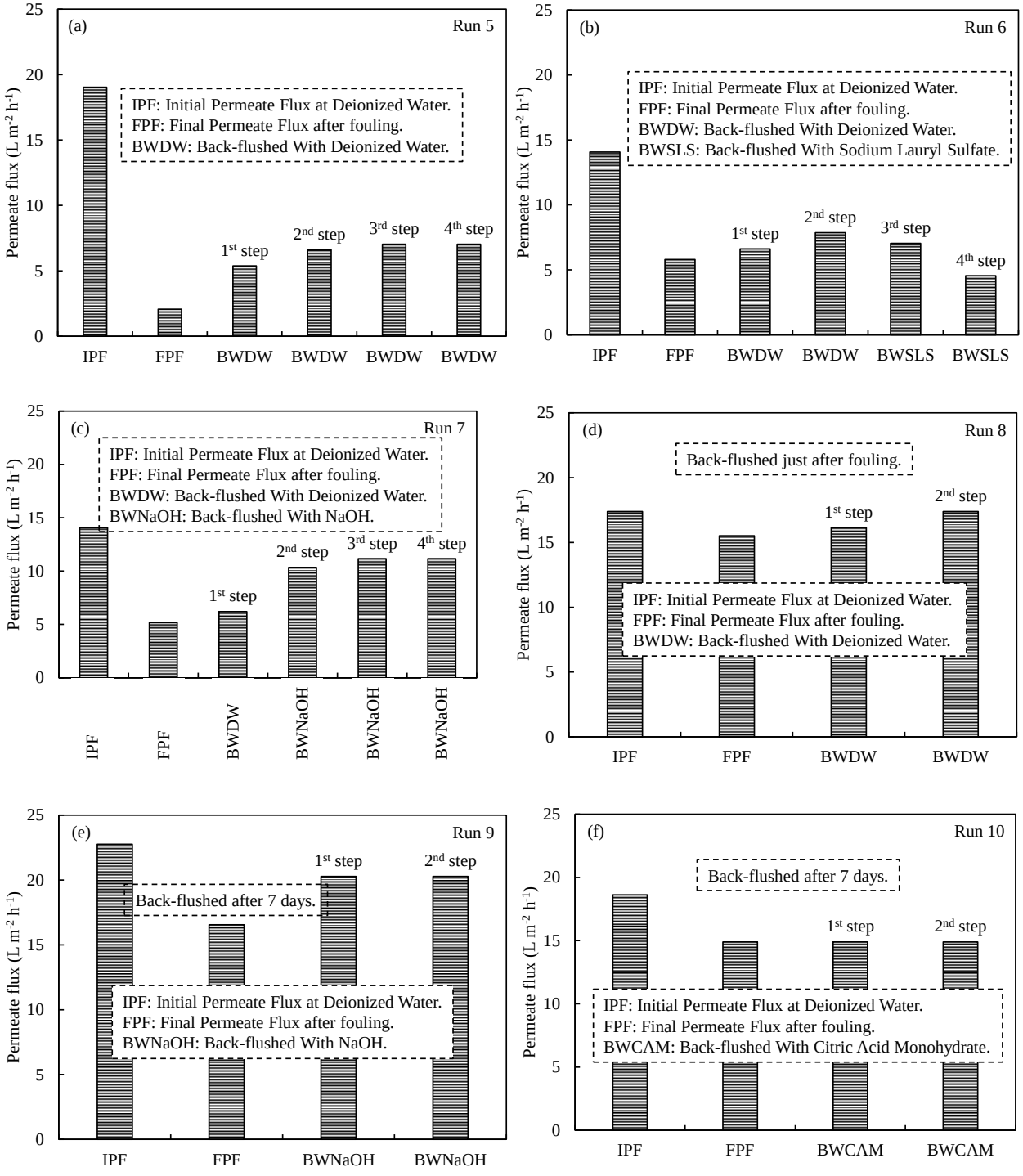

Figure 2.5 Permeate flux changes by each permeate flux recovery operation. (a) Back-flushing by DW (Run 5), (b) Back-flushing by DW followed by sodium lauryl sulfate (Run 6), (c) Back-flushing by DW followed by NaOH (Run 7), (d) Back-flushing by DW just after fouling (Run 8), (e) Back-flushing after 7 days by NaOH (Run 9), and (f) Back-flushing after 7 days by citric acid monohydrate (Run 10). The RO membranes for Runs 5-7 were mainly fouled by organic aggregates in actual wastewater, but that for Runs 8-10 were mainly fouled by Fe colloids in synthetic contaminated source water.

However, additional back-flushing with NaOH solution at the 4th steps for 2 hours were not effective in permeate flux recovery of the membrane and the final salt rejection rate was found to be 98.0%.

Figure 2.5 (d) shows the permeate flux recovery phenomenon of Run 8 by back-flushing with DW just after fouling. An initial permeate flux of the membrane of 17.38 L m^{-2} h^{-1} was recorded with respect to DW. Then, it was used for the fouling experiment using synthetic contaminated source water with the Fe^{2+} concentration of 144 mg/L and TMP of 326 kPa (Table 2.5). After 16 hours operation the membrane was fouled and the permeate flux of 15.52 L m^{-2} h^{-1} with respect to DW was observed. Then, the fouled membrane was used for the permeate flux recovery experiment. In the 1st step it was back-flushed with DW for 30 minutes and the permeate flux was measured to be 16.14 L m^{-2} h^{-1} that was equivalent to the permeate flux recovery rate of 92.8%. Next, in the 2nd step it was again back-flushed with DW for 30 minutes and permeate flux recovered to 17.38 L m^{-2} h^{-1} that was equivalent to the permeate flux recovery rate of 100% and last of all, salt rejection rate was found to be 93.0%.

Figure 2.5 (e) shows the permeate flux recovery phenomenon of Run 9 by back-flushing with a NaOH solution at the concentration of 1,000 mg/L (pH 12.4). An initial permeate flux of the membrane of 22.76 L m^{-2} h^{-1} was recorded with respect to DW. Then, it was used for the fouling experiment using the synthetic contaminated source water with the Fe^{2+} concentration of 125 mg/L and TMP of 400 kPa (Table 2.5). After 16 hours operation the filtration was stopped and the membrane was kept on the experimental setup for 7 days to mature the fouling by Fe colloids. After maturation the permeate flux of 16.55 L m^{-2} h^{-1} with respect to DW was observed. Then, the fouled membrane was used for the permeate flux recovery experiment. In the 1st step it was back-flushed with the NaOH solution for 30 minutes and the permeate flux was measured to be 20.28 L m^{-2} h^{-1} that was equivalent to the permeate flux recovery rate of 89.1%. Next, in the 2nd step an additional back-flushing with NaOH for 30 minutes was not effective in permeate flux recovery. The final salt rejection rate was found to be 87.6%.

Figure 2.5 (f) shows the permeate flux recovery phenomenon of Run 10 by back-flushing with 10 mM citric acid monohydrate (pH 1.5). An initial permeate flux of the membrane of 18.62 L m^{-2} h^{-1} was recorded with respect to DW. Then, it was used for fouling experiment using synthetic contaminated source water with the Fe^{2+} concentration of 129 mg/L and TMP of 372 kPa (Table 2.5). After 21 hours operation the filtration was stopped and the membrane was kept on the experimental setup like Run 9 for 7 days to mature the fouling by Fe colloids. After the maturation the permeate flux of 14.90 L m^{-2} h^{-1} was observed with respect to DW. Then, the fouled membrane

was used for the permeate flux recovery experiment. The membrane was back-flushed 2 times with 10 mM citric acid monohydrate solution for each 30 minutes, but it was not effective in permeate flux recovery. Therefore, the citric acid monohydrate solution was thought to be an ineffective chemical in permeate flux recovery of fouled membrane with matured Fe colloids. The final salt rejection rate was found to be 70.0%.

In this study, the salt rejection rates in Runs 9 and 10 were found to be less than that of other runs. Here, it is noticeable that RO membranes of Runs 9 and 10 were found to be still fouled by Fe colloids after back-flushing with NaOH and citric acid monohydrate solution. In this case, several factors may influence in salt rejection rate such as the presence of Fe colloids in the membrane, applied pressure, cross flow rate, and ionic concentration in the solution (Kim and Hoek, 2005; Lee et al., 2010). Here, after back-flushing the remaining amount of Fe colloids at the membrane surface of Runs 9 and 10 hindered the back diffusion of solute from the membrane surface to the bulk solution that resulted in lower salt rejection rate. Similar result was experienced by Ng and Elimelech (2004), which supports the above discussion.

Figure 2.6 shows the relationship between the SS concentration of influent and the fouled flux. Here, operational time for fouling the membranes of Runs 5, 6, and 7 were 16, 18, and 16 hours, respectively. Besides, the SS concentrations in influent of Runs 5, 6, and 7 were 300, 136, and 46 mg/L, respectively. From the Figure 2.6 it is found that the fouled flux was linearly increased with the increasing of SS concentration at the R^2 value of 0.996.

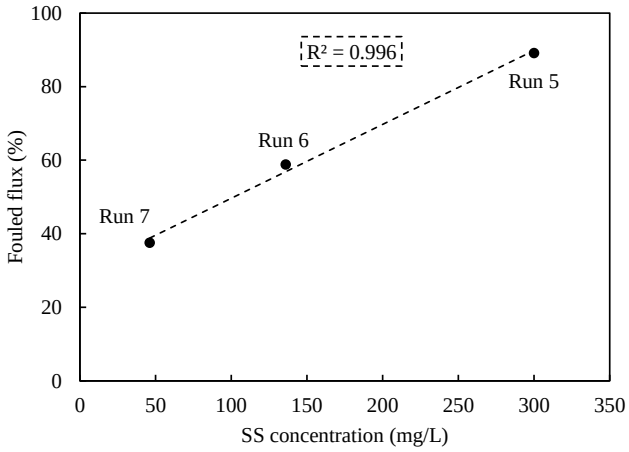

Figure 2.6 Relationship between the SS concentration in influent and fouling characteristics of a membrane, where the initial permeate flux of the Runs 5, 6, and 7 were 19.03, 14.07, and 14.07 L m^{-2} h^{-1}, respectively.

Figure 2.7 summarizes the permeate flux recovery rates of fouled membranes using different back-flushing ingredients. In a series of permeate flux recovery experiments the effectiveness of DW,

sodium lauryl sulfate, NaOH, and citric acid monohydrate solutions on permeate flux recovery rates on fouled membranes were examined, in which Runs 5, 6, and 7 were mainly fouled by organic aggregates and Runs 8, 9, and 10 were fouled by Fe colloids.

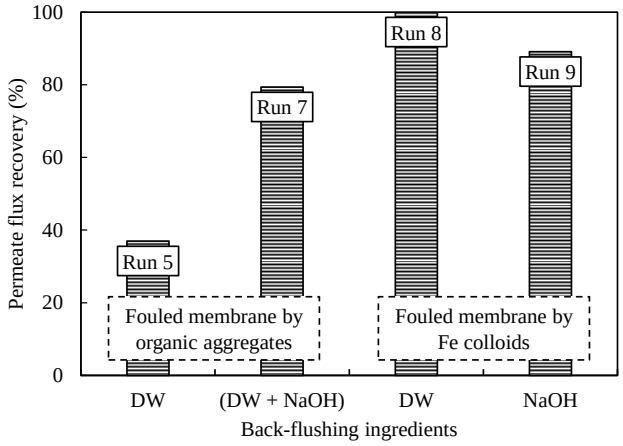

Figure 2.7 Permeate flux recovery rates of organic aggregates and Fe colloids fouled membranes by back-flushing with different back-flushing solutions, where the initial permeate flux of the Runs 5, 7, 8, and 9 were 19.03, 14.07, 17.38, and 22.76 L m^{-2} h^{-1}, respectively.

In this study, it was revealed that the single use of DW reached the permeate flux recovery rate of 37.0% for the membrane mainly fouled by organic aggregates (Figure 2.7, Run 5). But, the sodium lauryl sulfate solution showed an anti-behavior on permeate flux recovery of fouled membrane with organic aggregates (Figure 2.5 (b), Run 6). The DW followed by NaOH solution showed a better performance in permeate flux recovery of fouled membrane with organic aggregates, and the permeate flux recovery rate was calculated to be 79.4% (Figure 2.7, Run 7). The back-flushing with DW completely recovered the permeate flux of Fe colloidal fouled membrane, when back-flushing was applied just after fouling (Figure 2.7, Run 8). But, when back-flushing was applied after maturation of Fe colloids in the membrane unit with citric acid monohydrate it did not function at all (Figure 2.5 (f), Run 10). On the contrary, NaOH solution was found to be effective in permeate flux recovery of a matured Fe colloidal fouled membrane with the recovery rate of 89.1% (Figure 2.7, Run 9).

Although the causes of RO membrane fouling are complicated, several natures of particle surface such as, hydrophobic, hydrophilic, and surface charges are influenced the membrane fouling. In general, majority of RO membranes are fouled by natural organic matter, biopolymers, and colloids. In view of that, natural organic matter and colloids are thought to be key factors for RO membrane fouling that reported by Madaeni et al. (2010) and Malcolm (1985). The present study also supports this supposition, where organic aggregates and Fe colloids predominantly took part in the RO membrane fouling.

In the permeate flux recovery experiments, it was observed that DW was capable to washout the organic foulants that deposited on the surface of membrane like a soft cake layer. Afterward, NaOH showed good removal performances on the removal of foulants that remained after back-flushing by DW. NaOH can generate water-soluble soap micelles in the membrane unit by the saponification process and organic matters are hydrolyzed and increase the negative charges to a great extent of the organic molecules. Further, the hydrolyzed portions of organic matters weaken the adsorptive forces through the effect of repulsion force between negative charged functional groups and the membrane. This configuration creates a loose fouling layer that facilitates the mass transfer process and enhances the permeate flux recovery of a fouled membrane with organic aggregates. (Hong and Elimelech, 1997; Miller and Raney, 1993; Stumm and Morgan, 1996). The Fe colloids fouled membrane's permeate flux was possible to recovered completely by back-flushing with DW, just after fouling. Such a phenomenon suggested that Fe colloids just created physical clogging on the surface of membrane unit that easily washed away only by back-flushing with DW without any chemical addition. But, Fe colloids fouled membranes permeate flux after 7-days maturation was not possible to recover entirely by back-flushing even though chemicals of NaOH or citric acid monohydrate solution were used. Fe colloids are expected to transform into Fe oxides during the maturation. When membrane is fouled by Fe oxides, citric acid monohydrate is expected to be effective in permeate flux recovery, because Fe oxides are reduced by citric acid monohydrate solution (Kishimoto et al., 2011).

However, when divalent cations are coexistent with natural organic matter, it creates a denser adhesive fouling layer on the surface of a membrane. In such a case, citric acid monohydrate solution may not function at all. Alternatively, alkaline NaOH solution could be an effective chemical for the removal of Fe colloidal inorganic particles of a fouled membrane (Lee et al., 2010). This argument supports the present experimental results, where a NaOH solution at the concentration of 1,000 mg/L successively recovered the permeate flux of the matured Fe colloidal fouled membrane up to 89.1%. In this study, the main foulants in RO membrane operation were found to be organic aggregates and iron colloids. In the fouling by such foulants, I recommended sodium hydroxide solution at the concentration of 1,000 mg/L as an effective back-flushing chemical for the permeate flux recovery of both organic aggregates and iron colloids fouled membrane, back-flushing through the concentrate port at the flow rate of 1,100 mL/min.

2.4 Conclusion

Nowadays, RO membranes are considered to be one of the familiar technologies in water and wastewater treatment sector due to its low energy consumption and high quality water production

at a low cost. Therefore, I examined the applicability of a commercially available polyamide RO element to the treatment of synthetic contaminated source water containing with nitrite, nitrate, iron, manganese, and municipal sewage-derived contaminants, and sought an effective permeate flux recovery method for the fouled membrane.

The RO membrane was able to reject SS, BOD, COD and total coliform completely. Besides, the ions rejection rates were 98% for iron, 97% for manganese, 94% for chloride, 80% for nitrite, and 77% for nitrate, respectively. The ammonium rejection rate was found to be poor and it was only 45% probably due to its low molecular weight. As a result, a pre- or post-treatment process would be required to satisfy the drinking water quality standards, especially for ammonium.

Membrane fouling is one of the major drawbacks in the RO technology. In this study, organic aggregates and inorganic particles like iron colloids were found to be major membrane foulants, but dissolved matter in influent did not take part in membrane fouling. The back-flushing operation through the concentrate port could improve the permeate flux of a RO membranes fouled by organic aggregates to the permeate flux recovery rate of 37.0% using pure water, and 79.4% using pure water followed by the NaOH solution with the concentration of 1,000 mg-NaOH/L. The hydrolyzation and solubilization of organic matter by NaOH was inferred to be responsible for the permeate flux recovery of organic aggregates fouled membrane. On the contrary, the permeate flux of RO membrane fouled by iron colloids was completely recovered by back-flushing using pure water, when the back-flushing was applied just after fouling. This suggested that the membrane fouling by iron colloids was mainly caused by the physical clogging in the membrane element. In addition, NaOH solution showed a better performances in permeate flux recovery of matured iron colloidal fouled membrane and that was found to be up to 89.1%. For the permeate flux recovery of a fouled RO membrane by organic aggregates or iron colloids, I recommend back-flushing through the concentrate port at the flow rate of 1,100 mL/min using a sodium hydroxide solution at the concentration of 1,000 mg/L as a back-flushing solution.

2.5 References

Akther, H., Ahmed, M. S., Rasheed, K. B. S., (2009). Spatial and temporal analysis of groundwater level fluctuation in dhaka city. Asian Journal of Earth Sciences., 2 (2), 49-57.

Amjad, Z., Zibrida, J. F., Zuhl, R. W., (1998). Reverse Osmosis Technology: Fundamentals and Water Applications. Association of Water Technologies, Inc., Annual Convention & Exposition, Washington DC.

Ang, W. S., Yip, N. Y., Tiraferri, A., Elimelech, M., (2011). Chemical cleaning of RO membranes

fouled by wastewater effluent: Achieving higher efficiency with dual-step cleaning. Journal of Membrane Science., 382 (1-2), 100-106.

Baker, R. W., (2004). Membrane Technology and Applications. 2nd ed., John Wiley & Sons, Ltd, Chichester.

Chianese, A., Ranauro, R., Verdone, N., (1999). Treatment of landfill leachate by reverse osmosis. Water Research., 33 (3), 647-652.

Comerton, A. M., Andrews, R. C., Bagley, D. M., (2005). Evaluation of an MBR-RO system to produce high quality reuse water: Microbial control, DBP formation and nitrate. Water Research., 39, 3982-3990.

Fakhru'l-Razi, A., Pendashteh, A., Abidin, Z. Z., Abdullah, L. C., Biak, D. R. A., Madaeni, S. S., (2010). Application of membrane-coupled sequencing batch reactor for oilfield produced water recycle and beneficial re-use. Bioresource Technology., 101 (18), 6942-6949.

Funston, R., Ganesh, R., Leong, L. Y. C., (2002). Evaluation of technical and economic feasibility of treating oilfield produced water to create a new water resource, in: Ground Water Protection Council (GWPC), Colorado Spring, U.S., 16-17.

Gleick, P. H., Wolff, G. W., Cooley, H., Palaniappan, M., Samulon, A., Lee, E., Morrison, J., Katz, D., (2006). The world's water 2006-2006. The biennial report on fresh water resources. Island Press, Chicago.

Greenlee, L. F., Lawler, D. F., Freeman, B. D., Marrot, B., Moulin, P., (2009). Reverse osmosis desalination: Water sources, technology, and today's challenges. Water Research., 43, 2317-2348.

Hasan, S., Ali, M. A., (2010). Occurrence of manganese in groundwater of Bangladesh and its implications on safe water supply. Journal of Civil Engineering (IEB)., 38 (2), 121-128.

Hong, S., Elimelech, M., (1997). Chemical and physical aspects of natural organic matter (NOM) fouling of nanofiltration membranes. Journal of Membrane Science., 132 (2),159-181.

Hossain, D., Islam, M. S., Sultana, N., Tusher, T. R., (2013). Assessment of iron contamination in groundwater at tangail municipality , Bangladesh. Journal of Environmental Science and Natural Resources., 6 (1), 117-121.

Isaias, N. P., (2001). Experience in reverse osmosis pretreatment. Desalination., 133 (1-3), 57-64.

Kamar, F. H., Craciun, M. E., Nechifor, A. C., (2014). Heavy metals: sources, health effects, environmental effects, removal methods and natural adsorbent material as low-cost adsorbent: short review. International Journal of Scientific Engineering and Technology Research., 03 (14), 2974-2979.

Kim, S., Hoek, E. M. V., (2005). Modeling concentration polarization in reverse osmosis process. Desalination., 186 (1-3), 111-128.

Kishimoto, N., Iwano, S., Narazaki, Y., (2011). Mechanistic consideration of zinc ion removal by zero-valent iron. Water, Air, & Soil Pollution., 221, 183-189.

Le-Clech, P., Chen. V., Fane, T. A. G., (2006). Fouling in membrane bioreactors used in wastewater treatment. Journal of Membrane Science., 284 (1-2), 17-53.

Lee, S., Boo, C., Elimelech, M., Hong, S., (2010). Comparison of fouling behavior in forward osmosis (FO) and reverse osmosis (RO). Journal of Membrane Science., 365, 34-39.

Lloyd, D. R., (1985). Materials Science of Synthetic Membranes. American Chemical Society., 269, 273-294.

Loeb, S., Sourirajan, S., (1963). Sea water demineralization by means of an osmotic membrane. Advances in Chemistry Series., 38, 117-132.

Louie, J. S., Pinnau, I., Ciobanu, I., Ishida, K. P., Ng, A., Reinhard, M., (2006). Effects of polyether-polyamide block copolymer coating on performance and fouling of reverse osmosis membranes. Journal of Membrane Science., 280 (1-2), 762-770.

Madaeni, S. S., Samieirad, S., (2010). Chemical cleaning of reverse osmosis membrane fouled by wastewater. Desalination., 257 (1-3), 80-86.

Malcolm, R., (1985). Geochemistry of stream fluvic and humic substances, in humic substances in soil, sediment and water, ed. by G. R. Aliken, D. M. McKnight, and P. MacCarthy, 181-2009, Wiley-Interscience Publication, New York.

Mi, B., Elimelech, M., (2010). Organic fouling of forward osmosis membranes: Fouling reversibility and cleaning without chemical reagents. Journal of Membrane Science., 348 (1-2), 337-345.

Miller, C. A., Raney, K. H., (1993). Solubilization-emulsification mechanisms of detergency. Colloids and Surfaces A: Physicochemical and Engineering Aspects., 74, 169-215.

Ng, H. Y., Elimelech, M., (2004). Influence of colloidal fouling on rejection rate of trace organic contaminants by reverse osmosis. Journal of Membrane Science., 244, 215-226.

Perry, R. H., Green, D. W., (1997). Perry's Chemical Engineers' Handbook. 7th ed., McGraw-Hill, New York.

Rice, E. W., Baird, R. B., Eaton, A. D., Clesceri, L. S., (2012). Standard Methods for the Examination of Water and Wastewater. 22nd Edition. Washington, DC: American Public Health Association, American Water Works Association, Water Environment Federation.

Richardson, S. D., Plewa, M. J., Wagner, E. D., Schoeny, R., DeMarini, D. M., (2007). Occurrence, genotoxicity, and carcinogenicity of regulated and emerging disinfection byproducts in drinking water: a review and roadmap for research. Mutation Research/Reviews in Mutation Research., 636 (1-3), 178-242.

Service, R. F., (2006). Desalination freshens up. Science., 313 (5790), 1088-1090.

Stumm, W., Morgan, J. J., (1996). Aquatic Chemistry: Chemical Equilibria and Rates in Natural Waters, 3rd Ed., Wiley-Interscience Publication, New York.

Uddin, M. S., Kurosawa, K., (2011). Effect of chemical nitrogen fertilizer on the release of arsenic from sediment to groundwater in Bnagladesh. Procedia Environmental Sciences., 4, 294-302.

Vrijenhoek, E. M., Hong, S., Elimelech, M., (2001). Influence of membrane surface properties on initial rate of colloidal fouling or reverse osmosis and nanofiltration membranes. Journal of Membrane Science., 188 (1), 115-128.

Chapter III
Organic Aggregates and Iron Colloids Removal through Active Surface-charge Control Depth Filtration

3.1 Introduction

The reverse osmosis (RO) experiments in Chapter II revealed that the RO process can produce good quality potable water. However, a few foulants like organic aggregates and iron (Fe) colloids were found to be problematic for the continuous operation of the system. Accordingly, a pre-treatment of suspended solids (SS) like organic aggregates and Fe colloids should be introduced prior to the RO process. In this aspect, the application of depth filtration can be an alternative, cost-effective, and easy pre-treatment method. Depth filtration is a conventional technology and has been widely used for water and wastewater treatment using different filtration media like natural silica, anthracite, charcoal, and various fabric materials. In depth filtration, SS and colloidal particles are removed from a water stream by capturing them on porous media. The most significant advantage of depth filtration is its relatively small head loss and a high resistance to clogging in compared with other unconventional membrane technologies like microfiltration (MF), ultrafiltration (UF), and nanofiltration (NF).

Over the last half century, depth filtration process in porous bed has become more common in wastewater treatment area due to the stringent effluent quality standards (Darby et al., 1991). In this method, solid particles in suspension are generally adsorbed on or retained by the media while filtration. However, the effectiveness of particles removal depends on the surface forces acting between particles and filter grains. The latter is significant when distance between particles and filter grains are in the order of nanometers (Jegatheesan and Vigneswaran, 2003).

Numerous complementary research works have been performed to clearly understand the effects of media material on removal of SS by depth filtration (Tien and Payatakes, 1979). Still in recent years, depth filtration models cannot completely account for the fundamental insights concurring with a large variety of solid loading rate for wastewater filtration (Ding et al., 2015). It is well known that tiny particles separation is a very complex process and influenced by several factors such as wastewater characteristics, types of SS, and the operation mode of filtration (Darby and Lawler, 1990). When filtration proceeds over time without back-washing, effluent quality may be improved but clogging of filter bed will result in an increase in head loss and a decrease in filtration flux (Jackson and Letterman, 1980). Clogging and head loss are influenced by various factors like particle size distribution, particle concentration, particle surface chemistry, filter media size, and media type (Cushing and Lawler, 1998). A filter media with an uneven media size distribution normally have a greater chance of clogging than uniform filter media. The formation of clogging depends on the size distribution of SS, fine bedload, and channel sediments. Large fine particles

diameter more than 30 µm are subjected to mechanical filtration rather than surface phenomena such as the van deer Waals force. Medium sized particles between 3 and 30 µm are retained by both filtration mechanisms. Adhesion of colloidal particles and bacteria are exclusively due to physiochemical process (Brunke, 1999).

In general, performance of a filter is quantified by particle removal efficiency and head loss across the packed bed. Since, filtration is often thought to be a unit operation at post-treatment stage in wastewater treatment process, a secure removal of SS is required to satisfy the specific standard limit. In depth filtration mechanism, large and submicron particles, colloidal, and insoluble materials are removed while passing through a tortuous path before it is able to reach the other side (Ison and Ives, 1969). Figure 3.1 shows the flow of fluid and particles through depth filter media.

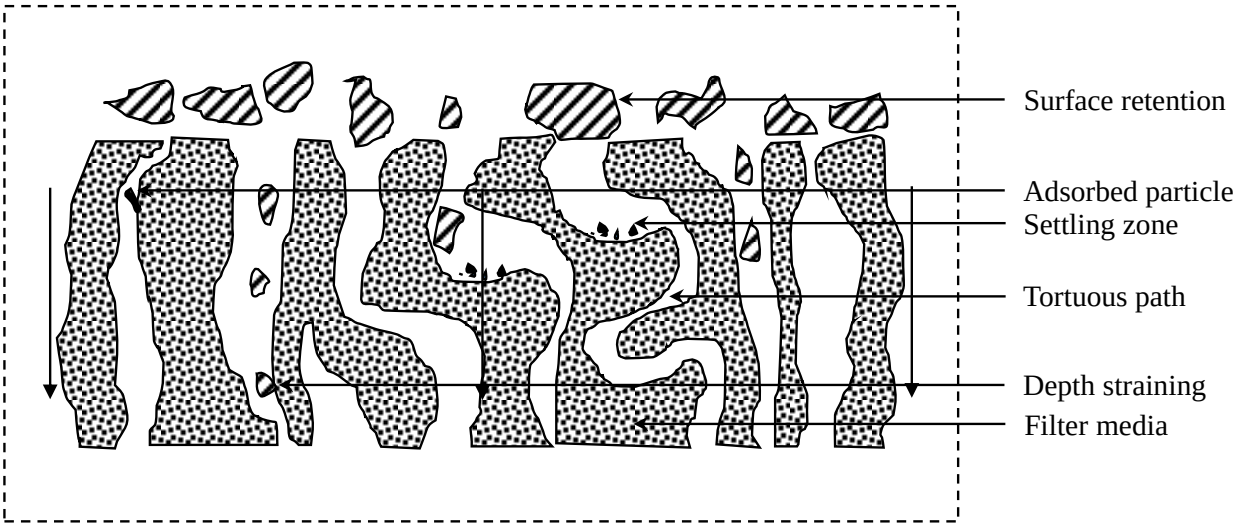

Figure 3.1 Flow of fluid and particles through depth filter media.

It is logical that particles larger than the pore size would be easily removed by mechanical filtration that is termed as sieving, straining, or size exclusion. In addition, adsorption and attraction mechanisms are also observed in depth filtration, where particles are adsorbed by the electro-kinetic force or surface affinity. Relatively large particles impact the filter medium through inertia, and relatively small particles impact through random Brownian motion. In these process particles are finally adsorbed on the filter medium by the van der Waals force or the interaction in the electric double layers (EDLs) of the surfaces (Stephan and Chase, 2001). However, the removal of particles smaller than the pore size and microorganisms like total coliform (TC) and general bacteria (GB) are less intuitive. In this case, an electro-kinetic effect in charge modified depth filter media would be able to remove these submicron particles, colloidal materials, and insoluble contaminants (Hou et al., 1980). Natural particles and colloids in water usually have a negative surface charge. Therefore, if filter media have an opposite surface charge against particles in water the particle removal performances of the system will be enhanced (Goldberg and Glaubig, 1987; Jefferson et al., 2005).

Considering this notion a laboratory scale depth filtration system was developed using a conducting carbon fiber felt made from polyacrylonitrile fibers with 5.3 μm in diameter as filter media, in which surface charge of filter media was actively controlled with a direct current (DC) power supply. In this system, wastewater filtration was performed under a positive surface charge of the filter media and back-washing was performed under a negative surface charge. These operations would enhance the particle rejection and back-washing effect through electrostatic interactions between particles and media surface (Kishimoto et al., 2010). The specific objectives of this research was to find out an optimum condition of the active surface-charge control depth filter for the removal of fouling materials of the RO membrane such as organic and inorganic particles. In addition, efficacy of this system on desorption of particles from filter media at the back-washing step was also explored.

3.2 Materials and Methods

3.2.1 Experimental Setup

Figure 3.2 shows the experimental setup. The laboratory scale experimental system was composed of a filter module, a feed pump (RP-1000, EYELA, Japan), a digital DC power supply (AD-8735D, AND, Japan), and a high power ultrasonic cleaner (SUS-200, Shimadzu, Tokyo, Japan).

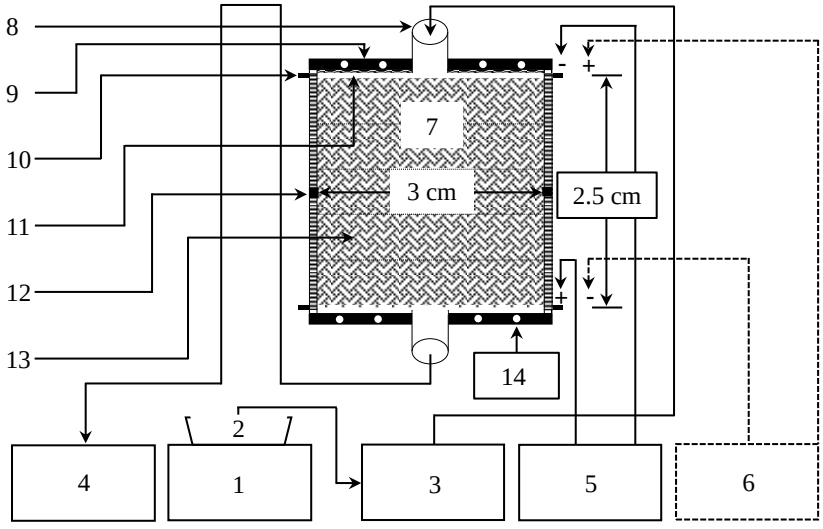

Figure 3.2 Laboratory scale experimental setup. 1: Ultrasonic cleaner, 2: Influent, 3: Feed water pump, 4: Effluent, 5: DC power supply in filtration mode, 6: DC power supply in back-washing mode, 7: Filter module, 8: Acrylic tube, 9: Acrylic resin cover, 10: Porous stainless steel plate, 11: Polytetrafluoroethylene mesh, 12: Silicon rubber, 13: Carbon fiber felt, and 14: Bolts.

The filter module was constituted of a filter bed chamber made of silicon rubber with 2.5 cm height and two covers made of acrylic resin with an inlet or outlet. Five sheets of carbon fiber felt (Weight per area: 250 g/m^2; Kanai Juyo Kogyo, Osaka, Japan) with 3 cm in diameter and 0.5 cm in thickness were stacked in the filter module. Two porous stainless steel (ANSI304) plates with 5 mm pores were set at the upper and lower end of the filter module as a counter electrode and a conductor to

the carbon fiber felt, respectively. A polytetrafluoroethylene mesh sheet with 1 mm in thickness was inserted between upper stainless steel plate sheet and carbon fiber felt as a separator. The empty volume of filter bed chamber was 17.7 cm^3.

3.2.2 Experimental Procedure and Operational Conditions

Before each experimental run the filter module was washed with deionized water (DW) of electrical conductivity (EC) less than 1 µS/cm, unless and until particles were not detected in the effluent. In this study, Run 1 was conducted to observe the kaolin particle removal efficiency in DW with no electric charge to the filter bed, Run 2 was conducted to observe the effect of conductivity on kaolin particle removal performances with no electric charge, and Run 3 was conducted to observe the effect of electric charge to the filter bed on kaolin particle removal performances.

The kaolin particle removal efficiency in synthetic contaminated source water was observed in Runs 4 and 5 at pH 6.7 and 7.8, respectively. The Runs 4 and 5 demonstrated the effect of synthetic contaminated source water pH on kaolin particle removal performances at around neutral pH. Run 6 was demonstrated to observe the effect of anionic surfactant on kaolin particle removal performances. The Fe and kaolin particle removal performances were observed in Runs 7 and 8 at pH 4.6 and 8.6, respectively. The Runs 7 and 8 demonstrated the effect of acidic and alkaline pH on kaolin particle and Fe colloids removal performances. Moreover, the effect of anionic surfactant in Fe and kaolin particle removal performances were observed in Runs 9 and 10 at pH 3.8 and 7.9, respectively. The Runs 9 and 10 were demonstrated to observe the effect of anionic surfactant on kaolin and Fe colloids removal performances at acidic and alkaline pH. Here, the objectives of doing several runs were to find out the exact parameters that influence on the kaolin particle and Fe colloids removal performances.

Tables 3.1 and 3.2 show the operational conditions and the synthetic influent characteristics of Runs 1-10, respectively. The potential of the conducting carbon felt against the counter electrode in the filter module was set to +1.0 V at filtration mode of Runs 3-10, though the potential was not applied at Runs 1-2 (Table 3.1). At the back-washing mode, the potential was reversely changed to -1.0 V at Runs 3-10 and the potential was not applied at Runs 1-2. The terminal voltage was set ±1.0 V, because this terminal voltage was within the potential window of water electrolysis, where electricity was used only for charging of the EDLs of filter media and the counter electrode (Ho et al., 1990). The back-washing solutions were flowed from the opposite direction of filtration mode at all experimental runs following the Figure 3.2 to remove the clogged or retained particles in the filter media, which is defined as washout step. The filtration hydraulic loading and filtrated water

volume of Runs 1-10 was 283 L m^{-2} min^{-1} and 800 mL, respectively. On the other hand, the back-washing hydraulic loading and back-washed water volume of Runs 1-10 was 1,274 L m^{-2} min^{-1} and 1,000 mL, respectively.

Table 3.1 Operational conditions of Runs 1-10.

Empty volume of the filter module	= 17.7 cm^3
Applied voltage in Runs 1-2	= Not applied
Applied voltage in Runs 3-10	= +1.0 V
Filtration hydraulic loading of Runs 1-10	= 283 L m^{-2} min^{-1}
Filtrated water volume of Runs 1-10	= 800 mL
Back-washing hydraulic loading of Runs 1-10	= 1,274 L m^{-2} min^{-1}
Back-washed water volume of Runs 1-10	= 1,000 mL

Table 3.2 Synthetic influent characteristics of Runs 1-10.

Runs	Spiked concentration/L in influent						Measured concentration/L in influent						
	DW (L)	SCSW (L)	Kaolin (mg)	NaCl (mg)	SLS (mg)	Fe^{2+} (mg)	pH	Zeta potential (ζ) (mV)	EC (µS/cm)	Suspended solid (SS) (mg)	Turbidity (mg/L-kaolin)	Color (Pt-Co)	Fe^{2+} (mg)
Run 1	1	×	100	0.0	0.0	0.0	7.4	-34.1 ± 1.8	3	93.0	87.0	142.5	0.0
Run 2	1	×	100	292.2	0.0	0.0	5.9	-21.2 ± 4.1	560	94.0	95.0	120.0	0.0
Run 3	1	×	100	292.2	0.0	0.0	5.9	-21.2 ± 4.1	550	88.0	83.5	117.5	0.0
Run 4	×	1	100	0.0	0.0	0.0	6.7	-30.5 ± 2.2	480	93.0	84.0	187.5	0.0
Run 5	×	1	100	0.0	0.0	0.0	*7.8	-26.5 ± 6.3	670	92.0	86.5	170.0	0.0
Run 6	1	×	100	292.2	100	0.0	6.6	-47.4 ± 7.0	770	90.0	83.0	162.5	0.0
Run 7	1	×	100	292.2	0.0	10	4.6	-5.4 ± 1.2	580	111.0	101.0	155.0	12.8
Run 8	1	×	100	292.2	0.0	10	*8.6	-37.4 ± 4.4	600	108.0	104.0	260.0	5.6
Run 9	1	×	100	292.2	100	10	3.8	-42.3 ± 2.6	870	108.0	103.0	330.0	9.9
Run 10	1	×	100	292.2	100	10	*7.9	-30.5 ± 1.4	830	108.0	76.5	225.0	5.4

DW=Deionized Water; SCSW=Synthetic Contaminated Source Water (Table 3.3); SLS=Sodium Lauryl Sulfate; EC=Electrical Conductivity; *The pH was increased adding 50 mM-NaOH.

Table 3.3 shows the synthetic contaminated source water characteristics of Runs 4 and 5. Here, the influent used in Runs 4-5 was municipal wastewater of Ryukoku University diluted by a 5-time with normal tap water. After that, it was kept in room temperature for about 2 months. As a result, organic matter was decomposed into inorganic carbon, nitrate (NO_3^-), and ammonium (NH_4^+). Consequently, NO_3^- and NH_4^+ concentrations were found to be higher than biochemical oxygen demand (BOD) and chemical oxygen demand (COD) (Table 3.3). The synthetic contaminated source water was filtrated using a glass fiber filter with 1-µm particle rejection (GF/B, Whatman, Japan) just before experimental runs.

Table 3.3 Water quality of synthetic contaminated source water filtrated for Runs 4 and 5.

SS (mg/L)	EC (µS/cm)	pH	DO (mg/L)	Turbidity (mg/L-kaolin)	Color (Pt-Co)	NO_2^- (mg/L)	NO_3^- (mg/L)	NH_4^+ (mg/L)	BOD (mg/L)	COD (mg/L)
0.0	620	7.1	8.0	0.0	16.5	0.0	93.0	28.2	3.9	20.8

EC=Electrical Conductivity.

In the back-washing experiments, DW was used as back-washing solution in Runs 1-2 and a sodium chloride (NaCl) solution with NaCl concentration of 5 mM (292.2 mg/L) (EC=580 µS/cm) was used in Runs 3-10. In the preparation of the influent of Runs 1-10 a high power ultrasonic cleaner was operated for 30 minutes to promote the dispersion of fine particles. The ultrasonic cleaner was continuously operated during the filtration operation too. In this experimental study, kaolin powder of 0.1-4.0 µm in diameter (Nacalai, Tesque, Kyoto, Japan), NaCl, sodium lauryl sulfate ($CH_3(CH_2)_{11}OSO_3Na$), and ferrous sulfate heptahydrate ($FeSO_4.7H_2O$) were used for the source of micro particles, electron conductor, anionic surfactant, and ferrous ion, respectively. Moreover, 50 mM (200 mg/L) sodium hydroxide (NaOH) was used as alkaline solution to increase the pH in Runs 5, 8, and 10, respectively.

3.2.3 Analytical Methods

The pH, dissolved oxygen (DO), and EC were measured with a pH meter (B-212, Horiba, Japan), a DO meter (LDO, HQ10, Hach, USA), and an EC meter (Twin cond, B-173, Horiba, Japan), respectively. A pH controller (FD-02, Series-B, Japan) was used to adjust the pH. Turbidity and color were measured with a digital turbidity/color meter (Aqua Doctor, WA-PT-4DG, Kyoritsu Chemical-Check Lab, Japan). Concentrations of nitrite (NO_2^-), NO_3^-, and NH_4^+ were determined by colorimetric method (4500-NO_2^- B) (Rice et al, 2012), cadmium reduction method (4500-NO_3^- E) (Rice et al., 2012), and phenate method (4500-NH_3 F) (Rice et al., 2012), respectively. Ferrous ion (Fe^{2+}) was measured by phenanthroline method (3500-Fe B) (Rice et al., 2012). The BOD was measured by 5-day BOD test (5210 B) (Rice et al., 2012) and COD was measured by closed reflux colorimetric method (5220 D) (Rice et al., 2012). Particle size distributions of kaolin suspension and Fe colloids in influent, effluent, and back-washed water were measured with a laser diffraction particle size analyzer (SALD-300V, Shimadzu, Kyoto, Japan). Zeta potential was measured with a zeta potential meter (ZEECOM ZC-2000, Microtec, Funabashi, Japan). Total coliform (TC) and general bacteria (GB) were measured by test papers for TC and GB (Sibata, Saitama, Japan) using colony count, most-probable-number (MPN) method with thermostat incubator (CALBOX, CB-101, Sibata, Saitama, Japan). Filtrate was collected as effluent and the mass of kaolin in the filtrate was measured as SS using glass fiber filter with 0.7 µm particle rejection (GF/F, Whatman, Japan).

DW with the EC less than 1 μS/cm was used for the dilution and preparation of standard solution, as obtained from a water purification system (Autostill, WA5000, Yamato, Japan).

3.3 Results and Discussion

3.3.1 Zeta Potential of Particles

Figure 3.3 shows the zeta potentials of particles at Runs 1-10 depending on pH and artificially spiked ingredients, namely kaolin particles, NaCl, sodium lauryl sulfate, and $FeSO_4.7H_2O$ in the influent (Table 3.2). Here, the zeta potential of kaolin particles was found to be -34.1 mV in DW at pH 7.4 (Run 1). But, when NaCl was added to the suspension (Runs 2 and 3), pH decreased to 5.9 and zeta potential increased to -21.2 mV, which would be caused by protonation with the decrease in pH (Adelkhani et al., 2009; Kishimoto et al., 2010; Yukselen and Kaya, 2003).

However, the zeta potential of kaolin suspension in synthetic contaminated source water in Run 4 and 5 was found to be -30.5 and -26.5 mV at pH 6.7 and 7.8, respectively. In this case, pH was increased by the addition of NaOH in Run 5. Therefore, the zeta potential of kaolin particle in synthetic contaminated source water showed reverse behavior with pH due to the effect of positively charged sodium ion (Na^+) in the kaolin suspension, which accords with the experimental results of Moayedi et al. (2011).

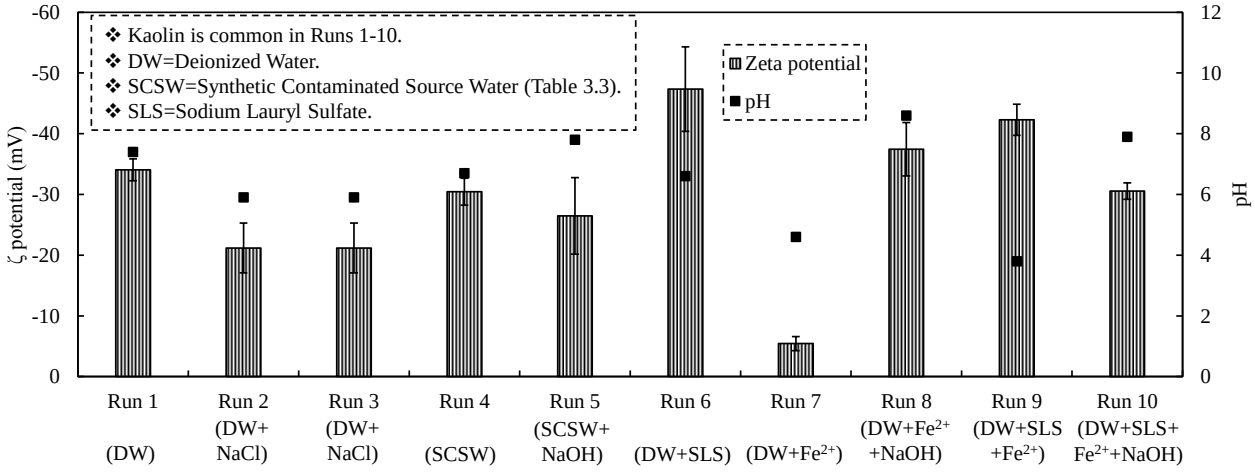

Figure 3.3 Zeta potential characteristics of Runs 1-10, where kaolin was used as a model common micro particles in Runs 1-10, sodium lauryl sulfate was used in Runs 6, 9, and 10, and Fe was used in Runs 7-10. The error bars depict the unbiased standard deviation.

The zeta potential of Run 6 was found to be -47.4 mV, which was lower than that of other runs, where kaolin particle and sodium lauryl sulfate were diluted with DW at pH 6.6. Since sodium lauryl sulfate is a negatively charged anionic surfactant, the adsorption of sodium lauryl sulfate onto the kaolin particle may take part in decreasing the zeta potential regardless of pH in the solution.

In the case of Runs 7 and 8 the zeta potentials of kaolin suspension in DW with Fe ions were found to be -5.4 and -37.4 mV at pH 4.6 and 8.6, respectively. Since, the zeta potential of ferric hydroxide ($(Fe(OH)_3$) is reported to be positive at pH less than around 6 (Hamamoto, 2016). The zeta potential in Run 7 was found to be higher than that of all runs, though the value was still negative. On the contrary, when the pH of Run 7 was increased to 8.6 (Run 8) the zeta potential decreased to -37.4 mV due to deprotonation effect (Yukselen and Kaya, 2003).

The zeta potentials of Runs 9 and 10 were found to be -42.3 and -30.5 mV at pH 3.8 and 7.9, respectively. Here, kaolin particle, sodium lauryl sulfate, and $FeSO_4.7H_2O$ were diluted in DW. The zeta potential in Run 9 was found to be lower than Run 10. In the case of Run 9 negatively charged head of sodium lauryl sulfate (SLS) was associated with positively charged Fe colloids in Run 9. As a result, Fe colloids covered by SLS that hydrophobic tails are exposed to the outer side namely, bulk water. Then, other SLSs were associated with SLSs adsorbed on the Fe colloids by hydrophobic interaction. Consequently, the surface of the Fe colloid was covered by negatively charged heads of SLSs, which result in the low zeta potential. In Run 10, negatively charged surface of Fe colloids prevent the adsorption of SLS onto the Fe colloids. Accordingly, the zeta potential observed in Run 10 was higher than that in Run 9.

At a glance, the zeta potential characteristics of kaolin particles in pure water, synthetic contaminated source water, anionic surfactant, and Fe-contaminated water are summarized here. The zeta potential of kaolin particles and kaolin particles with $Fe(OH)_3$ in pure water was found to increase with the decrease in pH probably due to the protonation effect (Runs 1, 2, 3, 7, and 8). However, the increment in zeta potential with the increment in pH was observed in Runs 4 and 5, where synthetic contaminated source water was added. Adsorption of positive ions/or organic ions in synthetic contaminated source water onto the kaolin surface might be responsible for such a phenomenon. However, extensive researches will be required for elucidating the mechanism in the future.

3.3.2 Effect of Conductivity and Electric Charge on Particle Separation

Figure 3.4 (a-f) show the volume-based kaolin suspension particle size distribution of influent and effluent of Runs 1-3. Here, the conductivity in influent of Runs 1-3 were 3, 560, and 550 µS/cm, respectively (Table 3.2) and a terminal voltage of +1.0 V was applied for Run 3 alone (Table 3.1). In addition, it is notable that the diameter of kaolin particles used in the experiments was in the range of 0.1-4.0 µm. However, the kaolin particle diameter increased to the range of 0.139-8.200

μm in the influent of Run 1 (Figure 3.4 (a)), 0.139-68.431 μm in the influent of Run 2 (Figure 3.4 (c)), and 0.139-58.126 μm in the influent of Run 3 (Figure 3.4 (e)), because of self-flocculation.

Figure 3.4 (b) and (d) show the particle size distribution of effluent in Runs 1 and 2. From these graph it is observed that the particles larger than 6.965 μm were decreased by filtration without impressed voltage. This result indicates that the particles larger than 6.965 μm were removed by the sieving mechanism and the adsorption mechanism by van der Waals forces.

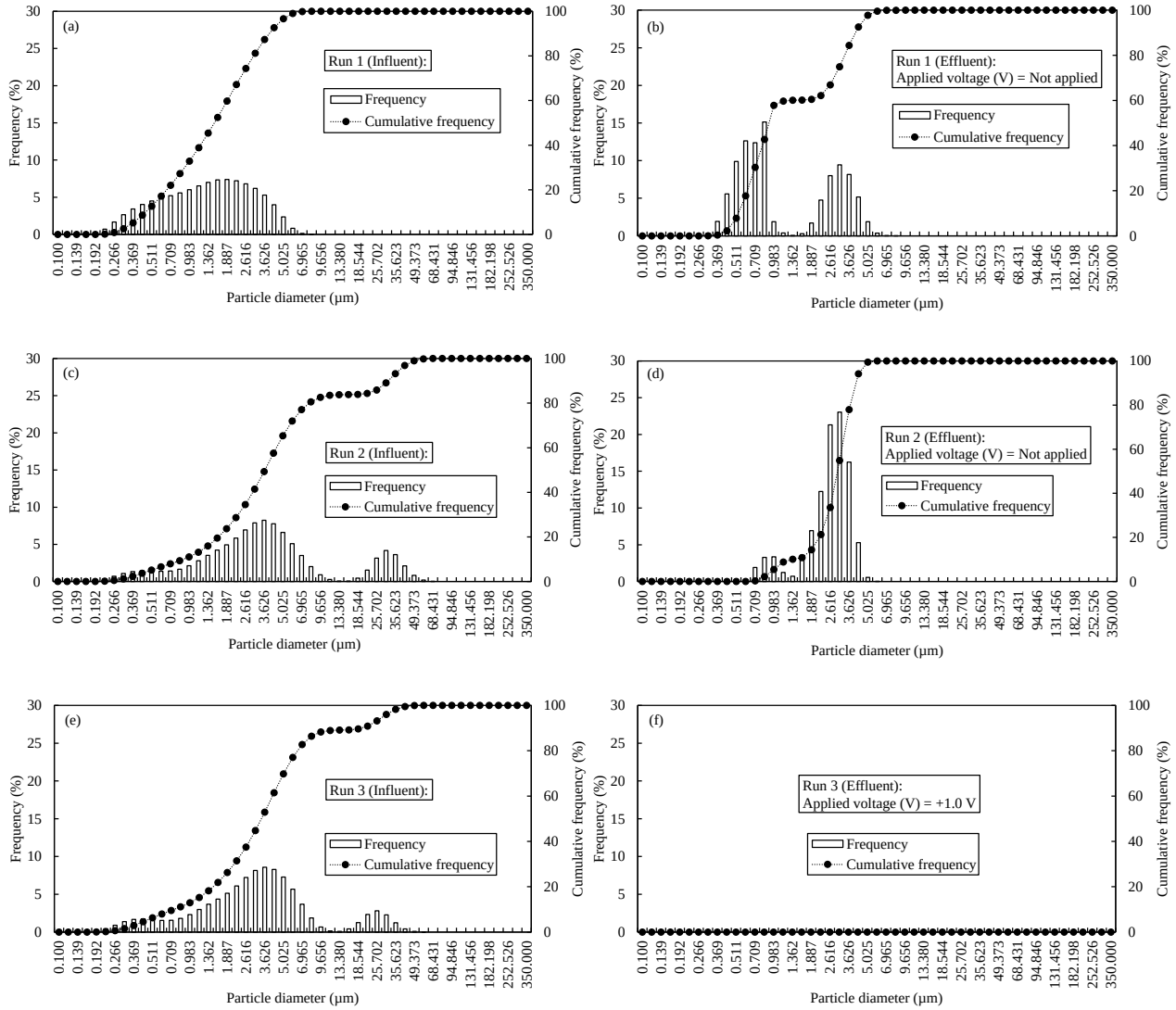

Figure 3.4 (a-f) Volume-based kaolin suspension particle size distribution of influent and effluent of Runs 1-3, where as a solvent for kaolin particle, DW was used in Run 1 and DW with 5 mM-NaCl was used in Runs 2-3.

Figure 3.4 (f) shows the particles were completely removed by the depth filtration with the impressed voltage at +1.0 V. Accordingly, it was inferred that smaller particles less than 6.965 μm were mainly removed by electro-kinetic adsorption mechanism. On the other hand, smaller particles within the range of 0.100-0.266 μm in the effluent of Run 1 (Figure 3.4 (b)) and 0.100-0.434 μm in

the effluent of Run 2 (Figure 3.4 (d)) were found to be decreased without electric charge and thought to be due to the effect of self-aggregation of small particles during the filtration.

Figure 3.5 shows the SS, turbidity, and color removal efficiency of Runs 1-3. The influent of Run 1 with the EC of 3 µS/cm was filtrated without application of terminal voltage and SS removal efficiency was found to be 92.2%. But, when the influent of Run 2 with the EC of 560 µS/cm was filtrated without application of terminal voltage like Run 1, SS removal efficiency was found to be a little bit more than Run 1, and it was found to be 97.3%. Due to addition of NaCl in Run 2, the ionic strength of the solution was intensified and the thickness of the electrical double layer was decreased, which helped to enhance the particles contact with the filter media and affected in particle removal efficiency (Huang et al., 1999). Moreover, the application of terminal voltage (+1.0 V) in Run 3 showed 100% removal efficiency of all parameters (Figure 3.5) probably due to the electrostatic attraction between the particles and the filter media (Foess and Borchardt, 1969).

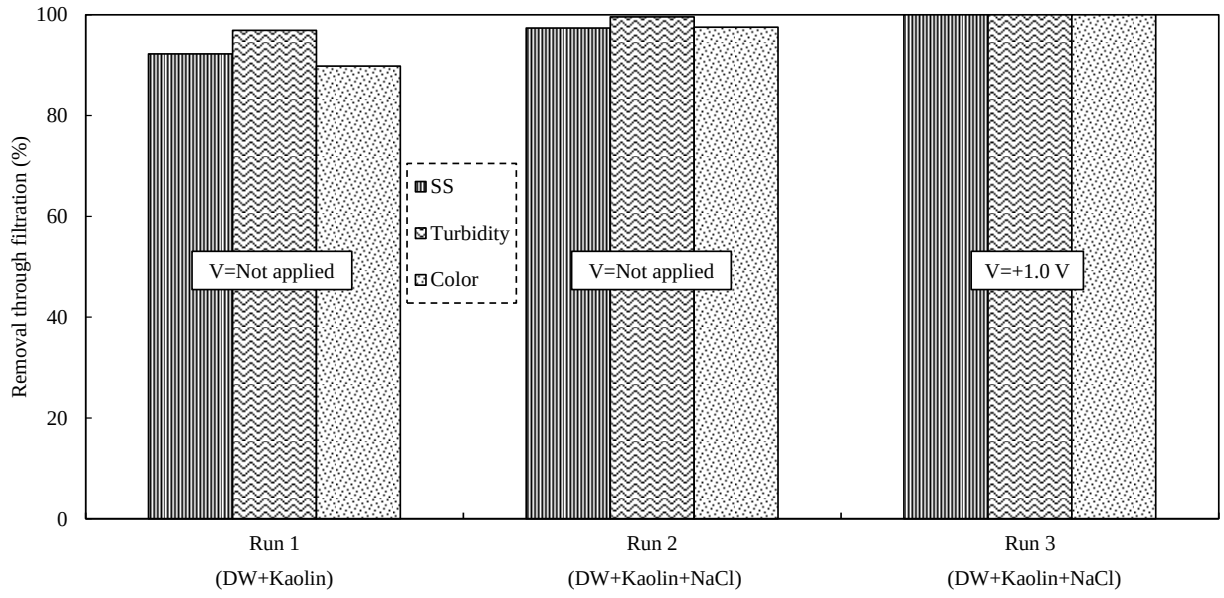

Figure 3.5 SS, turbidity, and color removal efficiency of Runs 1-3 at the filtration hydraulic loading of 283 L m^{-2} min^{-1}, without application of terminal voltage in Runs 1 and 2, and +1.0 V terminal voltage was applied in Run 3.

From the above discussions it can be concluded that the kaolin particles in size more than 6.965 µm in diameter were physically clogged by the pore space of the filter module and physically adsorbed on the filter media by van der Waals forces, but the kaolin particles less than 6.965 µm were mainly trapped by the electrostatic adsorption onto the filter media. Considering the 100% removal efficiency of all indices in Run 3, a terminal voltage of +1.0 V was adopted at the following experiments (Runs 4-10) using synthetic contaminated source water, anionic surfactant, and Fe-contained water.

3.3.3 Kaolin Particle and Iron Removal Performances in Synthetic Contaminated Source Water and Anionic Surfactant Contained Water through Filtration

The SS, turbidity, color, and Fe removal performances were observed on Runs 4-10 at the terminal voltage of +1.0 V with the filtration hydraulic loading of 283 L m^{-2} min^{-1} (Table 3.1). Since Fe^{2+} was spiked in the influent of Runs 7-10 at the concentration of 10 mg/L, SS in the influent was found to be a little bit more than that of Runs 1-6 (Table 3.2). Figure 3.6 (a-n) show the volume-based particle size distribution of influent and effluent of Runs 4-10. The particle size distribution of influent in Runs 4, 5, and 6 (Figure 3.6 (a), (c), and (e)) show the similar pattern to that in influent of Run 1 (Figure 3.4 (a)), though the influent in Runs 4, 5, and 6 had the similar EC of 480, 670, and 770 µS/cm to that in Run 2 (EC=560 µS/cm) and 3 (EC=550 µS/cm). Figure 3.7 shows the SS, turbidity, color, and Fe removal efficiency of Runs 4-10. In the case of Runs 4-6, SS removal efficiency was found to be lower than that of other runs, where synthetic contaminated source water (Table 3.3) was used for the dilution of kaolin particles in Runs 4 and 5 and, kaolin particles with sodium lauryl sulfate was diluted with DW in Run 6.

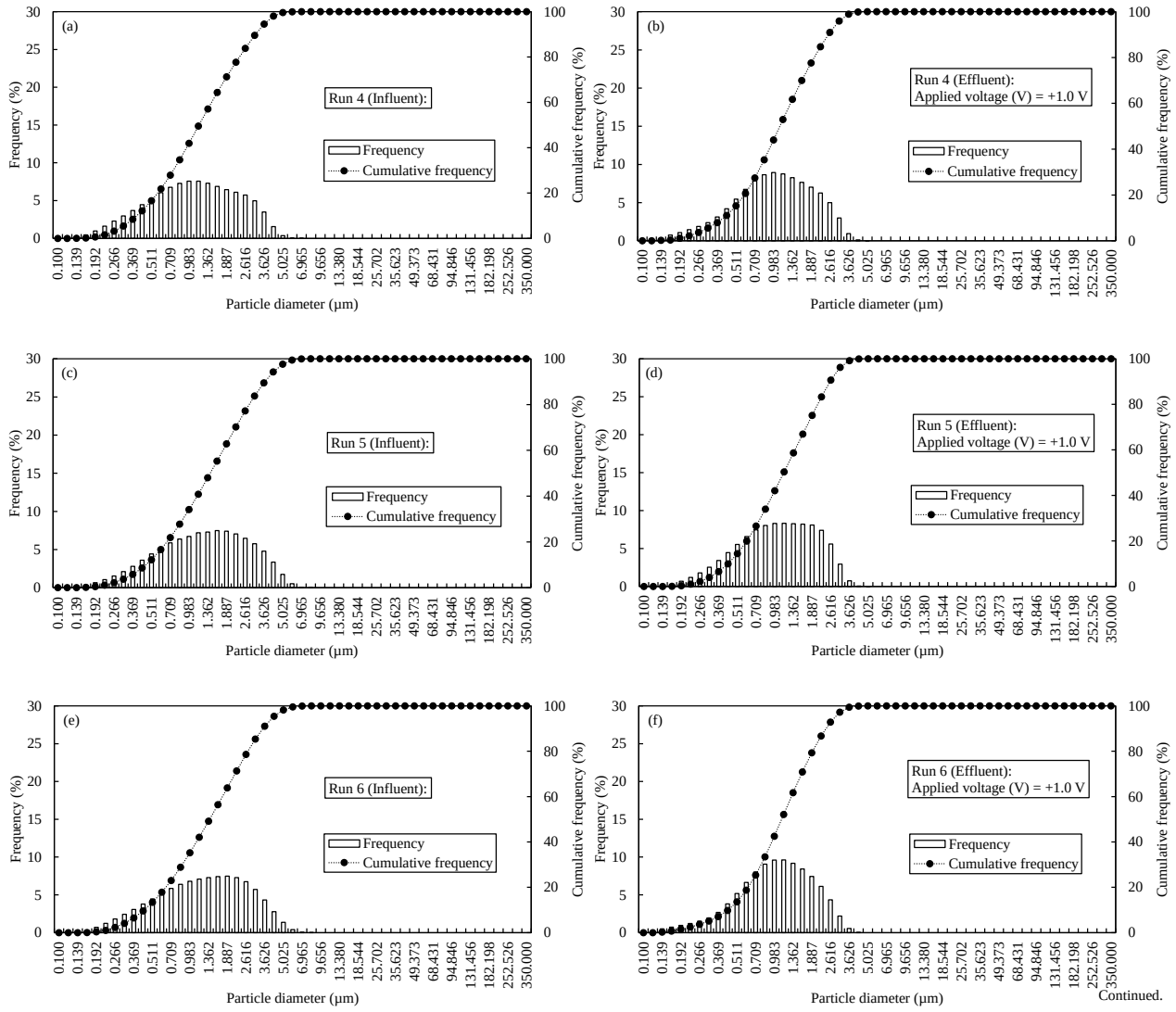

Continued.

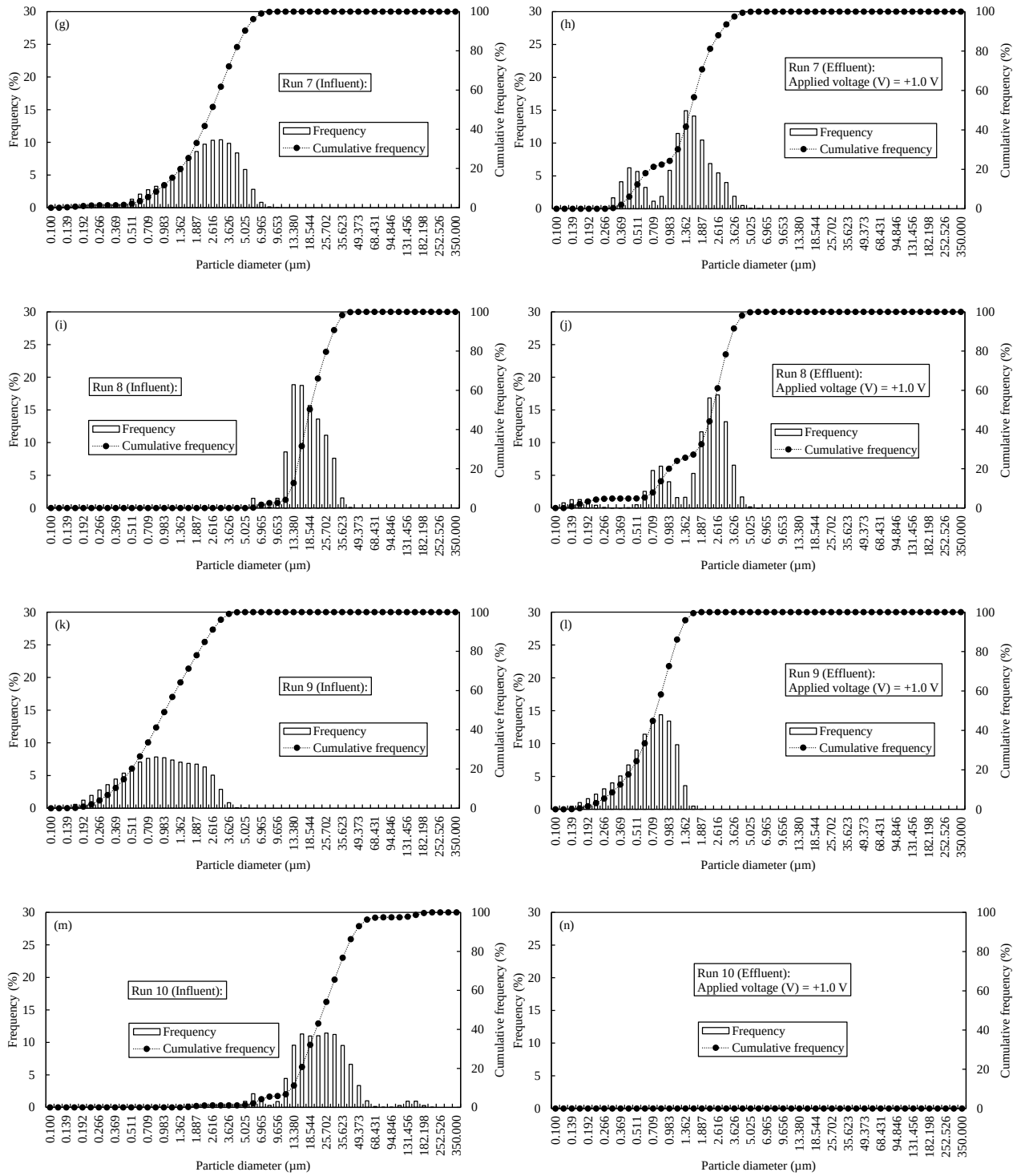

Figure 3.6 (a-n) Volume-based kaolin suspension particle size distribution of influent and effluent of Runs 4-10, where synthetic contaminated source water (Table 3.2) was used as a solvent in Runs 4 and 5. Sodium lauryl sulfate at the concentration of 100 mg/L was used in Runs 6, 9, and 10, and Fe was spiked at the concentration of 10 mg/L in Runs 7-10.

The SS removal efficiency was 22.2% in Run 4 at pH 6.7, 45.7% in Run 5 at pH 7.8, and 51.1% in Run 6 at pH 6.6, respectively, though 100% removal efficiency was observed at Run 3. In Run 6, SS removal efficiency was found to be decreased due to the addition of sodium lauryl sulfate

probably due to the adsorption of negatively charged sodium lauryl sulfate onto the filter media, which changed the surface charge of filter media from positive to negative. Besides, SS removal efficiency in Runs 4 and 5 were found to be much lower than Run 6. Here, it is assumed that anionic surfactant-like compounds were contained in the wastewater, affected seriously in charge-based particle removal mechanism of the depth filtration system (Besra et al., 2006; Stumm and Morgan, 1962).

Figure 3.6 (g) and (i) show the particle size distribution of Runs 7 and 8 in the influent of kaolin suspension with Fe. The particles in the influent were found to be in the range of 0.118-9.653 μm in Run 7 and 4.268-41.938 μm in Run 8. Although Fe was spiked at the same concentration of 10 mg/L in Runs 7 and 8, the particle size distribution showed the different pattern. This was happened due to the difference in the oxidizing behavior of Fe at acidic and alkaline pH. In the case of Run 8, Fe was completely oxidized at pH 8.6 following the equations 1 and 2 and the $Fe(OH)_3$ flocs were accumulated in the solution, which formed larger particles in comparison with original kaolin particles.

$$4Fe^{2+} + O_2 + 4H^+ \rightarrow 4Fe^{3+} + 2H_2O \quad (1)$$

$$Fe^{3+} + 3OH^- \rightarrow Fe(OH)_3\downarrow \quad (2)$$

As a result, SS removal efficiency in Run 8 was nearly equal to100% (Figure 3.7). The Fe removal efficiency of 96.4% in Run 8 supported the above discussion. The less amount of Fe removal efficiency in Run 7 was thought to be due to the partial oxidation of Fe at acidic pH of 4.6, which is supported by the low Fe removal efficiency of 29.9% as shown in Figure 3.7. The un-oxidized Fe easily passed through the filter module, because both the filter module and the Fe were positively charged.

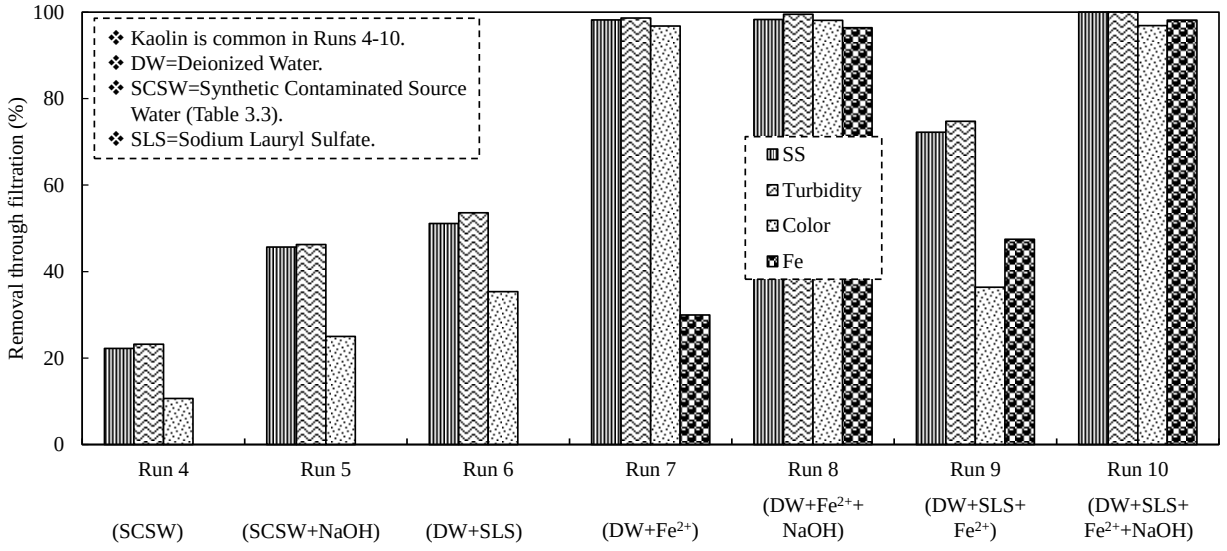

Figure 3.7 SS, turbidity, color, and Fe removal efficiency of Runs 4-10 at the filtration hydraulic loading of 283 L m^{-2} min^{-1}, with the applied terminal voltage of +1.0 V.

Figure 3.6 (k) and (m) show the particle size distribution of Run 9 and 10 in the influent of kaolin suspension with sodium lauryl sulfate and Fe. Here, the particles were found within the range of 0.118-5.025 µm in Run 9 and 0.983-214.498 µm in Run 10. The influent particle size distribution of Runs 9 and 10 show the similar pattern to that of Runs 7 and 8. Moreover, the influent particle size distribution of Runs 6 and 9 were found in the same range like Run 1 (Figure 3.4 (a)), though sodium lauryl sulfate was added in Runs 6 and 9. This result suggests that sodium lauryl sulfate did not take part in particle aggregation. The SS removal efficiency in Run 9 was not so high (72.2%) due to the presence of anionic surfactant as aforementioned in Run 6 and the removal efficiency of Fe was also low (47.5%) due to the acidic pH as was mentioned in Run 7.

On the contrary to Run 9, the SS removal efficiency and the Fe removal efficiency in Run 10 was 100% and 98.1%, respectively. Although sodium lauryl sulfate was present with the Fe colloids in the influent of Run 10, unlike Run 6 sodium lauryl sulfate could not influence on SS and Fe removal performances in Run 10 due to the stronger aggregation of kaolin suspension with Fe colloids at pH 7.9. Similar results were observed by Lay et al. (1995).

From the above experimental results it could be summarize that, kaolin particle removal performances were significantly affected by the contaminated source water (Runs 4 and 5) as well as anionic surfactant-contained water (Run 6) regardless of pH. The complete kaolin particle removal was observed in the pure water (Run 3) and pure water with Fe at alkaline pH (Run 10). Similarly, Fe removal performances were found to be affected in acidic pH (Runs 7 and 9) due to the partial oxidation, and 96.4% Fe removal was observed in Run 8 and 98.1% was observed in Run 10 at slightly alkaline pH.

3.3.4 Evaluation of Total Coliform (TC) and General Bacteria (GB) Removal Performances through Filtration

Figure 3.8 shows the total coliform (TC) and general bacteria (GB) removal performances. This experiment was conducted to observe the TC and GB removal performances through filtration at the hydraulic loading of 283 L m^{-2} min^{-1} with the terminal voltage of +1.0 V. To conduct this experiment, municipal wastewater of Ryukoku University was diluted by a 5-time with normal tap water. Then it was used as influent for the source of TC and GB. Here, the TC and GB concentration in the influent was found to be 88,800 CFU/mL and 116,000 CFU/mL, respectively. The filtrated water volume was 2,000 mL. In this experimental study, the TC and GB removal efficiency through filtration was found to be 23.7% and 30.3%, respectively. Similar removal efficiencies were observed by Green et al. (1997) and Schaub and Sorber (1997).

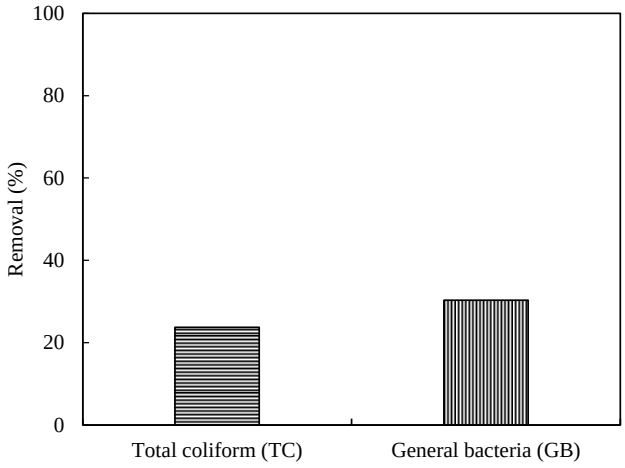

Figure 3.8 TC and GB removal performances through filtration with the terminal voltage of +1.0 V and at the filtration hydraulic loading of 283 L m^{-2} min^{-1}.

3.3.5 Effect of Back-washing on Kaolin Particle and Iron Washout from Filter Media

A series of back-washing experiments were demonstrated on Runs 1-10 at the back-washing hydraulic loading of 1,274 L m^{-2} min^{-1}, using a back-washing solution of DW for the Runs 1-2 and 5 mM-NaCl solution (EC=580 μS/cm) for the Runs 3-10. At the back-washing mode, -1.0 V potential was applied at Runs 3-10 and the potential was not applied at Runs 1-2 (Figure 3.2). Figure 3.9 (a-j) show the volume-based particle size distribution in back-washed water of Runs 1-10. As a whole, the particles diameter of the back-washed water in Runs 1-10 were found to be in the range of 0.139-68.431 μm. Here, part of particles in back-washed water of all the runs were found to be aggregated. The particle aggregation in back-washed water may occur through aeroflocs mechanism due to air intrusion while shifting the operation mode from filtration to the back-washing (Oliveira et al., 2014).

Figure 3.10 shows the SS, turbidity, color, and Fe washout removal performances of Runs 1-10. Here, the washout removal efficiency is defined as the ratio of the amount of particles washed away by the back-washing to the amount of particles removed at the filtration step. The SS washout removal efficiency in Run 3 was higher (72.5%) than that in Run 1 (60.0%) and slightly higher than that in Run 2 (68.2%).

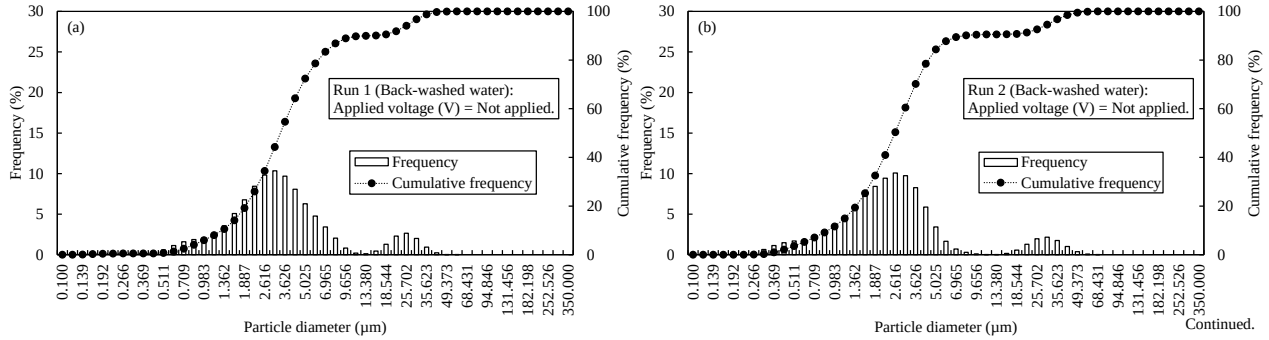

Continued.

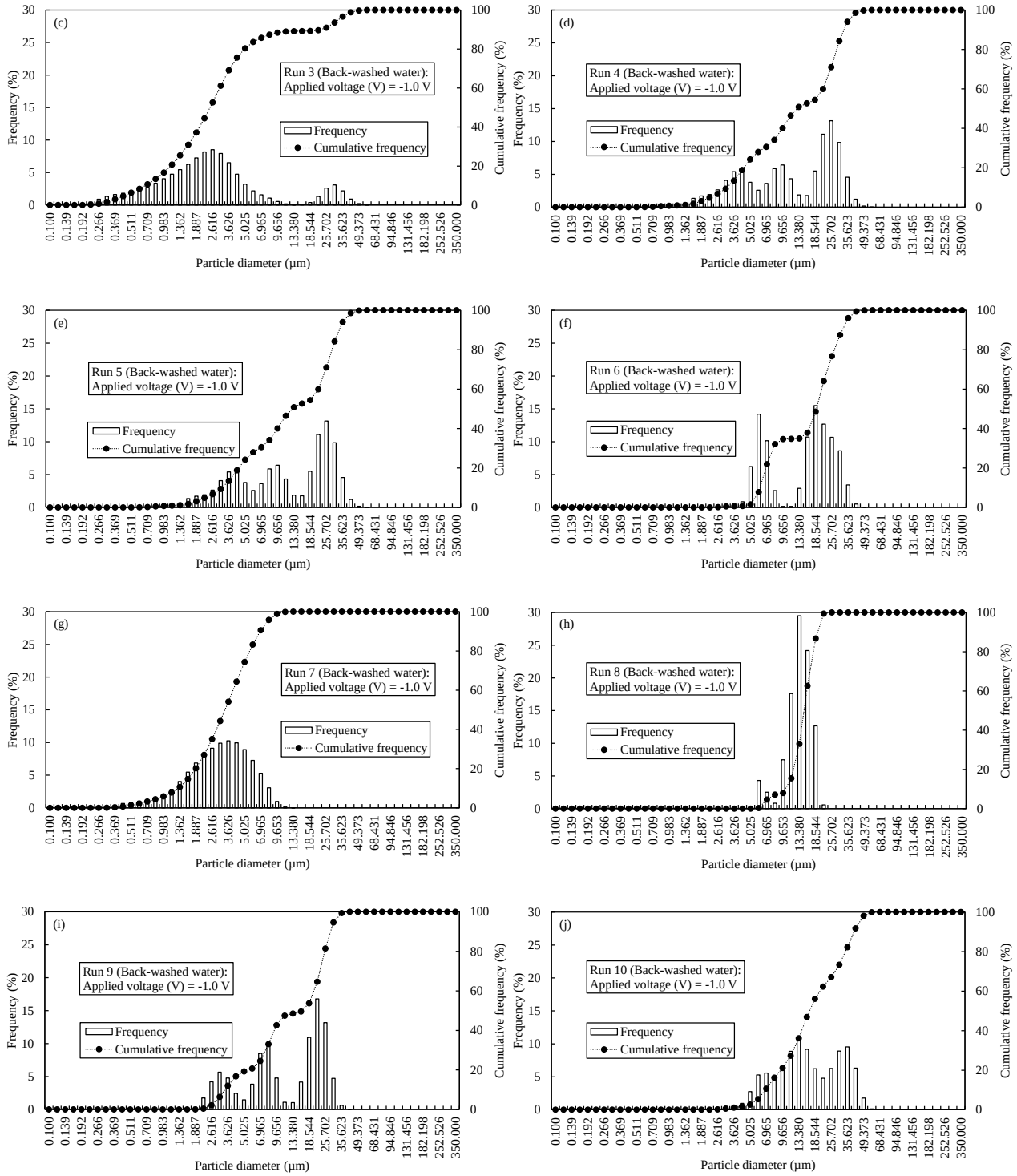

Figure 3.9 (a-j) Volume-based kaolin suspension particle size distribution in back-washed water of Runs 1-10, where the particles in Runs 1-6 were mainly kaolin and Runs 7-10 were kaolin with Fe colloids.

The higher washout removal efficiency in Run 3 was achieved for the application of terminal voltage of -1.0 V, which generated a repulsive fore against the kaolin particles and facilitated in washout removal process. Similar result was observed by Min et al. (2013) which supports this discussion.

Among the Runs 1-10, SS washout removal efficiency in Runs 6, 9, and 10 remained low, namely 7.8%, 4.6%, and 12.5%, respectively (Figure 3.10). Since sodium lauryl sulfate was added into the influent of Runs 6, 9, and 10, it is inferred to inhibit the repulsive force mechanism through the linkage between the filter medium and particles by the hydrophobic tails in the surfactant.

In the case of Runs 4 and 5, sodium lauryl sulfate was not added in the influent, but kaolin particle was diluted in the wastewater shown in Table 3.3. Here, the SS washout removal efficiency was found to be relatively low, namely 59.5% in Run 4 and 55.0% in Run 5. In these cases, such a low washout removal efficiency is predicted due to the presence of anionic surfactant-like compounds in the wastewater, which affected in repulsion mechanism.

The SS washout removal efficiency in Runs 7 (45.9%) and 8 (50.7%) were found to be lower than that in Run 3 (72.5%), but to be higher than that of Runs 6, 9, and 10. In Runs 7 and 8 Fe was spiked into the influent without addition of sodium lauryl sulfate. As a result, SS washout removal was not so much hindered by Fe like the Runs 6, 9, and 10. However, SS washout removal efficiency in Run 7 was found to be a little bit less than Run 8. In this case, the un-oxidized Fe^{2+} was positively charged at pH 4.6. As a result, the application of negative potential in the back-washing step created an attracting force between the Fe^{2+} and the filter media instead of repulsive force, which hindered in SS washout removal efficiency in Run 7.

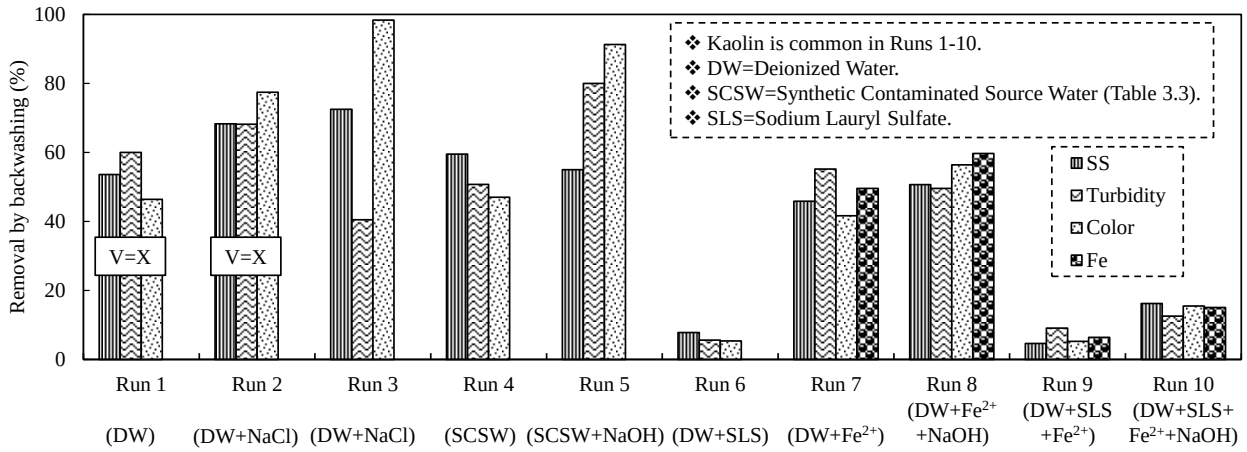

Figure 3.10 SS, turbidity, color, and Fe washout removal performances of Runs 1-10 by back-washing at the back-washing hydraulic loading of 1,274 L m^{-2} min^{-1}, where terminal voltage was not applied in Runs 1 and 2, and -1.0 V terminal voltage was applied in Runs 3-10.

The Fe washout removal efficiency was measured in Runs 7-10. The Fe washout removal efficiency in Run 8 (59.7%) was to some extent higher than that of Run 7 (49.6%). Fe was completely oxidized at alkaline pH and formed hydroxide flocs in Run 8. As a result, a thin soft cake layer of $Fe(OH)_3$

would be formed on the surface of filter media, which were washed away easily at the high back-washing hydraulic loading of 1,274 L m^{-2} min^{-1} from the surface of filter media during the back-washing stage. But, in the case of Runs 9 (6.4%) and 10 (15.1%) the Fe washout removal efficiencies were found to be comparatively very low with respect to Run 8 (59.7%). Since, sodium lauryl sulfate was present in the influent of Runs 9 and 10, which influenced Fe washout removal performances in the back-washing step. This can be explained in such a way that the positively charged hydrophobic tails of sodium lauryl sulfate covered the oxidized or un-oxidized Fe and the application of negative potential in the back-washing step created an attracting force that captured the Fe and hindered in washout removal performances.

From the above discussions it can be summarized that simple back-washing has the potentiality for the washout of physically clogged particles if the particles are deposited over the surface of the filter media like a cake layer. The washout removal efficiency by back-washing of the particles can be enhanced if a repulsive force is created between the particles and the filter media. On the other hand, the washout removal efficiency can be decrease dramatically if the particles are in contact with the anionic surfactant or an anionic surfactant-like compounds, because these types of surfactants inhibit in repulsive force mechanism between the particles and the filter media.

3.4 Conclusion

In this study, an effect of active control potential on filter medium was demonstrated at the terminal voltage of +1.0 V at the filtration operation and of -1.0 V at the back-washing operation using kaolin particle suspensions. An electric current was not observed, when the terminal voltage was impressed, because the applied terminal voltage of ±1.0 V was within the potential window of water electrolysis. Accordingly, the electricity was used only for charging the electrical double layers of filter media and counter electrode. This symptom denotes the zero energy consumption technique and this operation could be highly effective in enhancing charge-based particle separation mechanism in depth filtration.

The zeta potential of kaolin suspension in pure water and synthetic contaminated source water with or without an anionic surfactant showed the negative values, but it varied in a wide range depending on the pH of the solution and iron contamination. The kaolin particle removal efficiency in filtration was observed 100% at the terminal voltage of +1.0 V in the kaolin suspension in 5 mM sodium chloride solution at the hydraulic loading of 283 L m^{-2} min^{-1}. However, the kaolin particle removal efficiency decreased to 22.2-45.7% in synthetic contaminated source water and 51.1% in an anionic surfactant-contained water. On the contrary, the kaolin particle washout removal efficiency was

observed 72.5% at the terminal voltage of -1.0 V at the back-washing hydraulic loading of 1,274 L m^{-2} min^{-1}. But, the kaolin particle washout removal efficiency was decreased to 55.0-59.5% in wastewater and 4.6-12.5% in an anionic surfactant-contaminated water. The iron colloids suspension washout removal performances was observed to be 59.7% in an anionic surfactant-free water, but 6.4% in an anionic surfactant-contained water.

Moreover, total coliform and general bacteria removal efficiency were found to be 23.7% and 30.3%, respectively. Therefore, the application of electric charge technique in the depth filtration would be effective in removing colloidal size particles like inorganic and organic particles in the sewage contaminated water, though the removal of total coliform and general bacteria was not expected very much. From this experimental study, I recommend 0.283 m^3 m^{-2} min^{-1} hydraulic loading for the removal of organic aggregates and iron colloids with the terminal voltage of +1.0 V. For the washout of organic aggregates and iron colloids from the filter media I recommend the hydraulic loading of 1.27 m^3 m^{-2} min^{-1} with 5 mM sodium chloride contained pure water with the terminal voltage of -1.0 V.

3.5 References

Adelkhani, H., Nasoodi, S., Jafari, A. H., (2009). A study of the morphology and optical properties of electropolished aluminum in the Vis-IR region. International Journal of Electrochemical Science., 4, 238-246.

Besra, L., Sengupta, D. K., Roy, S. K., (2006). Influence of unadsorbed and weakly adsorbed flocculants on separation properties of kaolin suspensions. International Journal of Mineral Processing., 78 (2), 101-109.

Brunke, M., (1999). Colmation and depth filtration within streambeds: Retention of particles in hyporheic interstices. International Review of Hydrobiology., 84 (2), 99-117.

Cushing, R. S., Lawler, D. F., (1998). Depth filtration: fundamental investigation through three-dimensional trajectory analysis. Environmental Science & Technology., 32, 3793-3801.

Darby, J. L., and Lawler, D. F., (1990). Ripening in depth filtration: effect of particle size on removal and head loss. Environmental Science & Technology., 24 (7), 1069-1079.

Darby, J. L., Lawler, D. F., Wilsusen, T. P., (1991). Depth filtration of wastewater: particle size and ripening. Research Journal of the Water Pollution Control Federation., 63 (3), 228-238.

Ding, B., Li, C., Dong, X., (2015). Percolation-based model for straining-dominant deep bed filtration. Separation and Purification Technology, 147, 82-89.

Foess, G. W., Borchardt, J. A., (1969). Electrokinetic phenomena in the filtration of algal suspensions. Journal American Water Works Association., 61 (7), 333-338.

Goldberg, S., Glaubig, R. A., (1987). Effect of saturating cation, pH and aluminum and iron oxide on the flocculation of kaolinite and montmorillonite. Clays and Clay Minerals., 35 (3), 220-227.

Green, M. B., Griffin, P., Seabridge, J. K., Dhobie, D., (1997). Removal of bacteria in subsurface flow wetlands. Water Science and Technology., 35 (5), 109-116.

Hamamoto, S., (2016). Enhanced coagulation by the control of electrostatic interaction between contaminants and metal hydroxide flocs. Master Thesis of Ryukoku University (In Japanese).

Ho, K. C., Singleton, D. E., Greenberg, C. B., (1990). The influence of terminal effect on the performance of electrochromic windows. Journal of The Electrochemical Society., 137 (12), 3858-3864.

Hou, K., Gerba, C. P., Goyal, S. M., Zerda, K. S., (1980). Capture of latex beads, bacteria, endotoxin, and viruses by charge-modified filters. Applied and Environmental Microbiology., 40 (5), 892-896.

Huang, C., Pan, J. R., Huang, S., (1999). Collision efficiencies of algae and kaolin in depth filter: The effect of surface properties of particles. Water Research., 33 (5), 1278-1286.

Ison, C. R., Ives, K. J., (1969). Removal mechanisms in deep bed filtration. Chemical Engineering Science., 24 (4), 717-729.

Jackson, G. E., Letterman, R. D., (1980). Granular media filtration in water and wastewater treatment, part 1. C R C Critical Reviews in Environmental Control., 10 (4), 339-373.

Jefferson, B., Sharp, E. L., Goslan, E., Henderson, R., Parsons, S. A., (2005). Application of charge measurement to water treatment process. Water Science and Technology: Water Supply., 4 (5-6), 49-56.

Jegatheesan, V., Vigneswaran, S., (2003). Mathematical modelling on deep bed filtration. Proceedings of MODSIM International Congress on Modelling and Simulation., 4, 1805-1810.

Kishimoto, N., Kawasaki, H., Sasaki, T., Sasaki, S., (2010). Effect of active control of electric potential of filter medium on depth filtration. Water Science & Technology., 62 (5), 1022-1027.

Lay, M. L., Wu, H. M., Huang, C. H. (1995). Study of the zeta potential of Fe(O)OH colloids. Journal of Materials Science., 30, 5473-5478.

Min, F., Zhao, Q., Liu, L., (2013). Experimental study on electrokinetic of kaolinite particles in aqueous suspensions. Physicochemical Problems of Mineral Processing., 49 (2), 659-672.

Moayedi, H., Huat, B. B. K., Kazemian, S., Daneshmand, S., Moazami, D., Niroumand, H., (2011). Electrophoresis of suspended kaolinite in multivalent electrolyte solution. International Journal of Electrochemical Science., 6, 6514-6524.

Oliveira, C., Rodrigues, R. T., Rubio, J., (2014). Operating parameters affecting the formation of kaolin aerated flocs in water and wastewater treatment. Clean-Soil, Air, Water., 42 (7), 909-916.

Rice, E. W., Baird, R. B., Eaton, A. D., Clesceri, L. S., (2012). Standard Methods for the Examination of Water and Wastewater. 22nd Edition. Washington, DC: American Public Health Association, American Water Works Association, Water Environment Federation.

Schaub, S. A., Sorber, C. A., (1997). Virus and bacteria removal from wastewater by rapid infiltration through soil. Applied and Environmental Microbiology., 33 (3), 609-619.

Stephan, E. A., Chase, G. G., (2001). A preliminary examination of zeta potential and deep bed filtration activity. Separation and Purification Technology., 21 (3), 219-226.

Stumm, W., Morgan, J. J., (1962). Chemical aspects of coagulation. American Water Works Association., 54 (8), 971-994.

Tien, C., Payatakes, A. C., (1979). Advances in depth bed filtration. ALChE Journal., 25 (5), 737-759.

Yukselen, Y., Kaya, A., (2003). Zeta potential of kaolinite in the presence of alkali, alkaline earth and hydrolysable metal ions. Water Air and Soil Pollution., 145 (1), 155-168.

Chapter IV
Inorganic Nitrogen and Microorganisms Removal through Electrolysis

4.1 Introduction

Chapter II revealed that the reverse osmosis (RO) process had a potential to produce potable water with acceptable water quality from the contaminated source water. However, the rejection efficiency of inorganic nitrogen such as ammonia was relatively low even if the RO process was applied. Therefore, a process assisting the RO process should be introduced for the removal of inorganic nitrogen. Furthermore, a membrane fouling was a serious threat for extended operation of the RO process. In order to remove foulants from the feed water in the RO process, the depth filtration with the active control of the surface charge of the filter media was discussed as a pre-treatment technique in Chapter III. The depth filtration successfully removed particulate foulants from the contaminated source water. However, the removal efficiencies of total coliform (TC) and general bacteria (GB) remained low, which would cause the biofouling of the RO membrane. Accordingly, a pre-treatment technique for the removal of TC and GB should be also introduced prior to the RO process in this study.

Electrolysis is a technique to promote non-spontaneous chemical reactions driven by electric potential. The electrolysis principle was first formulated by Michael Faraday in 1820. In an electrochemical cell, an application of electric voltage moves cations and anions to cathodes and anodes, respectively, and results in the reduction of cations and oxidization of anions (Chopra et al., 2011). The electrochemical water treatment concept was first inaugurated at the beginning of the nineteenth century in the United Kingdom (UK). After that, it has been widely used elsewhere in the field of water and wastewater treatment due to its high effectiveness, lower maintenance cost, and rapid removal of pollutants. Besides, electrolysis offers prospective advantages over conventional treatment process such as coagulation, flocculation, and sedimentation, because it can be operated at normal temperature and pressure with a relatively simple equipment (Bejan et al., 2005).

The invention of electricity and the availability of electrical power have facilitated the enhancement of the electrochemical technologies to the door point of many fields (Chen, 2004). Nowadays, these technologies are commonly employed in many places to deal with water treatment for the removal of nitrogenous compounds particularly nitrate (NO_3^-), nitrite (NO_2^-), and ammonia (NH_3)/ammonium (NH_4^+) along with microbial organisms like TC and GB (Lin and Wu, 1996; Pavlovic et al., 2014). Because, it shows comparatively high treatment efficiency, negligible amount of sludge production, small area consumption, and quite low investment cost (Genders et

al., 1996; Duarte et al., 1998). Therefore, electrolysis may be a suitable candidate as a pretreatment technique for inorganic nitrogen removal from the contaminated source water.

Conversely, electrolysis is by some means considered as challenging task in wastewater treatment due to its low current efficiency, formation of insulating deposits on the electrode surface, and expensive electrode materials. However, in the last decades numerous cathode materials have been studied by several researchers in electrochemical denitrification such as, copper (Cu), iron (Fe), zinc (Zn), platinum (Pt), iridium (Ir), lead (Pd), and gold (Au). Some electrodes like Cu and Fe presented quite efficient promoter for NO_3^- reduction (Dash and Chaudhari, 2005; Ureta-Zanartu and Yanez, 1997). Nevertheless, NO_3^- removal from potable water, wastewater, and concentrated solutions that come from the reverse osmosis (RO), electro-dialysis, and ion exchange resin is a critical issue in environmental protection. To solve this issue, copious research works on biological, catalytic, and electro-catalytic methods have been looked at for the removal of NO_3^- (Polatides et al., 2005). The electrochemical reduction of NO_3^- leads to a relatively broad spectrum of products, such as nitrogen gas (N_2), hydroxylamine (NH_2OH), nitrous oxide (N_2O), nitric oxide (NO), and NH_3 (Gootzen et al., 1997). The pattern of NO_3^- reduction on catalysts and electro-catalysts can be stated as follows (Katsounaros and kyriacou, 2007):

$$\begin{array}{ccccccc} & & & & NO_{(g)} & & \\ & & & & \uparrow & & \\ NO_3^- & \rightarrow & NO_2^- & \rightarrow & NO & \rightarrow & NH_2OH \rightarrow NH_3 \\ & & & & \downarrow & & \\ & & & & N_2O_{(g)} & \rightarrow & N_{2(g)} \end{array}$$

However, in an electrochemical cell first of all, NO_3^- is mainly reduced to NO_2^- and NH_3 in the course of cathodic cycle following the reactions 1 and 2. Secondly, the produced NO_2^- and NH_3 are oxidized to NO_3^- and N_2 in the anodic cycle following the reactions 3 and 4 (Bouzek et al., 2001).

Reactions in the cathodic cycle:

$$NO_3^- + H_2O + 2e^- \rightarrow NO_2^- + 2OH^- \quad (1)$$

$$2NO_3^- + 12H_2O + 16e^- \rightarrow 2NH_3 + 18OH^- \quad (2)$$

Reactions in the anodic cycle:

$$NO_2^- + H_2O \rightarrow NO_3^- + 2H^+ + 2e^- \quad (3)$$

$$2NH_3 \rightarrow N_2 + 6H^+ + 6e^- \quad (4)$$

On the contrary, during the electrochemical reduction of NO_3^-, simultaneous electrochemical oxidation of NH_3 to N_2 is to some extent very difficult at a constant potential (Li et al., 2009). Thus, it seems to be very tough to find out the appropriate conditions to perform both cathodic reduction of NO_3^- and anodic oxidation of the produced NH_3 in an electrochemical flow cell (Vanlangendonck et al., 2005).

In general, electrolysis of water containing sufficient amount of chloride ion (Cl^-) produces chlorine (Cl_2) by anodic oxidation. Then, Cl_2 reacts with water (H_2O) and forms hypochlorous acid (HOCl) following the equations 5 and 6. Further, HOCl reacts with the NH_3 and converts it into N_2 through break-point chlorination mechanism (Pressley et al., 1972).

$$2Cl^- \rightarrow Cl_2 + 2e^- \quad (5)$$

$$Cl_2 + H_2O \rightarrow HOCl + HCl \quad (6)$$

In this regards, titanium (Ti)/titanium oxide (TiO_2) or rubidium oxide (RuO_2) anode has been advocated for the efficient removal of NH_3 with the appropriate amount of Cl^- concentration in the electrolyte, for example 1g/L (Feng et al., 2003).

Therefore, in this study I intended to find out the appropriate conditions to perform both cathodic reduction of NO_3^- to NO_2^- and NH_3 and along with anodic oxidation of the produced NH_3 with the presence of suitable Cl^- concentration to occur break-point chlorination. In addition, a cation exchange membrane was inserted between the two-compartment electrochemical flow cell to evaluate the NO_3^- removal performances, where cation exchange membrane functioned to block the migration of anions and water molecules to anode compartment, but allowed cations to move to the cathodic compartment. The objective of this research was to find out an optimum condition in response to the several parameters specially flow rate, electric charge, and Cl^- concentration to occur break-point chlorination for the removal of nitrogenous compounds along with total coliform and general bacteria.

4.2 Materials and Methods

4.2.1 Cyclic Voltammetry

A cyclic voltammetry (CV) was used to investigate NO_3^- reduction characteristics of copper cathode. Here, saturated silver/silver-chloride (Ag/AgCl) electrode was used as a reference electrode and a platinum coated titanium (Ti/Pt) electrode was used as a counter electrode. Working electrode was prepared by polishing the surface with an alumina-based abrasive (#800~#100, 3M, Japan). Test solution was prepared with reagent grade chemicals (Wako Chemical, Japan) of potassium sulfate (K_2SO_4) and potassium nitrate (KNO_3) diluted with deionized water (DW). The K_2SO_4 was used as a supporting electrolyte to ensure sufficient electrical conductivity (EC), since it is a strong electrolyte and fully ionized in water. The concentration of supporting electrolyte was determined considering the similarity to EC of general source water. The pH and EC of 1 mM K_2SO_4 solution was 6.8 and 290 µS/cm, respectively. On the other hand, the pH and EC of 1 mM K_2SO_4 with 1.42 mM KNO_3 solution was 5.3 and 440 µS/cm, respectively. The surface area of the working electrode was 1.0 cm^2. The potential sweep was cycled five times between +0.15 V to -1.23 V at a scan rate

of 50 mV/sec from forward to backward scan direction for getting stable polarization using an automatic polarization electrochemical system (HSV100, Hokuto Denko, Japan).

4.2.2 Experimental Apparatus for Electrolysis

Figure 4.1 shows the laboratory scale experimental setup. It was composed of a hand-made electrolytic flow cell, a feed pump (RP-1000, EYELA, Japan), and a direct current (DC) power supply (PW18-3AD, Kenwood, Japan). Figure 4.2 shows the structure of the electrolytic flow cell. The flow cell was divided into two compartments, namely cathodic and anodic by inserting a flat sheet cation exchange membrane (Nafion NE-1110, DuPont, USA) between two compartments.

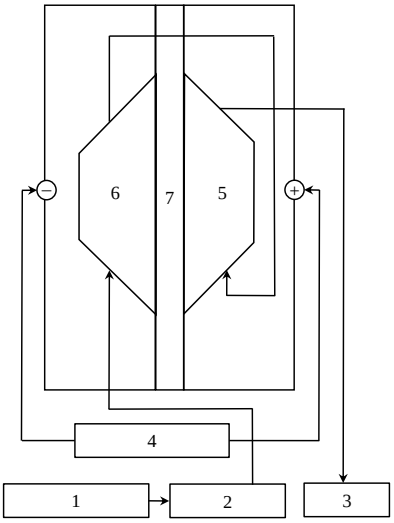

Figure 4.1 Laboratory scale experimental setup. 1: Synthetic water, 2: Feed water pump, 3: Effluent, 4: DC power supply, 5: Anode chamber, 6: Cathode chamber, and 7: Cation exchange membrane.

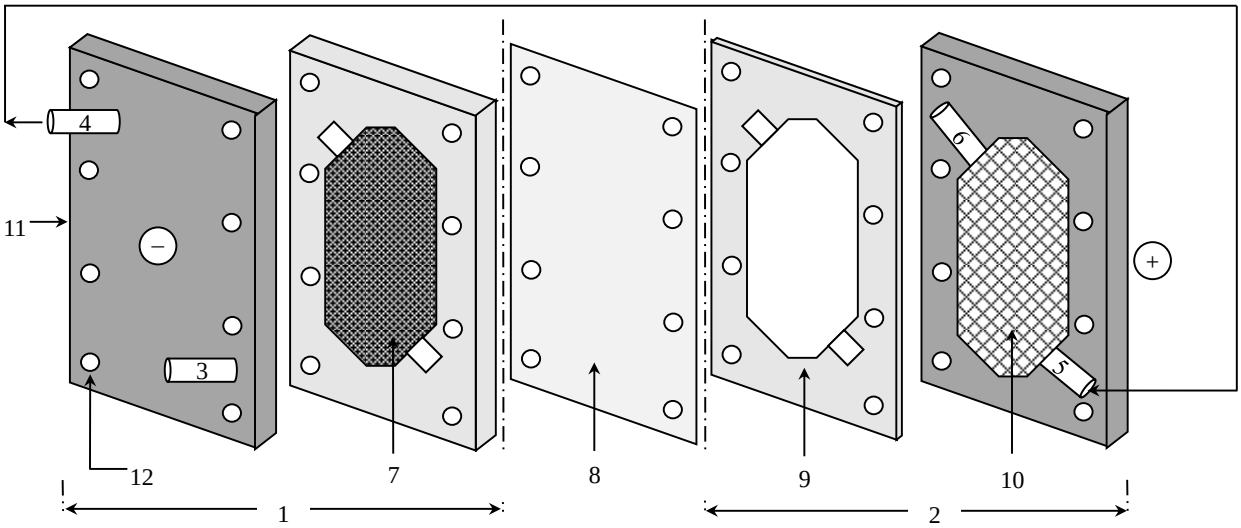

Figure 4.2 Structure of the electrolytic flow cell. 1: Cathodic compartment, 2: Anodic compartment, 3: Water inlet tube in the cathode chamber, 4: Water outlet tube in the cathode chamber, 5: Water inlet tube in the anode chamber, 6: Water outlet tube in the anode chamber, 7: Copper mesh, 8: Cation exchange membrane, 9: Silicon rubber sheet, 10: Polytetrafluoroethylene mesh, 11: Acrylic resin cover, and 12: Bolts.

Ten sheets of copper (Cu) meshes (#40/36, 0.28 mm in the diameter of Cu wire) with the configuration of 50 cm^2 constituted the cathode by stacking them in the cathodic chamber. The effective cathode area amounted to be 2,892 cm^2. The anodic compartment was equipped with a Ti/Pt plate electrode at the outside of the compartment with the effective area of 50 cm^2 and was filled with a polytetrafluoroethylene mesh sheet. The flame of the compartment was made of a silicon sheet with 4 mm in thickness for cathodic and 1 mm in thickness for anodic one. Accordingly, the empty volume of cathodic and anodic compartment was 20 cm^3 and 5.0 cm^3, respectively. All parts of the cell were fastened tightly with 8 bolts.

4.2.3 Experimental Procedure for Electrochemical Denitrification

Before each experimental run positive and negative terminals of the DC power supply was perfectly connected with the anode and the cathode, respectively. After that, the feed pump was switched on to feed the synthetic water as well as synthetic contaminated source water into the electrolytic flow cell. Then the DC power supply was turned on for galvanostatic electrolysis. All the runs were performed under air-conditioned room temperature at 25°C. For sampling and analysis the effluent from anodic compartment was collected by using laboratory grade glass bottles. Synthetic water ingredients used for the experiments are given in the Table 4.1.

Table 4.1 List of chemicals used in synthetic water for the electrochemical denitrification experiment.

Name of chemicals	Concentrations	Functions
Potassium sulfate (K_2SO_4)	174.25 (mg/L)/(1 mM)	Supporting electrolyte
Potassium nitrate (KNO_3)	144.43 (mg/L)/(1.42 mM)/NO_3^--N=20 (mg/L)/ NO_3^-=88.57 (mg/L)/NO_3^-=1.42 mM	Source of nitrate ion
Sodium chloride (NaCl)	100-800 (mg-Cl^-/L)/329.68-1318.72 (mg/L)	Source of chloride ion
Citric acid monohydrate ($C_6H_8O_7.H_2O$)	10,507 (mg/L)/50 mM	Used to remove oxide layers of copper meshes
Sodium bicarbonate ($NaHCO_3$)	8,400 (mg/L)/100 mM	Used to adjust the pH
Sulfuric acid (H_2SO_4)	Density (1.84 g/mL)	Used to adjust the pH

Table 4.2 Characteristics of synthetic contaminated source water in electrochemical denitrification experiment.

SS (mg/L)	EC (µS/cm)	pH	NO_2^- (mM)	NO_3^- (mM)	NH_4^+ (mg/L)/(mM)	COD (mg/L)
0.0	270	7.0	0.0	0.0	5.28/0.29	41.0

SS=Suspended Solids; EC=Electrical Conductivity.

Table 4.2 shows the characteristics of synthetic contaminated source water characteristics, which was a filtrated municipal wastewater in Ryukoku University was diluted by a 5-time with normal

tap water. The filtration of the wastewater was performed using a glass fiber filter with 1µm particle rejection (GF/B, Whatman, Japan). The synthetic water as well as synthetic contaminated source water was fed into the cathodic compartment, and then its effluent flowed into the anodic compartment. Before each experimental operation Cu meshes were submersed into 50 mM citric acid monohydrate ($C_6H_8O_7.H_2O$) solution for 5 minutes for removing the oxide layers. Then, they were washed with deionized water (DW) water for several times and used for the experiment.

4.2.4 Analytical Methods

The pH and EC was measured by a pH meter (B-212, Horiba, Japan) and an EC meter (Twin cond, B-173, Horiba, Japan), respectively. The concentrations of NO_2^- and NO_3^- were determined by the ion chromatography (PIA-1000, Shimadzu, Japan) and NH_4^+ was determined by the phenate method (4500-NH_3 F) (Rice et al., 2012). Total chlorine and free chlorine was measured by a chlorine meter (HI95711, Hanna Instruments, Romania). Total coliform (TC) and general bacteria (GB) were measured by test papers for TC and GB (Sibata, Saitama, Japan) using colony count, most-probable-number (MPN) method with thermostat incubator (CALBOX, CB-101, Sibata, Saitama, Japan). DW of EC less than 1 µS/cm was used for the dilution and preparation of standard solution, as obtained from a water purification system (Autostill, WA5000, Yamato, Japan).

4.3 Results and Discussion

4.3.1 Cyclic Voltammetry on Copper as Cathode Material

Figure 4.3 (a) shows the cyclic voltammogram (CV) of 1 mM K_2SO_4 (EC=290 µS/cm) at the scan rate of 50 mV/s on copper as a working electrode. The CV was developed in combination with the capacitive or non-faradic and faradic current. The graph in Figure 4.3 (a) shows small amount of non-faradic current that was used for the accumulation or removal of electrical charges on the electrode and electrolyte solution near the electrode.

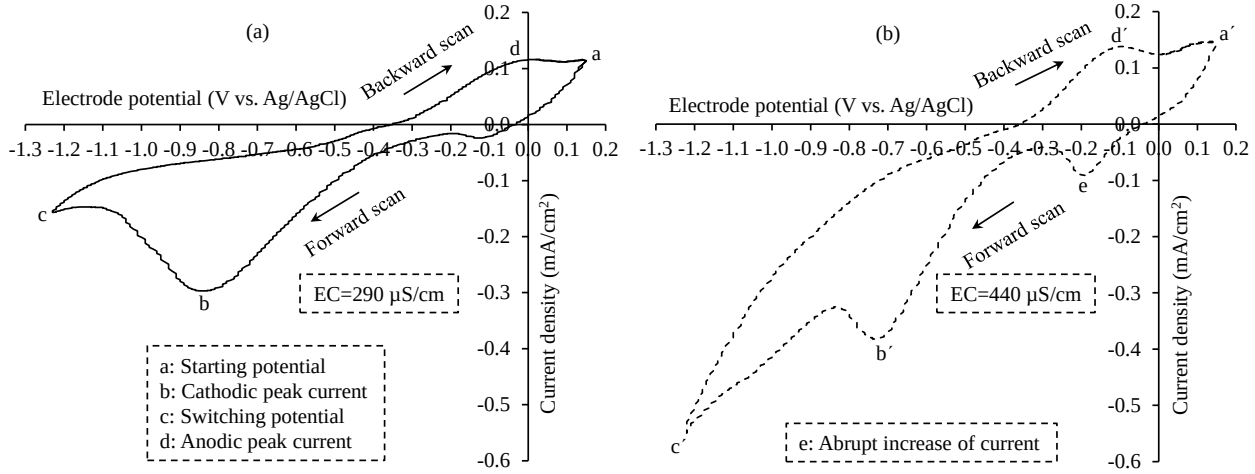

Figure 4.3 Cyclic voltammograms of (a) 1mM K_2SO_4, and (b) 1mM K_2SO_4 with 1.42 mM KNO_3 at the scan rate of 50 mV/s using a copper as working electrode with a surface area of 1.0 cm^2.

Conversely, the faradic current higher than the non-faradic current was the result of electrochemical reactions at the electrode surface. Here, the CV developed two peak currents at the forward and backward scan directions namely, cathodic b and anodic d peak current. In this study, Figure 4.3 (a) and (b) showed the similar CV pattern, but Figure 4.3 (b) showed higher electrolytic current than Figure 4.3 (a) which was caused by the higher EC of the used electrolytic solution.

On the other hand, Figure 4.3 (b) shows the CV of 1mM K_2SO_4 with 1.42 mM KNO_3 (EC=440 µS/cm) under the same condition. This CV curve showed two cathodic peak currents at point e and b´. Accordingly, NO_3^- was mainly reduced by the cathodic reduction at the negative potential of -0.2 V at point e and the reduced species were thought to be stable intermediate byproducts such as NO_2^- or NH_3 (De et al., 2004). Significantly, at the backward scan direction another recognizable abrupt increase of anodic current was not observed, except anodic peak current d´, which denotes that the reduced species such as NO_2^- was not re-oxidized to NO_3^-. This phenomenon indicates one step NO_3^- reduction mechanism such as NO_3^- into NO_2^- (reaction 1), NO_3^- into NH_3 (reaction 2) or NO_3^- into N_2 following the equation 7 (Thinh et al., 2007):

$$2NO_3^- + 6H_2O + 10e^- \rightarrow N_2 + 12OH^- \qquad (7)$$

4.3.2 Influence of Volumetric Electric Charges and Flow Rates on Conversion of Nitrate to Nitrite and Ammonia

In this study, a series of electro-reduction experiments were conducted in the synthetic solution with 1.42 mM of NO_3^- and 1 mM of K_2SO_4 at an initial pH of about 5.5 (Table 4.1). Figure 4.4 (a) shows the effect of volumetric electric charges on transformation of NO_3^- to NO_2^- and NH_4^+ at a constant flow rate of 20 mL/min, which was equivalent to the space velocity (SV) of 1.0 min^{-1}. Here, total nitrogen (TN) indicates the sum of NO_3^-, NO_2^-, and NH_4^+ nitrogen concentration. The applied electrolytic current ranged from 0.10 to 2.90 A, which were equivalent to the volumetric electric charges from 300 to 8,700 C/L.

At these volumetric electric charges the main reduced intermediate products were found to be NO_2^- and NH_4^+. De et al. (2004) also detected similar intermediate nitrogenous compounds, which coincide with this experimental results. Here, the enhancement of NO_3^- reduction with the increase in volumetric electric charges were observed at 300, 1,500 and 2,700 C/L, where NO_3^- concentrations were measured 1.18, 0.92, and 0.71 mM, respectively. This result indicates that 16.9% of the initial NO_3^- was reduced at 300 C/L, 35.2% at 1,500 C/L and 50.0% at 2,700 C/L. In these cases, an increase in the reduction rate of NO_3^- at higher electrolytic current was thought to be reasonable. Since, an electrochemical reduction rate of an element depends on electrolytic

current under electron transfer-controlled condition. This statement was true for the volumetric electric charges of 300 to 2,700 C/L, where NO_3^- reduction rate increased with the increase in supplied electric charge that supports with the experimental results of Li et al. (2010).

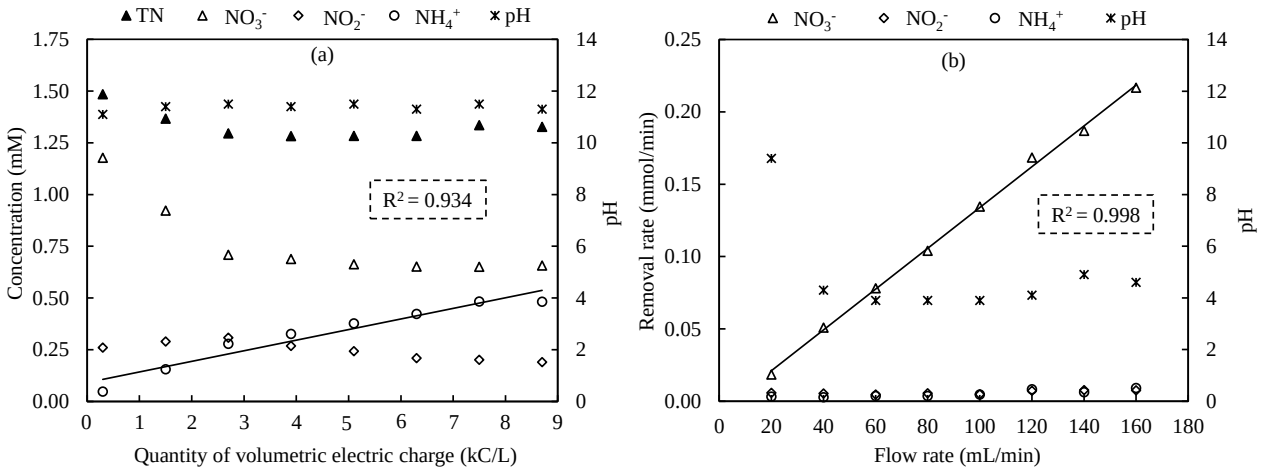

Figure 4.4 Effect of (a) Volumetric electric charges, and (b) Flow rates on transformation of NO_3^- to NO_2^- and NH_4^+. The flow rate was set at 20 mL/min (SV: 1.0 min^{-1}) for Figure 4.4 (a), and the volumetric electric charge was fixed at 1,500 C/L for Figure 4.4 (b).

However, NO_3^- reduction rate was found to be unchanged from the volumetric electric charges of 2,700 to 8,700 C/L. In these cases, it can be supposed that applied excess electric charges were consumed for hydrogen evolution at the cathode and hydrogen was adsorbed on the cathode which affected on NO_3^- reduction process. In the case of NO_2^-, it slightly increased with the increase in volumetric electric charges from 300 C/L to 2,700 C/L, within the range of 0.26-0.31 mM. After that, it marginally decreased up to the volumetric electric charges of 8,700 C/L, where NO_2^- was found to be 0.19 mM. Here, NO_2^- concentration gradually decreased with the increase in volumetric electric charges may be occurred due to the hydrogen evolution, where it could play an important role in cathodic reduction of NO_3^- to NO_2^- (De et al., 2000; Polatides et al., 2005; Prashad et al., 2005). On the other hand, hydrogen evolution did not play any inhibition role in NH_4^+ formation from NO_3^-. A clear linear relationship between NH_4^+ formation and the volumetric electric charges was observed at the R^2 value of 0.934 in Figure 4.4 (a).

The pHs of all treated solutions in the effluent were found to be increased from about 5.5 to 11.5. This was happened mainly due to the reactions forming hydroxide ions (OH^-) during the electrochemical reduction of NO_3^- (equations 1 and 2). The high pH along with almost constant TN concentration of electrolyzed effluent recommends that NO_3^- was mainly transformed into NO_2^- and NH_3 according to the equations 1 and 2 in the cathode chamber (Chiang et al., 1995; Dash and Chaudhari, 2005; Li and Liu, 2009; Lin and Wu, 1996).

Figure 4.4 (b) shows the effect of flow rates on NO_3^- removal rate and formation rates of NO_2^- and NH_4^+ at the volumetric electric charge of 1,500 C/L. These experiments were also conducted using the same synthetic solution in Figure 4.4 (a) (Table 4.1). From Figure 4.4 (b) it is observed that the NO_3^- removal rate was linearly increased with the increase in flow rates at the R^2 value of 0.998. This phenomenon can be ascribed to the enhancement of the mass transfer processes.

4.3.3 Influence of Chloride Ion Concentration on Reduction of Nitrogenous Compounds

Figure 4.5 (a), (b), (c), and (d) show the variation of TN, NO_3^-, NO_2^-, NH_4^+, and chloramines concentration after electrolysis with the presence of different dozes of NaCl. These experiments were performed with 1mM K_2SO_4, 1.42 mM NO_3^-, and varied Cl^- concentration of 100, 200, 400, and 800 mg/L, respectively (Table 4.1). In addition, Figure 4.5 (e) and (f) show NH_4^+ and chloramines concentration in the same effluent at Cl^- concentration of 400 and 800 mg/L at pH 5, 7, and 9, respectively. The pH of the effluent was adjusted by adding buffer solution of 100 mM sodium bicarbonate ($NaHCO_3$) with sulfuric acid (H_2SO_4) (Table 4.1).

It is well known that Cl^- is converted into active Cl_2 through an anodic reaction in an electrochemical cell according to the equation 5. After that, the produced Cl_2 rapidly hydrolyses to HOCl according to the equation 6. Next, NH_3 in water reacts with HOCl and typically formed chloramines, namely monochloramine (NH_2Cl), dichloramine ($NHCl_2$), and trichloramine or nitrogen trichloride (NCl_3) depending on the pH, temperature, reaction time, and other surrounding environmental conditions according to the equations (8-10). And finally, chloramines are oxidized into N_2 or N_2O according to the equations 15 and 16 (Kim et al., 2005; Rajeswar and Ibanez, 1997).

$$NH_3 + HClO \rightarrow NH_2Cl + H_2O \quad (8)$$

$$NH_2Cl + HClO \rightarrow NHCl_2 + H_2O \quad (9)$$

$$NHCl_2 + HClO \rightarrow NCl_3 + H_2O \quad (10)$$

$$2NH_2Cl \rightarrow NHCl_2 + NH_3 \quad (11)$$

$$2NH_2Cl + HOCl \rightarrow N_2 + 3HCl + H_2O \quad (12)$$

$$NH_2Cl + NHCl_2 \rightarrow N_2 + 3HCl \quad (13)$$

$$2NHCl_2 + H_2O \rightarrow N_2O + 4HCl \quad (14)$$

The above equations can be summarized as follows:

$$2NH_3 + 3Cl_2 \rightarrow N_2 + 6HCl \quad (15)$$

$$2NH_3 + 4Cl_2 + H_2O \rightarrow N_2O + 8HCl \quad (16)$$

$$NH_3 + 3Cl_2 \rightarrow NCl_3 + 3HCl \quad (17)$$

From Figure 4.5 (a) and (b) it is observable that, NO_3^- was transformed into NO_2^- and NH_4^+ in the

similar trend. As a result, NH_4^+ and chloramines were accumulated with an increase in volumetric electric charges due to addition of small amount of Cl^- concentration of 100 and 200 mg/L, respectively, but any significance decrease in TN was not observed.

Form Figure 4.5 (c) it is observable that, NH_4^+ formation was enhanced with the increase in volumetric electric charges in the range of 300 to 2,700 C/L and it gradually decreased over 2,700 C/L. The chloramines concentration were increased gradually with the volumetric electric charges of 300 to 7,500 C/L, but it decreased at the volumetric electric charge of 8,700 C/L, where TN also dropped. This result indicates that chloramines were denitrified at 8,700 C/L.

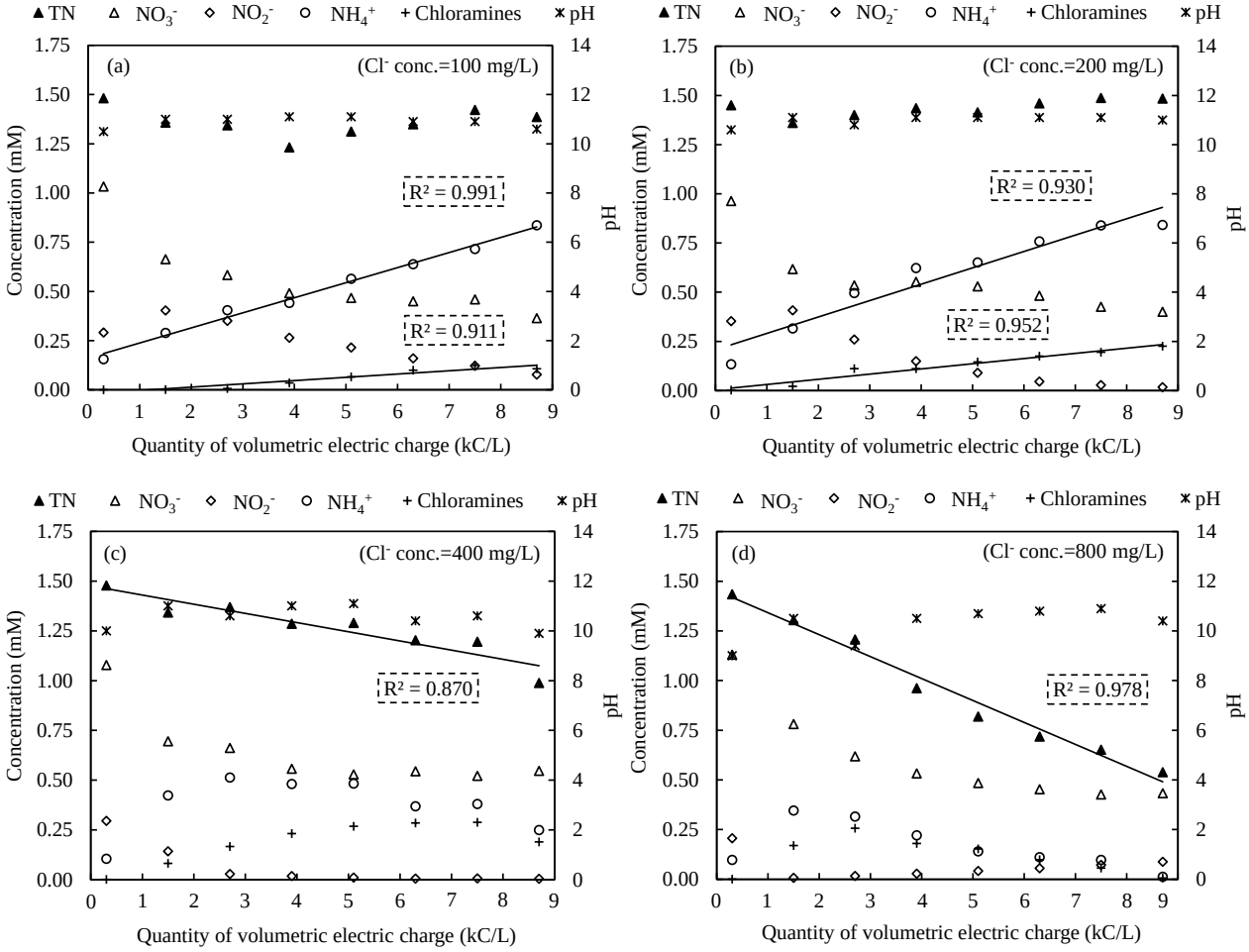

Figure 4.5 Variation of TN, NO_3^-, NO_2^-, NH_4^+, and chloramines concentration in the effluent at (a) Cl^- concentration of 100 mg/L, (b) Cl^- concentration of 200 mg/L, (c) Cl^- concentration of 400 mg/L, and (d) Cl^- concentration of 800 mg/L.

From Figure 4.5 (d) it is observable that, NH_4^+ accumulation rate was enhanced with the increase in volumetric electric charges in the range of 300 to 1,500 C/L, and it gradually decreased with the volumetric electric charges over 1,500 C/L. The complete consumption of NH_4^+ was observed at the volumetric electric charge of 8,700 C/L. The formation of chloramines were increased from the volumetric electric charges of 300 to 2,700 C/L, and it followed the similar trend like NH_4^+ over

2,700 C/L. Finally, TN decreased linearly with the increase in volumetric electric charge at the R^2 value of 0.978. Here, at the volumetric electric charge of 8,700 C/L, TN was found to be 0.54 mM that was composed of NO_3^-, NO_2^-, NH_4^+, and chloramines with the concentrations of 0.43, 0.09, 0.01, and 0.01 mM, respectively.

Figure 4.6 (a) and (b) show the NH_4^+ and chloramines concentrations in the effluents at pH 5, 7, and 9, respectively. This experiment was conducted to observe the effect of pH on break-point chlorination to remove NH_4^+ and chloramines, where Cl^- concentration of 400 mg/L was used for Figure 4.6 (a) and Cl^- concentration of 800 mg/L was used for Figure 4.6 (b). Here, NH_4^+ and chloramines concentration were found to be comparatively lower at neutral pH (pH=7) than acidic (pH<7) and alkaline (pH>7) condition (Figure 4.6 (a)). Likewise, the NH_4^+ and chloramines were not detected at the volumetric electric charge of 5,100 C/L at pH 7 (Figure 4.6 (b)). But, when the pH was in alkaline condition, 8,700 C/L was required for the complete consumption of NH_4^+ and chloramines (Figure 4.5 (d)). He et al. (2015) observed the similar experimental results that supports the above discussion.

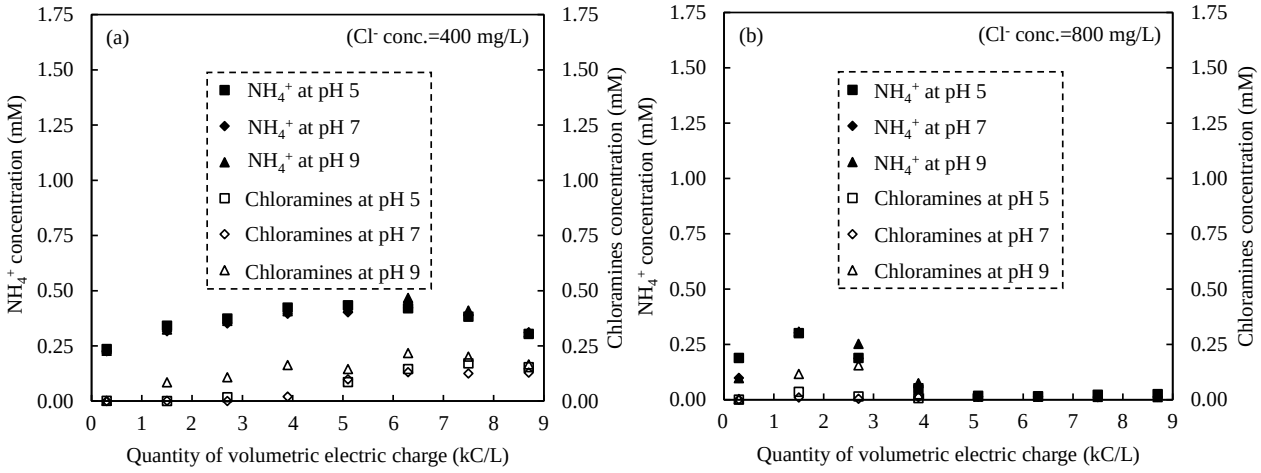

Figure 4.6 NH_4^+ and chloramines concentration in the same effluent at Cl^- concentration of 400 mg/L at pH 5, 7, and 9 for (a), and NH_4^+ and chloramines concentration in the same effluent at Cl^- concentration of 800 mg/L at pH 5, 7, and 9 for (b).

Figure 4.7 (a) and (b) show the variation of NH_4^+ concentration after electrolysis with the synthetic contaminated source water (Table 4.2), where Cl^- was not added for Figure 4.7 (a) and Cl^- was added for Figure 4.7 (b) at the final concentration of 800 mg/L. Here, the NH_4^+ concentration in effluent in Figure 4.7 (a) was almost the same as that in the influent. As a result of no addition of Cl^-, the production rate of free chlorine was inferred to keep low and the produced chlorines were consumed by reduced chemicals in synthetic contaminated source water, which constrained the break-point chlorination. On the contrary, when Cl^- of 800 mg/L was added in the synthetic

contaminated source water, the NH_4^+ concentration in effluent was gradually decreased with the increasing of volumetric electric charges (Figure 4.7 (b)) through the break-point chlorination mechanism. Similar results were experienced by Li et al. (2009) and Pletcher and Poorabedi (1979), which accords with my experimental results.

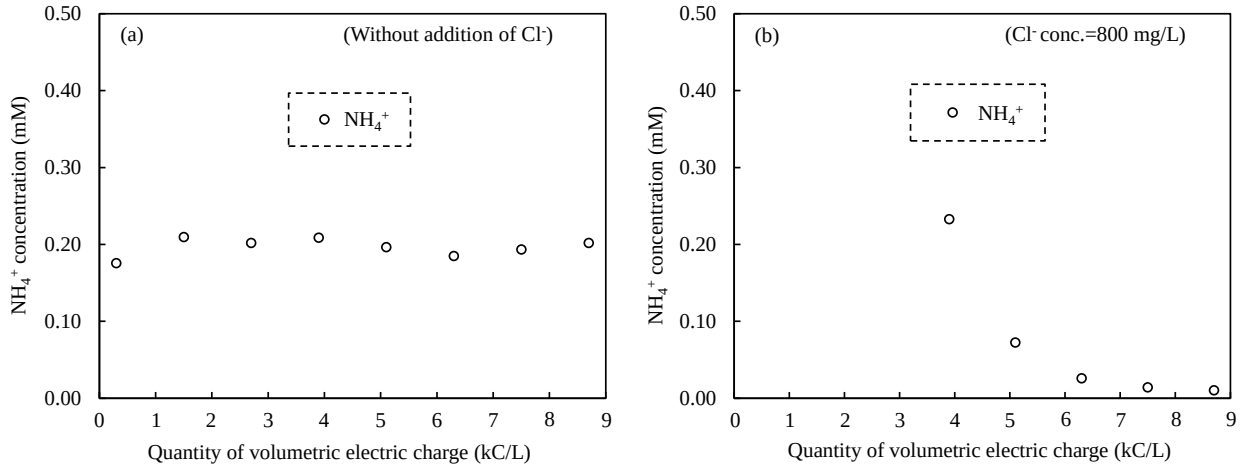

Figure 4.7 Variation of NH_4^+ concentration in the effluent at (a) Without addition of Cl^- in the synthetic contaminated source water, and (b) With the addition of Cl^- concentration of 800 mg/L in the synthetic contaminated source water.

Figure 4.8 shows the production of free Cl_2 at different dozes of NaCl without NO_3^- addition. From this figure it is seen that, free Cl_2 production rate at the Cl^- concentration of 100, 200, 400, and 800 mg/L was linearly increased with respect to the volumetric electric charges at the R^2 value of 0.989, 0.958, 0.988, and 0.981, respectively. This results means that the current efficiency for Cl_2 production did not depend on the volumetric electric charges. The current efficiency increased with the rise in Cl^- from 0.4% for 100 mg-Cl^-/L to 6.1% for 800 mg-Cl^-/L.

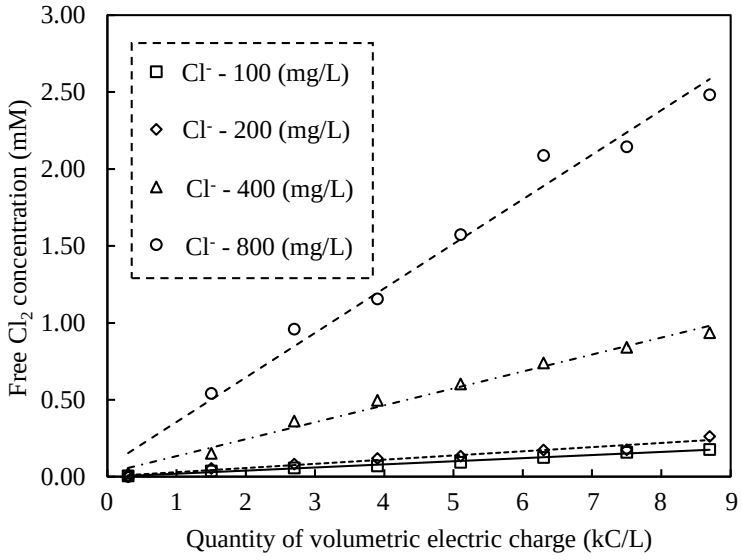

Figure 4.8 Production of free Cl_2 without addition of NO_3^- at different Cl^- concentration. The test solution contained 1mM of K_2SO_4 as a supporting electrolyte.

The enhancement of NH_3 removal under higher current densities was caused by the increase in anodic potential, which was favorable to the electrochemical generation of Cl_2. Because the standard potential of the anodic oxidation of Cl^- (1.36 V vs. SHE) is higher than that of the anodic oxidation of water (1.23 V vs. SHE) (Ureta-Zanartu and Yanez, 1997). The electrode potential of anodic oxidation of Cl^- can be described by the following Nernst's equation.

$$E = E^0 - \frac{RT}{2F} ln \frac{a^2Cl^-}{PCl_2} \quad (18)$$

Where, E is an electrode potential [V], E^0 is the standard potential [V], R is the gas constant (8.314 J K^{-1} mol^{-1}), T is an absolute temperature [K], a_{Cl^-} is an activity of Cl^- [M], and P_{Cl2} is the partial pressure of Cl_2 [atm.]. Since a_{Cl^-} is positively related to Cl^- concentration, an increase in Cl^- concentration results in a decrease in E, which can promote the anodic oxidation of Cl^- into Cl_2. Thus, an increase in electric charge and Cl^- concentration promoted the production of HOCl via the enhancement of electrochemical generation of free chlorine, which enhanced the oxidization of NH_3.

4.3.4 Effect of Electrochemically Produced Chlorine to Occur Break-point Chlorination on Ammonia Nitrogen Removal

Figure 4.9 (a), (b), (c), and (d) show the variation of total Cl_2, free Cl_2, and combined Cl_2 concentration after electrolysis with the presence of different dozes of NaCl (Table 4.1). When Cl^- is added to water, HOCl is generated via the anodic oxidation of chlorine ions. Since HOCl is a weak acid, the following chemical equilibrium is established.

$$HOCl \leftrightarrow H^+ + OCl^- \quad (19)$$

In general, both HOCl and OCl^- altogether are known as free chlorine. These two species exist in an equilibrium condition depending on the pH and temperature. As the pH increases, the ratio of HOCl to OCl^- decreases. Since the pKa of HOCl is 7.5, HOCl is the dominant species below pH 7.5 and OCl^- is the dominant species above pH 7.5 (Reger et al., 2010). The stoichiometric weight ratio of free chlorine as Cl_2 to NH_3 as N is 5.1 for NH_2Cl formation according to the equation 8. After NH_2Cl formation, $NHCl_2$ forms when additional Cl_2 is added according to the equation 9. This formation rates depend on pH, temperature, and mixing condition (Chapin, 1929). Similarly, NCl_3 forms when additional chlorine reacts with $NHCl_2$ following the equation 10. The sum of combined and free chlorine in a sample is known as total chlorine. Combined chlorine includes chloramines of NH_2Cl and $NHCl_2$. Figure 4.9 (a), (b), (c), and (d) show the variation of total Cl_2, free Cl_2, and combined Cl_2 concentration at the Cl^- concentration of 100, 200, 400, and 800 mg/L, respectively, where influent NO_3^- concentration in all these experiments were 1.42 mM.

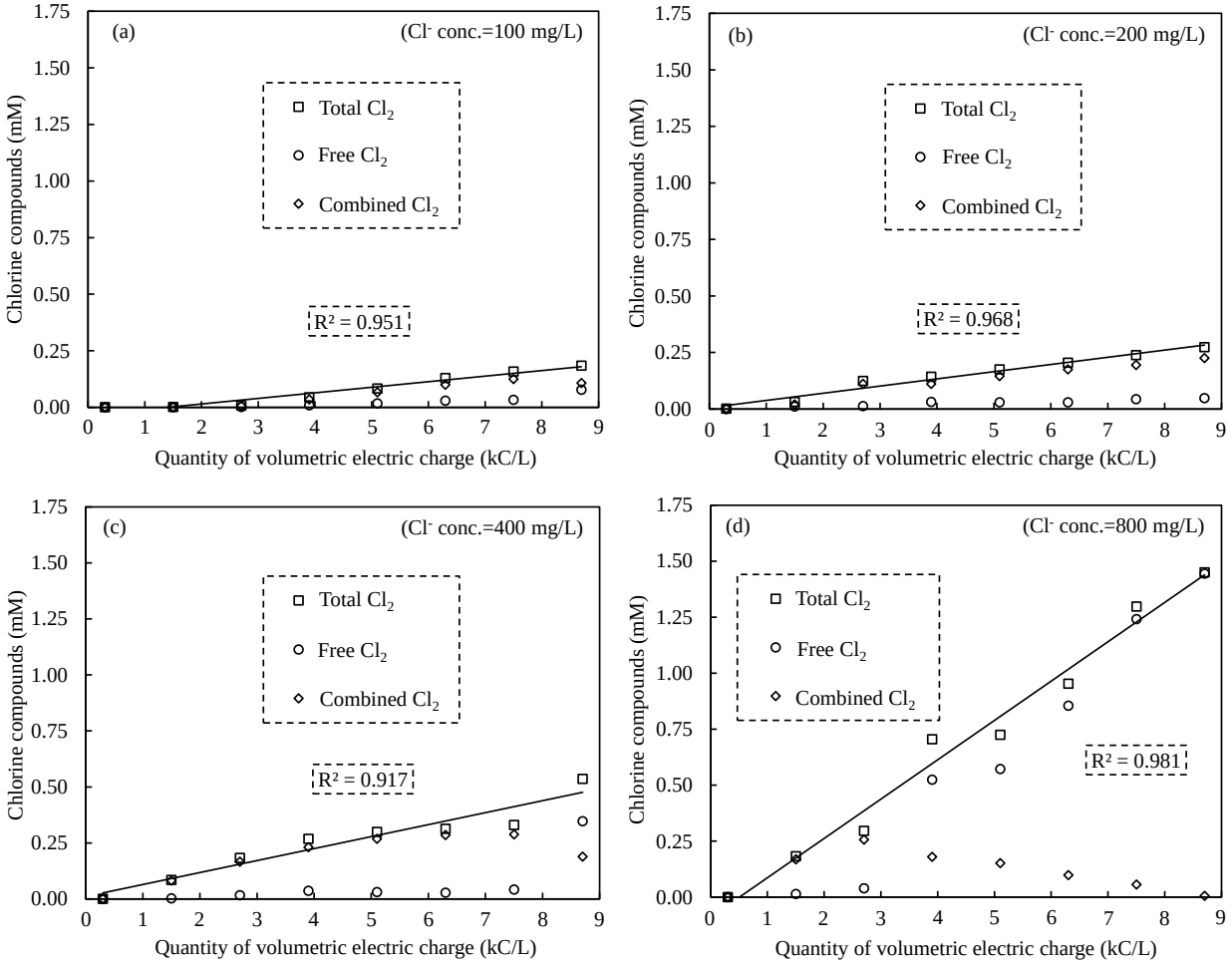

Figure 4.9 Variation of total Cl_2, free Cl_2, and chloramines in the effluent at (a) Cl^- concentration of 100 mg/L, (b) Cl^- concentration of 200 mg/L, (c) Cl^- concentration of 400 mg/L, and (d) Cl^- concentration of 800 mg/L.

From these graphs it is clearly observable that, total Cl_2 increased linearly with the increase in volumetric electric charges at the R^2 value of 0.951 (Figure 4.9 (a)), 0.968 (Figure 4.9 (b)), 0.917 (Figure 4.9 (c)), and 0.981 (Figure 4.9 (d)), respectively. Here, at the Cl^- concentration of 100 and 200 mg/L free Cl_2 accumulation was found to be less than that of chloramines. Similarly, at the Cl^- concentration of 800 mg/L free Cl_2 was found to be less than chloramines from the volumetric electric charges of 300 to 2,700 C/L due to insufficient Cl_2 production. But, the electric charges over 2,700 C/L at the Cl^- concentration of 800 mg/L produced the sufficient amount of Cl_2 for the complete ammonia oxidation. As a result, free Cl_2 was found to be gradually increased and chloramines gradually decreased over 2,700 C/L.

When Cl_2 consumption for TN removal was estimated by subtracting the residual free Cl_2 and 1.5 times of chloramines in Figure 4.9 (c) and (d), and from the produced free Cl_2 in Figure 4.8, the relationship between TN removal and Cl_2 consumption in the case of Cl^- concentration of 400 and 800 mg/L was plotted in Figure 4.10. The slope of the regression line was found to be 0.783 mM-

N/mM-Cl_2, which is equivalent to the molar ratio of Cl_2 consumption to TN removal of 1.28. Based on the equations 15 and 16, the theoretical molar ratio of chlorine to NH_3 is projected to be 1.5 for N_2 evolution and 2 for N_2O evolution.

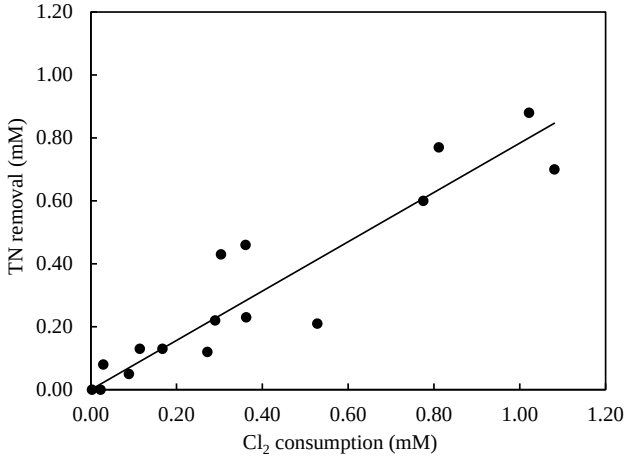

Figure 4.10 Relationship between TN removal and Cl_2 consumption at Cl^- concentration of 400 and 800 mg/L. The Cl_2 consumption was corrected by the residual free Cl_2 and residual chloramines.

In this study, the observed molar ratio for TN removal was found to be slightly smaller than the theoretical molar ratio, which was due to uncertainty of several factors, such as contact time, water temperature, concentrations of ammonium and chlorine, and pH of estimation of Cl_2 consumption for chloramine accumulation. But, it was close to the theoretical molar ratio for N_2 evolution. Therefore, nitrogenous compound removal pathway in this experiment was inferred to be the N_2 evolution following the equation 15. For the complete removal of ammonia, I recommend 5,100 C/L volumetric electric charge with the chloride ion concentration of 800 mg/L at pH 7.

4.3.5 Evaluation of Total Coliform (TC) and General Bacteria (GB) Removal Performances

This experiment was conducted to observe the total coliform (TC) and general bacteria (GB) removal performances through electrolysis. To conduct this experiment, municipal wastewater in Ryukoku University was diluted by a 5-time with normal tap water. Then, it was used as influent for the source of TC and GB. Here, the TC and GB concentration in the influent was found to be 66,200 CFU/mL and 80,800 CFU/mL, respectively. In the electrolysis experiment the electrochemical flow cell was operated within the volumetric electric charges of 300-8,700 C/L at the flow rate of 20 mL/min. The effluent volume for each operation was 200 mL. Figure 4.11 (a) and (b) show the TC and GB removal performances through electrolysis. Here, the TC removal efficiency was found to be 97.1% at the volumetric electric charge of 300 C/L and 98.9% at the volumetric electric charge of 1,500 C/L, respectively. The TC and GB removal efficiencies were found to be 100% at the volumetric electric charges of over 1,500 C/L (Figure 4.11 (a)), almost 100% at any volumetric electric charge in the range of 300-8,700 C/L (Figure 4.11 (b)), respectively.

Similar results were experienced by Haaken et al. (2014). Therefore, I recommend over 300 C/L volumetric electric charge for the complete removal of total coliform and general bacteria.

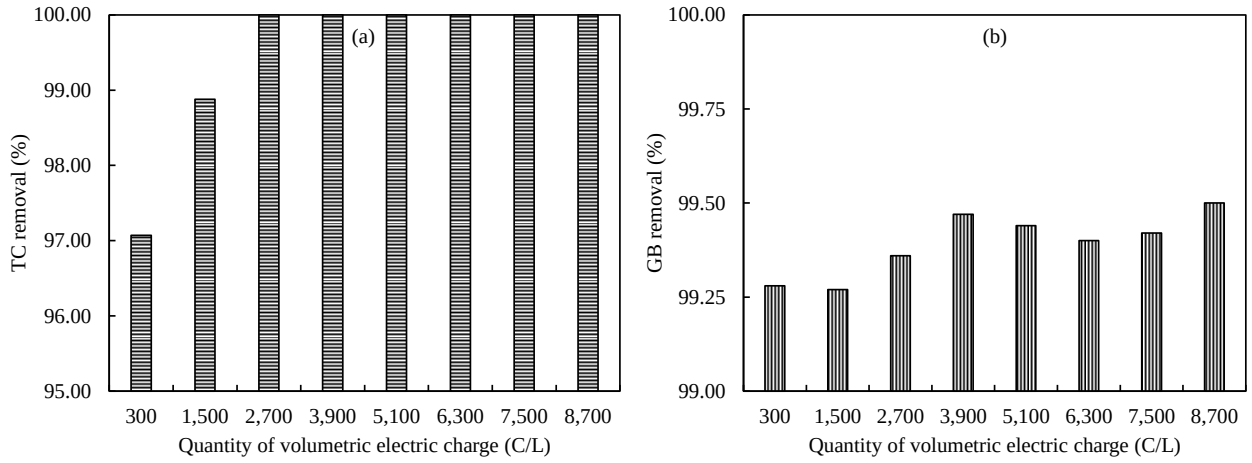

Figure 4.11 (a) and (b) TC and GB removal performances through electrolysis in the volumetric electric charges of 300-8,700 C/L at the flow rate of 20 mL/min.

4.4 Conclusion

In this study, a rapid electrochemical removal technique of nitrogenous compounds such as nitrate, nitrite, and ammonia was demonstrated using a two-compartment electrochemical flow cell with copper mesh cathode and platinum-coated titanium anode. A cation-exchange membrane was employed between the compartments for separating anodic and cathodic reactions in the electrochemical cell. Nitrogenous compounds removal efficiency was evaluated using synthetic water containing 1.42 mM nitrate with chloride ion concentration of 100-800 mg/L. The effect of volumetric electric charges, flow rates, and Cl^- concentrations were examined to find out appropriate condition to occur break-point chlorination mechanism. The volumetric electric charge was regulated by changing the electrolytic current. Volumetric electric charges enhanced the conversion of nitrate into nitrite and ammonia as well as anodic production of chlorine, but it did not change the current efficiency. Flow rates also enhanced the electrochemical reactions due to the promotion of mass transfer process. Chloride ion concentration improved the current efficiency of chlorine production by decreasing the electrode potential for Cl_2 evolution. As a result, total nitrogen removal was accelerated via the break-point chlorination mechanism.

However, the current efficiency remained at a low level, a maximum value of 6.1% at the chloride ion concentration of 800 mg/L. In spite of the low current efficiency, 1.42 mM (NO_3^--N=20 mg/L) initial nitrate was decreased to 0.48 mM (NO_3^--N=6.78 mg/L) without nitrite and ammonia accumulation during 1.0 minute contact time for nitrate reduction and 15 seconds contact time for

chlorine production at the volumetric electric charge of 5,100 C/L and Cl^- concentration of 800 mg/L at pH 7. As a consequence, this research provided a feasible approach for the rapid removal of nitrogenous compounds from contaminated water source. Finally, I would like to propose 5,100 C/L volumetric electric charge with 800 mg/L chloride ion concentration at pH 7 as an optimum operational condition for the removal of nitrogenous compounds along with total coliform and general bacteria.

4.5 References

Bejan, D., Sagitova, F., Bunce, N. J., (2005). Evaluation of electrolysis for oxidative deodorization of hog manure. Journal of Applied Electrochemistry., 35 (9), 897-902.

Bouzek, K., Paidar, M., Sadilkova, A., Bergmann, H., (2001). Electrochemical reduction of nitrate in weakly alkaline solutions. Journal of Applied Electrochemistry., 31, 1185-1193.

Chapin R. M. (1929). Dichloro-Amine. Journal of The American Chemical Society., 51 (7), 2112-2117.

Chen, G., (2004). Electrochemical technologies in wastewater treatment. Separation and Purification Technology., 38 (1), 11-41.

Chiang, L. C., Chang, J. E., Wen, T. C., (1995). Indirect oxidation effect in electrochemical oxidation treatment of landfill leachate. Water Research., 29 (2), 671-678.

Chopra, A. K., Sharma, A. K., Kumar, V., (2011). Overview of electrolytic treatment: An alternative technology for purification of wastewater. Archives of Applied Science Research., 3 (5), 191-206.

Dash, B. P., Chaudhari, S., (2005). Electrochemical denitrification of simulated ground water. Water Research., 39 (17), 4065-4072.

De, D., Englehardt, J. D., Kalu, E. E., (2000). Cyclic voltammetric studies on nitrate and nitrite ion reduction at the surface of iridium-modified carbon fiber electrode. Journal of The Electrochemical Society., 147 (11), 4224-4228.

De, D., Kalu, E. E., Tarjan, P. P., Englehardt, J. D., (2004). Kinetic studies of the electrochemical treatment of nitrate and nitrite ions on iridium-modified carbon fiber electrodes. Chemical Engineering & Technology., 27 (1), 56-64.

Duarte, H. A., Jha, K., Weidner, J. W., (1998). Electrochemical reductions of nitrates and nitrites in alkaline media in the presence of hexavalent chromium. Journal of Applied Electrochemistry., 28, 811-817.

Feng, C. P., Sugiura, N., Shimada, S., Maekawa, T., (2003). Development of a high performance electrochemical wastewater treatment system. Journal of Hazardous Materials., 103 (1-2), 65-78.

Genders, J. D., Hartsough, D., Hobbs, D. T., (1996). Electrochemical reduction of nitrates and nitrites in alkaline nuclear waste solutions. Journal of Applied Electrochemistry., 26, 1-9.

Gootzen, J. F. E., Peeters, P. G. J. M., Dukers, J. M. B., Lefferts, L., Visscher, W., Veen, J. A. R. V., (1997). The electrolytic reduction of NO_3^- on Pt, Pd and Pt + Pd electrodes activated with Ge. Journal of Electroanalytical Chemistry., 434 (1-2), 171-183.

Haaken, D., Dittmar, T., Schmalz., V., Worch, E., (2014). Disinfection of biologically treated wastewater and prevention of biofouling by UV/electrolysis hybrid technology: Influence factors and limits for domestic wastewater reuse. Water Research., 52, 20-28.

He, S., Huang, Q., Zhang, Y., Wang, L., Nie, Y., (2015). Investigation on direct and indirect electrochemical oxidation of ammonia over Ru-Ir/TiO_2 anode. Industrial & Engineering Chemistry Research., 54 (5), 1447-1451.

Katsounaros, I., Kyriacou, G., (2007). Influence of the concentration and the nature of the supporting electrolyte on the electrochemical reduction of nitrate on tin cathode. Electrochimica Acta., 52 (23), 6412-6420.

Kim, K. W., Kim, Y. J., Kim, I. T., Park, G. I., Lee, E. H., (2005). The electrolytic decomposition mechanism of ammonia to nitrogen at an IrO_2 anode. Electrochimica Acta., 50 (22), 4356-4364.

Li, L., Liu, Y., (2009). Ammonia removal in the electrochemical oxidation: Mechanism and pseudo-kinetics. Journal of Hazardous Materials., 161 (2-3), 1010-1016.

Li, M., Feng, C., Zhang, Z., Shen, Z., Sugiura, N., (2009). Electrochemical reduction of nitrate using various anodes and a Cu/Zn cathode. Electrochemistry Communications., 11 (10), 1853-1856.

Li, M., Feng, C., Zhang, Z., Sugiura, N., (2009). Efficient electrochemical reduction of nitrate to nitrogen using Ti/IrO_2-Pt anode and different cathodes. Electrochimica Acta., 54 (20), 4600-4606.

Li, M., Feng, C., Zhang, Z., Yang, S., Sugiura, N., (2010). Treatment of nitrate contaminated water using an electrochemical method. Bioresource Technology., 101 (16), 6553-6557.

Lin, S. H., Wu, C. L., (1996). Electrochemical removal of nitrite and ammonia for aquaculture. Water Research., 30 (3), 715-721.

Palvlovic, M. G., Pavlovic, M. M., Pavlovic, M. M., Nikolic, N. D., (2014). Electrochemical removal of microorganisms in drinking water. International Journal of Electrochemical Science., 9, 8249-8262.

Pletcher, D., Poorabedi, Z., (1979). The reduction of nitrate at a copper cathode in aqueous acid. Electrochimica Acta., 24 (12), 1253-1256.

Polatides, C., Dortsiou, M., Kyriacou, G., (2005). Electrochemical removal of nitrate ion from aqueous solution by pulsing potential electrolysis. Electrochimica Acta., 50 (25-26), 5237-5241.

Prashad, P. K. R., Priya, M. N., Palanivelu, K., (2005). Nitrate removal from groundwater using electrolyte reduction method. Indian Journal of Chemical Technology., 12, 164-169.

Pressley, T. A., Bishop, D. F., Roan, S. G., (1972). Ammonia-nitrogen removal by breakpoint chlorination. Environmental Science & Technology., 6 (7), 622-628.

Rajeswar, K., Ibanez, (1997). Environmental electrochemistry fundamentals and applications in pollution abatement. Academic Press Inc., San Diego, California.

Reger, D. L., Goode, S. R., Ball, D. W., (2010). Chemistry: Principles and Practice, Third Edition, USA.

Rice, E. W., Baird, R. B., Eaton, A. D., Clesceri, L. S., (2012). Standard Methods for the Examination of Water and Wastewater. 22nd Edition. Washington, DC: American Public Health Association, American Water Works Association, Water Environment Federation.

Thinh, N. V., Thoa, N. T. P., Hung, L. Q., (2007). Cyclic voltammetry study on the reduction of nitrate and nitrite on a copper electrode. Journal of Chemistry., 45 (2), 213-218.

Ureta-Zanartu, S., Yanez, C., (1997). Electroreduction on nitrate ion on Pt, Ir and on 70:30 Pt:Ir alloy. Electrochimica Acta., 42 (11), 1725-1731.

Vanlangendonck, Y., Corbiser, D., Lierde, A. V., (2005). Influence of operating conditions on the ammonia electro-oxidation rate in wastewaters from power plants. Water Research., 39 (13), 3028-3034.

Chapter V
Final Conclusion

5.1 Proposed Outline for the Integrated Water Treatment System in Contaminated Source Water

Considering the specific results of a series of experiments in this research, the following integrated water treatment system is proposed, which consists of three unit processes, namely, process I (Active Surface-charge Control Depth Filtration), process II (Electrolysis), and process III (Reverse Osmosis (RO)), respectively. Figure 5.1 shows the flow diagram of the proposed integrated water treatment system.

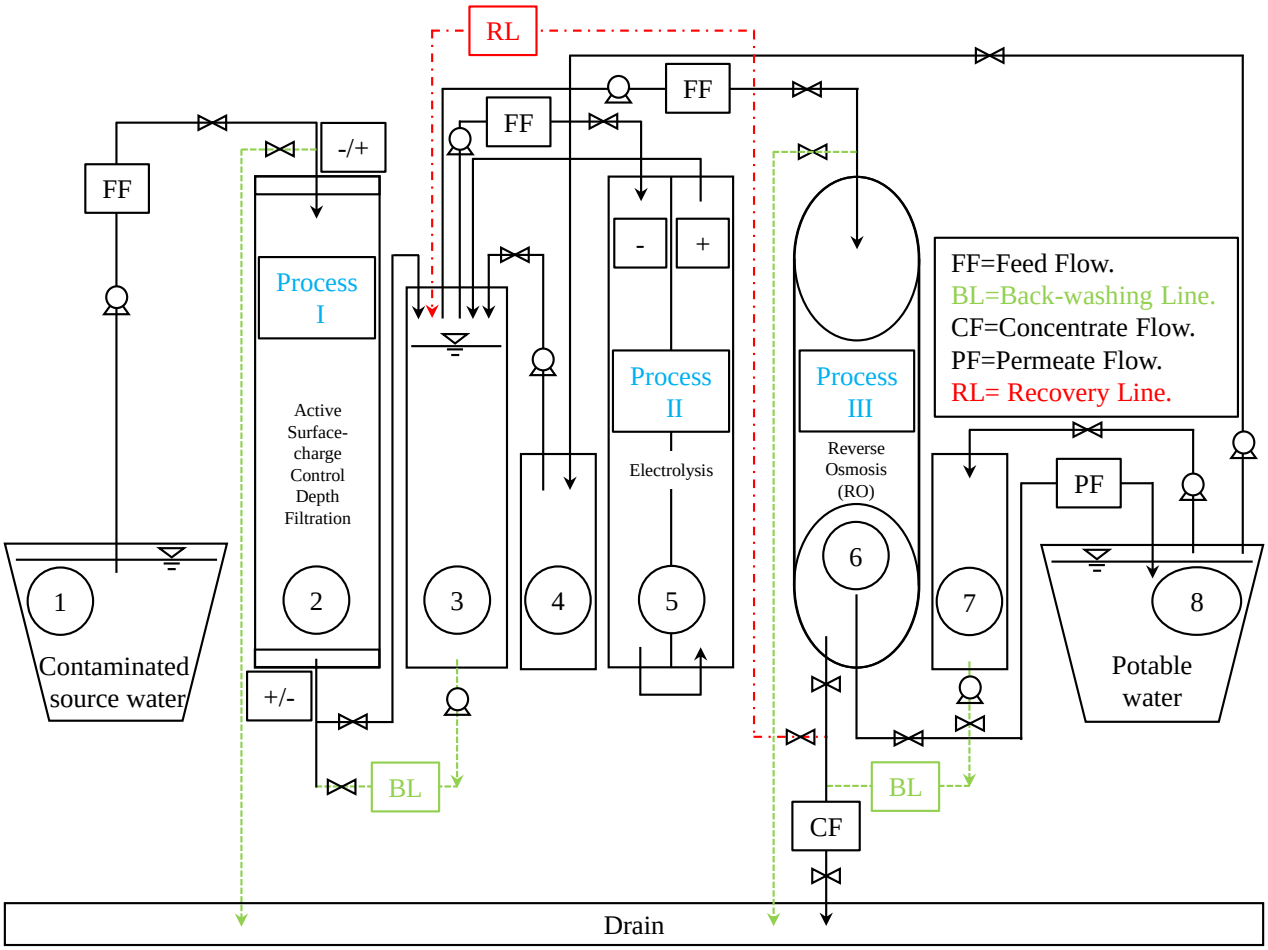

Figure 5.1 Integrated water treatment system flow diagram. 1; Contaminated source water reservoir, 2; Active surface-charge control depth filtration (Process I), 3; Effluent reservoir of process I along with back-washing tank for the Process I, 4; Sodium chloride (NaCl) and buffer solution tank to adjust the pH for the effluent of process I, 5; Electrolysis (Process II), 6; Reverse osmosis (RO) (Process III), 7; Back-flushing tank for the process III (NaOH conc.=1,000 mg/L), and 8; Potable water reservoir.

In this integrated system, I set active surface-charge control depth filtration at the first step. Then, electrolysis and RO are applied in parallel. The causes of such an arrangement are explained here:

In this integrated system, RO is the core technology for water purification. Since RO membrane is a very sensitive and sophisticated technology and the fouling is a main problem in RO operation. As a result, to protect the RO membrane from organic and inorganic fouling materials such as various suspended solids (SS) and colloids like iron (Fe) colloids, active surface-charge control depth filtration was used in the first step. Although active surface-charge control depth filtration is good for the removal of organic and inorganic particles, it cannot remove microorganisms like total coliform (TC) and general bacteria (GB) very much, which cause biofouling in RO membrane. Moreover, RO membrane shows lower performance for removing many nitrogenous compounds such as ammonia (NH_3). As a result, to remove the microorganisms along with NH_3, electrolysis was applied to the effluent from the Process I. In this system, the active surface-charge control depth filtration was installed prior to electrolysis to protect the electrochemical cell from various organic and inorganic particles that may hinder electrochemical reactions in process II through the deposition onto the electrodes. Finally, the RO was used at the end of this system for complete removal of physical, chemical, and biological contaminants to get a high quality potable water. The water quality parameters expected after RO treatment are shown in Table 5.1, when the RO membrane unit is operated at the permeate flux of 19.9 L m^{-2} h^{-1} with the transmembrane pressure (TMP) of 414 kPa. The water recovery (Rw) rate was calculated using the following equations:

$$\text{Water recovery (Rw) \%} = \left(1 - \frac{1}{R}\right) \times 100 = 1 - \frac{1}{5.2} \times 100 = 80.8\ \%$$

$$\text{Here, R = Concentration ratio} = \frac{EC_{(2{,}000\ mg/L\ NaCl)} - EC_{(528\ mg/L\ NaCl)}}{EC_{in\ (NaCl\ conc.=52.1\ mg/L)}}$$

Here, $EC_{(2{,}000\ mg/L\ NaCl)}$ = Maximum sodium chloride conc. in feed water (Dow Filmtec.)

EC = Electrical Conductivity

$$\text{Here, R = Concentration} = \frac{(4{,}400.0 - 1{,}161.6)\ \mu S/cm}{620.0\ \mu S/cm} = 5.2$$

$$\text{Final NaCl conc.} = A_{NaCl\ (mg/L)} + C_{in\ NaCl\ (mg/L)} \times R = 800\ mg/L$$

$$= (528.0 + 52.1 \times 5.2)\ mg/L = 798\ mg/L \approx 800\ mg/L$$

Here, A_{NaCl} = Sodium chloride (NaCl) addition

And, $C_{in\ NaCl}$ = Source water sodium chloride (NaCl) conc.

$$\text{Here, } A_{NaCl\ (mg/L)} = \frac{EC_{NaCl\ (\mu S/cm)}}{\alpha}$$

$$\alpha = \frac{EC_{NaCl\ (2{,}000\ mg/L)}}{\text{NaCl Conc. 2,000 mg/L}}$$

$$\alpha = \frac{4{,}400}{2{,}000} = 2.2$$

$$EC_{NaCl\ (\mu S/cm)} = A_{NaCl\ (mg/L)} \times \alpha = 528.0 \times 2.2 = 1{,}161.6\ \mu S/cm$$

Moreover, 5 minutes back-washing time is proposed for process I after every 50-m^3 m^{-2} water production at the back-washing hydraulic loading of 1.27 m^3 m^{-2} min^{-1}. This means that the water recovery in Process I is 87.3%. The proposed back-washing frequency for the RO elements and water consumption by 5-times back-washing are calculated to be 138 L/d (=19.9 L m^{-2} h^{-1} × 0.29 m^2 $element^{-1}$ × 23.92 h/d) and 5.5 L (=1.1 L min^{-1} × 5 min), respectively, 4.0% of produced water is consumed for back-washing in process III. Consequently, the water recovery of the whole system is expected to be 67.7% (=0.873 × 0.808 × (1-0.04)).

Table 5.1 Water quality parameters after RO treatment.

Sl. No.	Parameters	Initial contamination	Water quality after RO treatment	Potable water quality standards by WHO
01.	Suspended solids (SS)	16 ~ 100 (mg/L)	0.0 (mg/L)	0.0 (mg/L)
02.	Turbidity	36 ~ 197 (mg/L-kaolin)	0.0 ~ 1.0 (mg/L-kaolin)	< 1.0 (mg/L-kaolin)
03.	Color	140 ~ 190 (Pt-Co)	2 ~ 3 (Pt-Co)	< 1.0 (Pt-Co)
04.	Iron (Fe^{2+})	7.3 ~ 9.2 (mg/L)	0.1 ~ 0.2 (mg/L)	< 0.5 (mg/L)
05.	Manganese (Mn^{2+})	5.1 ~ 6.5 (mg/L)	0.2 (mg/L)	< 0.5 (mg/L)
06.	Nitrite nitrogen (NO_2^--N)	8.9 ~ 12.6 (mg/L)	0.0 (mg/L)	< 1.0 (mg/L)
07.	Nitrate nitrogen (NO_3^--N)	14.9 ~ 18.6 (mg/L)	6.78 (mg/L)	< 10.0 (mg/L)
08.	Ammonium nitrogen (NH_4^+-N)	2.4 ~ 3.8 (mg/L)	0.0 (mg/L)	< 0.5 (mg/L)
09.	Biochemical oxygen demand (BOD)	48.8 ~ 75.5 (mg/L)	0.0 ~ 1.0 (mg/L)	< 1.0 (mg/L)
10.	Chemical oxygen demand (COD)	88.6 ~ 127.9 (mg/L)	0.0 ~ 1.0 (mg/L)	< 1.0 (mg/L)
11.	Total coliform (TC)	29,333 ~ 122,000 (CFU/mL)	0.0 (CFU/mL)	0.0 (CFU/mL)
12.	General bacteria (GB)	80,800 (CFU/mL)	0.0 (CFU/mL)	0.0 (CFU/mL)

All the parameters are found to be below the acceptable level of potable water quality, which satisfy the potable water quality standards recommended by the world health organization (WHO). As a result, this integrated system can be used for the practical purpose in the water contaminated areas.

5.2 Energy Consumption Calculation of Each Process Based on the Experimental Conditions

Table 5.2 and 5.3 shows the operational conditions and energy cost of each process, respectively. The energy cost for feed pump operation in process I and II is not included in Table 5.3.

Table 5.2 Operational conditions of process I, II, and II.

Process I	Process II	Process III
Filtration terminal voltage= +1.0 V.	Volumetric electric charge=5,100 C/L.	Pressure boost pump 24 VAC (CPD6800, Aquatec, USA)=0.53 amps.
Back-washing terminal voltage= -1.0 V.	Voltage at 5,100 C/L volumetric electric charge=10.0 V.	Operating pressure=414 kPa.
Filtration hydraulic loading=283 (L m^{-2} min^{-1}).	-	Permeate flow rate=94.6 (mL/min) (36 GPD).
Back-washing hydraulic loading=1274 (L m^{-2} min^{-1}).	-	Back-washing flow rate=1,100 (mL/min) with 20 kPa.

This energy consumption was calculated based on 1-m^3 water production in each process separately.

The water production energy cost for process I, Process II, and process III were found to be 0.0 USD, 2.59 USD, and 0.35 USD, respectively, flowing the Japanese energy charge rate, 1kWh=19.52 Yen and 1 Yen=0.009366 USD. The overall cost for the potable water production was found to be 2.94 USD/m^3. Here, the energy cost for process I was zero, because the applied terminal voltage +1.0 V did not show any current consumption.

Table 5.3 Energy cost per cubic meter water production in process I, II, and II.

Energy cost per cubic meter water production in each process			Total energy cost per cubic meter potable water production
Active Surface-charge Control Depth Filtration (Process I)	Electrolysis (Process II)	Reverse Osmosis (RO) (Process III)	
0.0 (USD)	2.59 (USD)	0.35 (USD)	2.94 (USD)

5.3 Advantages of the Proposed Integrated System

The proposed system has a high quality potable water production capability at the minimum cost of 2.94 USD/m^3 except pumping cost at the water recovery of 67.7%. Long operational life-time with environment friendly, and comparatively less manpower would be needed for operation and maintenance.

5.4 Disadvantages of the Proposed Integrated System

Buffer solution chemicals like sodium bicarbonate ($NaHCO_3$) and sulfuric acid (H_2SO_4) will be necessary to control the feed water pH of process II. Sodium hydroxide (NaOH) will be needed for the back-washing in process III.

5.5 Recommendations for the Future Research

In this study, the water quality parameters of the three unit process were examined and demonstrated separately in the laboratory scale. As a result, a pilot study is recommended in the field level combining the three unit process into integrated system as a unit process for commercial application.

Peer-reviewed Journals and Conferences

Peer-reviewed Journals

- A.K.M. Ashadullah and Naoyuki Kishimoto, (2016). Influence of Operational Parameters on Rapid Nitrate Removal Using an Electrochemical Flow Cell. International Journal of Environmental Science and Development., 7 (7), 499-506.

- A.K.M. Ashadullah and Naoyuki Kishimoto, (2016). Applicability of a Reverse Osmosis (RO) membrane to the Treatment of Wastewater Contaminated with Nitrite, Nitrate, Iron, and Manganese. International Journal of Water and Wastewater Treatment., 2 (1), 1-9.

Conferences

- A.K.M. Ashadullah and Naoyuki Kishimoto, (2014): Effects of operational parameters on reduction of nitrate to ammonia using an electrochemical flow cell. Water and Environment Technology Conference, TWIns, Waseda University, Tokyo, Japan.

- A.K.M. Ashadullah and Naoyuki Kishimoto, (2015): Effects of operational parameters on electrochemical nitrate removal using an electrochemical flow cell. 2nd IWA Malayasia Young Water Professional Conference, Vivatel, Kualalumpur, Malaysia.

- A.K.M. Ashadullah and Naoyuki Kishimoto, (2015): Applicability of a reverse osmosis (RO) membrane to the treatment of wastewater contaminated with nitrite, nitrate, iron and manganese. Water and Environment Technology Conference, Nihon University, Tokyo, Japan.